The role of sphingosine-1-phosphate and its receptor S1PR1 in inflammation and cancer

Dissertation
zur Erlangung des Doktorgrades der Naturwissenschaften

vorgelegt beim Fachbereich Biochemie, Chemie und Pharmazie
der Johann Wolfgang Goethe-Universität
Frankfurt am Main

von
Benjamin Weichand
aus Rödermark (Urberach)

Frankfurt am Main, 2014

(D30)

vom Fachbereich 14 (Biochemie, Chemie und Pharmazie)

der Johann Wolfgang Goethe-Universität als Dissertation angenommen

Dekan: Prof. Dr. T. Prisner

Gutachter: Prof. Dr. R. Fürst
Prof. Dr. B. Brüne

Datum der Disputation: 08.12.2014

Genius is one per cent inspiration,
ninety-nine per cent perspiration.

Thomas Alva Edison

INDEX

LIST OF FIGURES

LIST OF TABLES

ABBREV.

3-MCA	3-methylcholanthrene
ABC	ATP-binding cassette
AC	adenylate cyclase
ACM	apoptotic cancer cell supernatant
ADORA2A	adenosine A2A receptor
AF488	AlexaFluor488
Akt	protein kinase B
AN	apoptotic neutrophils
AnxA1	annexin A1
AOM/DSS	azoxymethane/dextran sulfate sodium
AP-1	activator protein 1
APAF-1	apoptotic protease-activating factor-1
ARG1	arginase 1
ASC	apoptosis-associated speck-like protein containing a CARD
ATP	adenosine triphosphate
ATX	autotaxin
BAK	Bcl-2 homologous antagonist killer
BAX	Bcl-2 associated protein x
Bcl-2	B cell lymphoma 2
BH3	Bcl-2 homology domain 3
BMDM	bone marrow derived macrophage
BOK	Bcl-2-related ovarian killer
CARD	caspase recruitment domain
Casp1	caspase-1
CCL2/5	chemokine (C-C motif) ligand 2/5
CD	cluster of differentiation
CER	ceramidase
CHO	Chinese hamster ovary cell
CHX	cycloheximide
CK	ceramide kinase
CLR	C-type lectin receptor
CNS	central nervous system
CRE	causes recombination (enzyme)
CXCL13	chemokine (C-X-C motif) ligand 13
d	day
DAMP	danger associated molecular pattern

DC	dendritic cell
DIABLO	direct IAP-binding protein with low pI
DISC	death-inducting signaling cascade
DMEM	Dulbecco's modified Eagle's medium
EGF	epidermal growth factor
EGFR	epidermal growth factor receptor
EMT	epithelial-mesenchymal-transition
ER	endoplasmatic reticulum
ERK	extracellular-signal-regulated kinase
F4/80	EGF-like module-containing mucin-like hormone receptor-like 1
FACS	fluorescence-activated cell sorting
FADD	Fas-associated protein with death domain
FasL	Fas ligand
FasR	Fas receptor
FCS	fetal calf serum
Fizz1	resistin-like beta
GF	growth factor
GFP	green fluorescent protein
GM-CSF	granulocyte/macrophage-colony stimulating factor
Gy	gray (SI unit of absorbed radiation)
HDAC	histone deacetylase
HDL	high density lipoprotein
HER2	receptor tyrosine-protein kinase erbB-2
HMGB1	high-mobility group box 1
HO-1	heme-oxygenase 1
HSPC	hematopoietic stem and progenitor cell
i/mDC	immature/mature dendritic cell
IAP	inhibitor of apoptosis
IFNγ	interferon γ
Ig	immunoglobulin
IL	interleukin
iNOS	inducible nitric oxide synthase
IRAK	interleukin-1 receptor-associated kinase 1
IRF	interferon regulatory factors
IκBα	nuclear factor of kappa light polypeptide gene enhancer in B-cells inhibitor α
JAK2	Janus kinase 2
JNK	c-Jun N-terminal kinase

K_d	diffusion constant
KO	knockout
LGP2	RIG-I-like receptor 3
loxP	locus of X-over P1
LPS	lipopolysaccharide
LRR	leucine rich repeats
LXR	liver-X-receptor
m	minute
Mal	myelin and lymphocyte protein
MAPK	mitogen-activated protein kinase
MCL-1	myeloid cell leukemia 1
MCP-1	(see CCL2)
M-CSF	macrophage-colony stimulating factor
MDA5	melanoma differentiation-associated protein 5
MDSC	myeloid derived suppressor cell
mdT/meG	membrane allocating dTomato/eGFP fluorochrome
MMP9	matrix-metalloproteinase 9
MR	mannose receptor
mTOR	mechanistic target of rapamycin
MyD88	myeloid differentiation primary response gene (88)
NEO	neomycin
NFAT	nuclear factor of activated T-cells
NF-κB	nuclear factor kappa-light-chain-enhancer of activated B cells
NK cell	natural killer cell
NLR	NOD-like receptor
NLRP	NACHT, LRR and PYD domains-containing protein
PAF	platelet-activating factor
PAMP	pathogen associated molecular pattern
PDGF	platelet-derived growth factor
PGE_2	prostaglandin E_2
PI3K	phosphatidylinositol-3 kinase
PKC	protein kinase C
PLC	phospholipase C
PPA2	protein phosphatase A2
PPARγ	peroxisome proliferator-activated receptor γ
PRR	pattern recognition receptor
PyMT	polyoma middle T (oncogene)

qPCR	quantitative real-time polymerase chain reaction
Rac	Rho family GTPase
Ras	Ras subfamily of small GTPases
Rho	Rho GTPase
RIG-I	retinoic acid-inducible gene 1
RLR	RIG-I-like receptor
ROS	reactive oxygen species
RPMI	Roswell Park Memorial Institute medium
RTK	receptor tyrosine kinase
s	second
S1P	sphingosine-1-phosphate
S1PR	S1P receptor
SARM	sterile alpha and TIR motif containing 1
SGMS	sphingomyelin synthase
SMAC	second mitochondria-derived activator of caspases
SMase	sphingomyelinase
Sph	sphingosine
SphK	sphingosine kinase
SPL	sphingosine-1-phosphate lyase
SPNS2	spinster homolog 2
SPP	sphingosine phosphatase
STAT	signal transducer and activator of transcription
SURVIVIN	baculoviral inhibitor of apoptosis repeat-containing 5
TAM	tumor-associated macrophage
TGF-β	transforming growth factor beta
Th	T helper cell
TIR	Toll/Interleukin-1 receptor
TLR	Toll-like receptor
TNFα	tumor necrosis factor alpha
TRAF2	TNF receptor-associated factor 2
TRAM	TRIF-related adaptor molecule
TRIF	TIR-domain-containing adapter-inducing interferon-β
UbiC	ubiquitin C
VEGF	vascular endothelial growth factor
wt	wildtype
XCL1	chemokine (C motif) ligand

1 Summary

Immune cells are key players in several physiological and pathophysiological events such as acute and chronic inflammation, atherosclerosis and cancer. Especially in acute inflammation, macrophages are indispensable for the switch from the acute inflammatory phase to the resolution phase. Not only the phagocytosis of apoptotic cells, but especially the surrounding cytokines and mediators are able to switch macrophage polarization from inflammatory- to anti-inflammatory phenotypes. Within this cytokine environment, sphingosine-1-phosphate (S1P) plays an important role for immune cell activation, polarization and migration.

In the first part of my studies, I investigated the role of apoptotic cells (AC) and apoptotic cell supernatants (ACM) on the expression of S1P receptors (S1PR) on human and mouse macrophages. I could demonstrate that the stimulation of primary macrophages with AC or ACM significantly induces the expression of S1PR1. Considering that ACM is able to provoke alternative-like macrophage activation, I analyzed the S1PR1-inducing effect of mediators for classical- (IFNγ, LPS, GM-CSF) and alternative macrophage activation (IL-4, M-CSF, LXR-agonism, PPARγ-agonism). The enhanced expression of S1PR1 was achieved by stimulation with M-CSF, LXR-agonists and IL-4, but not with GM-CSF, PPARγ, IFNγ or LPS-stimulation. S1PR1 induction therefore seems to be a common, but not a general event during alternative macrophage activation. Although I could not identify the responsible factor within ACM, I could prove by ACM ultracentrifugation that soluble and particle fractions together are required for the observed S1PR1 induction. Furthermore, I could demonstrate that ACM-stimulation facilitates random and directed macrophage migration towards S1P *in vitro*. To substantiate my *in vitro* findings and prove a physiological relevance on macrophage migration *in vivo*, I followed up the S1PR1-mediated effects in a zymosan A-induced, self-resolving peritonitis mouse model. During the resolution phase, infiltrated macrophages commonly emigrate from the tissue to restore tissue homeostasis. However, the quantification of peritoneal resident macrophages revealed a significant elevation of macrophage numbers after the resolution phase in macrophage-S1PR1 deficient (S1PR1 KO) mice. Even though S1P can affect immune cell polarization, proliferation and survival, I could prove that exclusively emigration from the post-inflammatory peritoneum is affected in S1PR1 KO macrophages.

The second part of my studies concerned the role of sphingosine kinases (SphK) in tissue and hematopoietic cells as well as macrophage-S1PR1 in inflammation-induced (3-methylcholanthrene, 3-MCA) and oncogene-driven (polyoma middle T, PyMT) cancer in mice. In line with earlier findings, cancer growth was reduced by depletion of cancer cell SphK1 or SphK2 in 3-MCA mice, probably due to reduced S1P-dependent growth signaling and immune cell polarization. Interestingly, the effect of macrophage-S1PR1 knockout was less explicit as recent findings of self-amplifying S1PR1-STAT3-IL-6 signaling loops suggested. Although breast cancer growth was significantly slowed, the inflammation-induced cancer showed rather an accelerated growth, which might depend on the cancer type. Besides this effect on tumor growth, I discovered a pronounced reduction of lymphangiogenesis in the primary tumor of both cancer models. Furthermore, macrophage-S1PR1 KO PyMT mice exhibited an almost complete absence of lung metastasis, which occurs *via* the lymphatics. Transcriptome analysis of FACS-isolated tumor-associated macrophages by mRNA array revealed a strongly reduced expression of the inflammasome component NLRP3 in S1PR1 KO macrophages. This intracellular receptor/adaptor protein is an indispensable element for inflammatory reactions and the secretion of inflammatory mediators such as IL-1β or IL-18. The secretion of IL-1β was recently found to selectively induce lymphangiogenesis in mice. As I could confirm reduced IL-1β secretion after macrophage stimulation with LPS and simultaneous S1PR1 inhibition *in vitro*, this signaling pathway constitutes a promising target for further research in the field of TAM-induced lymphangiogenesis and lymph vessel-dependent metastasis.

In summary, I provided evidence for an induction of S1PR1 during alternative-like activation of macrophages with apoptotic cells or other alternative activating cytokines. This regulation strongly enhances macrophage migration towards S1P and contributes to the emigration of macrophages from the peritoneum into blood and lymph.

The finding of macrophage-S1PR1 involvement in cancer-induced lymphangiogenesis and metastasis adds a new aspect to the understanding of cancer development and metastasis formation. S1PR1 and TLR-induced inflammatory signaling crosstalk is presumably able to induce lymph vessel growth within the tumor and fosters secondary effects such as distant organ metastasis.

2 Kurzbeschreibung

Das Immunsystem mehrzelliger Organismen erfüllt eine Vielzahl verschiedener Funktionen, zu denen nicht nur die Abwehr von pathogenen Bakterien und Viren gehört, sondern auch Prozesse wie Wundheilung, Toleranzentwicklung und das Aufrechterhalten der Homöostase. Störungen in Funktion oder Regelkreisen des Immunsystems sind oftmals der Grund von Krankheiten oder Organstörungen wie sie sich bei Autoimmunerkrankungen, Demenz, Morbus Parkinson oder Krebserkrankungen beobachten lassen.

Eindringende Pathogene und durch Gewebeschädigungen freigesetzte Alarmmoleküle, führen zur Aktivierung gewebeständiger Immunzellen. Pathogen assoziierte molekulare Muster (PAMPs) oder mit Gefahr assoziierte molekulare Muster (DAMPs) werden durch hochspezifische Mustererkennungsrezeptoren (*pattern recognition receptor*, PRR) erkannt und induzieren die Sekretion von Entzündungsmediatoren wie IL-1β oder TNFα. Die Sekretion dieser hochpotenten Zytokine bewirkt nicht nur, dass Gewebezellen ein Selbstschutzprogramm aktivieren, sie fördert zudem das Einwandern von Immunzellen wie polymorphnukleärer Granulozyten (PMN) in das Entzündungsgebiet. Diese schnell einwandernden Immunzellen nehmen eingedrungene Pathogene auf und geben ihrerseits Botenstoffe ab, die zum Einwandern von Monozyten führen. Direkt nach der Infiltration in das entzündete Gewebe differenzieren Monozyten zu entzündlichen Makrophagen des Subtyps „M1“ und forcieren das Entzündungsgeschehen durch Freisetzung weiterer Entzündungsmediatoren. Im Verlauf der akuten Entzündung sterben die zuerst eingewanderten neutrophilen Granulozyten durch Apoptose und werden von Makrophagen mittels Phagozytose aus dem Gewebe entfernt. Dieser Prozess inaktiviert in den Makrophagen das Entzündungsprogramm und führt durch einen sogenannten Phänotypenwechsel zum alternativ-aktivierten „M2-ähnlichen“ Phänotyp. In diesem Zustand verändert sich das Genexpressionsprofil der Makrophagen und es werden zunehmend anti-entzündliche Botenstoffe wie TGF-β und Wachstumsfaktoren wie VEGF sekretiert. Diese verhindern einerseits das Einwandern weiterer Immunzellen und fördern andererseits die Regeneration des geschädigten Gewebes.

In meiner Arbeit konnte ich beweisen, dass es durch die Stimulation mit dem Überstand apoptotischer Zellen (ACM) oder den apoptotischen Zellen (AC)

selbst, zu einer Expressionssteigerung des Sphingosin-1-Phosphat Rezeptors 1 (S1PR1) kommt. Dieser Mechanismus war zudem nicht nur durch AC oder ACM induzierbar, vielmehr konnten unterschiedliche M2-polarisierende Mediatoren die Expression von S1PR1 in vergleichbarem Maße steigern. Zwar konnte ich den oder die S1PR1 induzierenden Faktor im ACM nicht identifizieren, jedoch zeigte sich durch Ultrazentrifugation, dass partikuläre und lösliche Bestandteile zusammen zur Induktion des S1PR1 benötigt werden.

Sphingosin-1-Phosphat (S1P) ist ein ubiquitär produziertes und sezerniertes Produkt des Membranlipidstoffwechsels, der von allen Zellen betrieben wird. Der Abbau von Membranlipiden, beispielsweise Sphingomyelin, führt über mehrere Hydrolyseschritte zur Freisetzung von Sphingosin, das durch die Sphingosinkinasen 1 und 2 (SphK1/2) zu S1P phosphoryliert werden kann. S1P ist in der Lage verschiedenste biologische Effekte auszulösen, zu verstärken oder abzumildern, je nachdem in welcher Menge und an welchem Ort es vorliegt. Intrazelluläres S1P besitzt, unter anderem, eine entzündungsfördernde Wirkung, da es nach TNFα Rezeptor vermittelter SphK1 Aktivierung den Transkriptionsfaktor NF-κB aktiviert. Größere Mengen von intrazellulärem S1P, wie sie auch nach Wachstumsfaktor-Rezeptor Aktivierung vorkommen, können durch membranständige Lipidtransporter wie ABC oder SPNS2 in den Extrazellularraum transportiert werden. Dieser so genannte von-innen-nach außen (*inside-out*) Signalweg stimuliert alle umliegenden Zellen durch ihre S1P Rezeptoren (S1PR). Alle 5 hochspezifischen S1PR können über ihre G-Protein Kopplung verschiedene Effekte wie Apoptoseresistenz, Proliferation oder Zellmigration beeinflussen oder auslösen.

Bereits seit mehreren Jahren ist bekannt, dass dendritische Zellen (DC) während der Entzündungsreaktion einen Phänotypenwechsel durchlaufen der letztendlich zum Auswandern aus dem Gewebe führt. Mit Hilfe spezifischer Migrationsexperimente konnte ich beweisen, dass die erhöhte Expression von S1PR1 auf Makrophagen *in vitro* zu einem vergleichbaren Effekt führt. Durch die vermehrte Stimulation des S1PR1 kam es zu einer erhöhten basalen Bewegungsrate und darüber hinaus zu einer gerichteten Bewegung der alternativ-polarisierten Makrophagen entlang eines S1P Gradienten.

Um eine physiologische Relevanz zu ermitteln, verwendete ich einen Mausstamm mit spezifischem Makrophagen-S1PR1 Knockout in einem Zymosan A induzierten Peritonitis Mausmodell. Durch die Injektion von

fluoreszierendem Zymosan konnte ich die Gesamtzahl der im Gewebe verbliebenen Makrophagen ermitteln, die von Beginn der Entzündung an im Peritoneum verweilten. Wie erwartet, war die Zahl der Makrophagen in den S1PR1 KO Mäusen gegenüber den Wildtypmäusen, 6 Tage nach Injektion von Zymosan A, tatsächlich signifikant erhöht. Mit dem Befund, dass der Makrophagen-S1PR1 KO weder Überleben noch Proliferation beeinflusst, konnte ich belegen, dass die Induktion von S1PR1 während der Entzündungsphase dazu dient, die Makrophagen nach der akuten Entzündung aus dem Gewebe auswandern zu lassen. Die von anderen Arbeitsgruppen postulierten Effekte für S1PR1 auf die Aktivierung von Makrophagen konnte ich in meinem experimentellen System nicht bestätigen. Nach 6 Tagen ergaben sich *in vivo* keine Unterschiede zwischen Wildtyp und S1PR1 KO Makrophagen in mRNA Expression oder in der Sekretion entzündlicher Zytokine.

In den letzten Jahrzehnten wurden vermehrt Hinweise darauf gefunden, dass S1P und seine Rezeptoren eine überaus wichtige Rolle im Krebsgeschehen spielen. Während früher die Meinung vorherrschte, dass ein Tumor nur aus unkontrolliert wachsenden, mutierten Zellen besteht, ist es heutzutage Konsens, dass Immunzellen eine tragende Rolle innerhalb eines Tumors einnehmen. Mutierte Zellen werden für gewöhnlich von Immunzellen erkannt und abgetötet. Sofern nicht alle Tumorzellen eliminiert werden können, kann es zur Entwicklung sogenannter schlafender Tumore kommen. Durch den Selektionsdruck, ausgeübt von Immunzellen, kann es mit der Zeit zur Selektion von Tumorzellen kommen, die sich die positiven Eigenschaften von Immunzellen auf Wundheilung und Zellteilung zu Nutze machen. Durch die Stimulation von Immunzellen, insbesondere Makrophagen, mit Entzündungsmediatoren oder Signalmolekülen wie S1P, kann es zur Aktivierung sogenannter Signaltransduktionsaktivatoren (STAT) kommen, die im Gegenzug eine dauerhafte, chronische Entzündung auslösen können. Die Sekretion von Zytokinen wie Interleukin 6 (IL-6) kann durch die Stimulation mit TNFα oder S1P verstärkt werden. IL-6 wiederum ist dazu in der Lage S1PR1 zu induzieren, was somit zu einer sich-selbst-verstärkenden Signalschleife führt. Das Zusammenspiel aus Tumorzellen und Immunzellen ist demzufolge in der Lage über den Aufbau einer chronisch entzündlichen Umgebung das Wachstum des Tumors so wie von Blut- und Lymphgefäßen zu fördern. Um den Einfluss der SphK1 und 2 und des Makrophagen-S1PR1 auf die

Tumorentstehung und -entwicklung zu ermitteln, nutzte ich 2 unterschiedliche Tumor-Mausmodelle: ein chronisch entzündliches Tumormodell, durch die Injektion von 3-Methylcholanthren (3-MCA) und ein endogenes Brustkrebsmodell (PyMT), in dem die Expression eines Onkogens zur Krebsentwicklung führt. Um einen möglichen Kompensationseffekt in Keimbahn-Knockout-Mäusen zu vermindern, schuf ich Knochenmarks-chimäre Mäuse durch den Transfer von SphK1KO oder SphK2KO Knochenmark in Wildtypmäuse und Wildtyp-Knochenmark (Wt) in die entsprechenden Knockoutmäuse. Durch diesen Transfer ließ sich im 3-MCA Modell der Einfluss der SphKs im Gewebe gegenüber dem Einfluss im hämatopoietischen System ermitteln. Wie durch frühere Studien bereits angedeutet wurde, bewirkte der Verlust der SphK1 im Tumorgewebe (SphK1KO-Wt) von 3-MCA Mäusen ein verringertes Tumorwachstum. Überraschenderweise war die Masse an gewachsenem Tumor in SphK1KO Mäusen, gegenüber den Wildtyp Kontrolltieren, gesteigert. Daraus schlussfolgerte ich, dass die SphK1 mehrere Rollen in einer Krebserkrankung einnehmen kann: einerseits kann sie durch das Fördern der Tumorzellproliferation und dem Aufbau einer entzündlichen Umgebung zum Tumorwachstum beitragen, andererseits scheint sie ebenso an der notwendigen Entzündung zum Abstoßen des Tumors beteiligt zu sein. Überraschenderweise kam es bei den SphK1KO Brustkrebsmäusen zu keiner Veränderung des Tumorwachstums. Die Anzahl der gebildeten Metastasen im PyMT Modell hingegen war deutlich erhöht. Wodurch dies vermittelt wurde konnte ich in meinen Analysen nicht klären, jedoch liegt der Schluss nahe, dass dies ebenfalls durch eine verminderte Abstoßungsreaktion durch die SphK1 defizienten Immunzellen bedingt sein könnte.

Bei den SphK2 Mäusen und ihren Chimären waren nahezu keine Effekte zu beobachten. Einzig der Verlust der SphK2 in Tumorzellen (SphK2KO-Wt) führte zu einem signifikant verzögerten Auswachsen des Tumors. Dies kann durch eine verminderte Fähigkeit in der Immunzellpolarisierung, durch extrazelluläre SphK2 und somit vermindertes extrazelluläres S1P, erklärt werden. Ein solcher Effekt konnte vor kurzem durch unsere Gruppe in einem Maus-Xenograft-Modell belegt werden. Diesen Effekt des verzögerten Wachstums konnte ich im PyMT Modell jedoch nicht beobachten. Anders als im SphK1KO-PyMT Modell kam es nicht zu einer vermehrten Lungenmetastasenbildung. Dieser Befund könnte bedeuten, dass der Verlust der SphK2 in den Brustkrebszellen, wie auch

im 3-MCA Modell, durch den Verlust der SphK2 in den Immunzellen aufgehoben wird, und somit nicht zum Tragen kommt.

Am bemerkenswertesten waren jedoch die Befunde aus den Mausmodellen der Makrophagen-S1PR1 KO Mäuse. Den Ergebnissen der letzten Jahre zu Folge, sollte es gerade im entzündungsvermittelten (3-MCA) Tumorgeschehen zu einer deutlich reduzierten Tumorbildung kommen. Allerdings entwickelten beide Mauslinien gleich viele Tumore, die in den Makrophagen-S1PR1 KO Mäusen sogar schneller wuchsen als im Wildtyp. Diesen nicht erklärbaren Befund versuchte ich im Brustkrebsmodell zu reproduzieren. Allerdings zeigten die PyMT S1PR1 KO Mäuse eine überdeutliche Verlangsamung des Tumorwachstums. Interessanterweise ging diese Verzögerung einher mit einem nahezu vollständigen Ausbleiben von Lungenmetastasen im S1PR1 KO Genotyp. Anschließende immunhistochemische Analysen zeigten, dass sich in beiden Tumormodellen, ungeachtet der Tumorentwicklung, deutlich weniger Lymphgefäße im primären Tumor bilden konnten. Die Dichte des Lymphsystems wurde bereits in mehreren Studien als ein bedeutender Faktor zur Metastasierung identifiziert. Da S1PR1 auf Makrophagen bislang noch nicht mit Lymphangiogenese in Verbindung gebracht wurde, entschied ich mich zur Analyse des Transkriptoms der Tumor assoziierten Makrophagen mittels FACS Zellsortierung und anschließendem mRNA array. Die Auswertung des arrays ergab, dass S1PR1 KO-Makrophagen deutlich weniger NLRP3 exprimieren und folglich nicht in der Lage sind effizient IL-1β zu produzieren. IL-1β erwies sich in früheren Studien als dazu in der Lage, gezielt Lymphangiogenese zu fördern. In ersten *in vitro* Experimenten konnte ich bestätigen, dass die Hemmung des S1PR1 nach Stimulation mit LPS *in vitro* zu deutlich verminderter IL-1β Freisetzungen aus Makrophagen führt. S1P scheint somit über S1PR1 die Sekretion von Entzündungsmediatoren zu verstärken. Weitere Experimente werden klären wie genau Entzündungs-Signalwege und S1PR1 zusammenwirken, um Lymphangiogenese zu ermöglichen bzw. zu fördern.

Anhand dieser Erkenntnisse erscheint die Inhibition von S1PR1 als ein neuer möglicher Weg um Lymphangiogenese und Metastasierung bei Krebserkrankungen zu beeinflussen und somit sekundäre Effekte zu reduzieren, wenn nicht sogar zu verhindern.

3 Introduction

3.1 Sphingolipids

The lipid class of sphingolipids was first characterized in 1884 in ethanolic brain extracts by the founder of brain biochemistry, Ludwig Thudichum. These extracts contained, besides already identified compounds, one class of lipids that shared structural similarities, although they possessed a high degree of structural diversity. Because of their variety and their versatile, sometimes contradictory roles on cellular functions, they were named “sphingolipids” after the enigmatic, riddle asking “sphinx” [1].

Throughout the following centuries, many researchers focused on the functions and involvements of sphingolipids and their metabolites in physiology and pathophysiology. Although many mysteries could be unraveled, sphingolipids live up to their name and provide sufficient questions for today’s research and future generations of researchers.

3.1.1 Sphingolipid structure and metabolism

All sphingolipids share, as the name indicates, one structural similarity. Just like phospholipids that share glycerol as their esterified backbone, all sphingolipids contain the aliphatic aminoalcohol sphingosine (Sph) (Figure 1) as their central element.

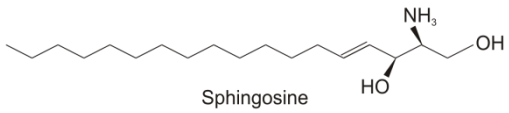

Figure 1. (2S,3R)-2-aminooctadec-4-ene-1.3-diol, Sphingosine

The condensation with fatty acids allows an almost infinite number of different sphingolipids, of which more than 300 different combinations have been identified in various mammalian cells [2]. These sphingolipids are predominantly localized in the so called “lipid rafts” within the plasma membrane and related membranes, where they contribute to membrane fluidity and integrity. Several glycosphingolipids have furthermore been identified to be involved in processes such as cell recognition or specific cell-cell interactions, processes that especially require glycosylation [3, 4].

Similar to phospholipids, the metabolic breakdown of membrane sphingolipids releases molecules that are able to influence intracellular targets directly or

indirectly. In a first step, sphingolipids, such as sphingomyelin or complex glycosphingolipids, are hydrolyzed to ceramide by sphingomyelinases (SMase). Ceramides can then be further degraded and used for the release of sphingosine (Sph) by ceramidases (CER) (Figure 2). Alternatively, ceramides can get phosphorylated by ceramide kinase to independent signaling molecules or used by sphingomyelin synthases (SGMS) for the re-synthesis of membrane lipids [1]. However, free ceramide has shown to be involved in several signaling pathways, such as regulation of cell proliferation and survival. A direct ceramide binding to phospholipase C (PKC) [5] or induction of cathepsin D-dependent lysis [6] is able to restrict cell growth and to induce apoptosis. Free sphingosine, released during ceramide degradation, possesses primarily pro-apoptotic properties by activating caspases, such as caspase-3 [7]. The simple phosphorylation, however, converts the pro-apoptotic sphingosine into the pro-survival mediator sphingosine-1-phosphate (S1P) and counteracts sphingosine effects. Since the discovery of these opposing consequences for cell development in the late 1990's [8], many researchers proposed the balance of Sph and S1P as an essential rheostat for cell death or survival [9].

3.1.2 Sphingosine kinases

Although the release of minor S1P amounts from hydrolysis of sphingosylphosphorylcholine by autotaxin (ATX) was identified *in vitro* [10], it is by now clear that S1P is predominantly formed by sphingosine kinases (SphK) from free sphingosine. The structure of SphKs is evolutionary highly conserved and almost all organisms express one or two SphK isoenzymes, which mostly differ in their N-terminal region. These structural differences most likely account for the altered affinities to the substrate and their distribution within the cell.

All human tissues ubiquitously express 2 SphK isoenzymes and several isoforms of those, which catalyze the ATP-dependent phosphorylation of sphingosine to S1P, after activation by upstream kinases. Inflammatory mediators, such as IL-1β [11] or TNFα [12], growth factors such as EGF [13], VEGF [14] or PDGF [15] and even S1P itself [16] are able to trigger SphK1 activation by activating extracellular signal-regulated kinases 1/2 (ERK1/2) and the subsequent phosphorylation of SphK1-Ser225. Not only is the activation of SphK1-induced by phosphorylation, but especially its localization within the cell. It was shown that SphK1 activation increases its affinity to phosphatidylserine,

which is predominantly located within the lipid rafts of the inner leaflet of the plasma membrane [17]. This translocation brings SphK1 into close proximity to SMase and CER that provide the substrate for SphK1 and allow rapid and efficient S1P production. The temporary activation of SphK1, however, is promptly reversed by protein phosphatase A2 (PPA2)-dependent Ser225 dephosphorylation [18] and mediates SphK1 detachment from the plasma membrane.

Contrary to SphK1, it is not yet clear which and how cytokines exactly induce the activation of SphK2. Although inflammatory cytokines (e.g. TNFα) or growth factors (e.g. VEGF) induce Sphk2 activity in a similar, ERK1/2-dependent manner [19], it is not completely explored if phosphorylation is required, and if yes, which serine/tyrosine residues have to be modified for SphK2 activity. Other than SphK1, SphK2 is not only expressed in the cytosol, but can be found in almost all cell compartments. SphK2 holds a nuclear localization sequence (NLS) that mediates its import into the nucleus [20], where it can bind to HDAC1 and 2 containing co-repressor complexes and inhibit Histone H3 acetylation by production of S1P [21] (Figure 2). This effect on transcriptional regulation might be one explanation for the observed inhibitory effects on cell proliferation and induction of apoptosis [22]. However, other research groups identified the relevance of SphK2 expression in heart mitochondria for cardioprotection [23] and its localization to the plasma membrane, which depends on its lipid binding domain in the N-terminus [24]. Furthermore, it was shown that apoptotic cells secrete a truncated but active form of SphK2 that contributes to the elevated amounts of S1P in apoptotic tissues [20]. This extracellular S1P production was shown to influence all surrounding cells and contributes to anti-inflammatory immune cell activation [20, 25]. The observed enrichment of SphK2 in the endoplasmatic reticulum, after serum deprivation, might therefore be an indicator for an increase in SphK2 secretion [26].

To identify the relevance of SphKs in living organisms, many experiments were carried out with the use of SphK1 and SphK2 knockout mice. Although SphK1 was considered to be the more important isoform, its deficiency did not affect the development or homeostasis of mice. Even the “triple zero” genotype ($SphK1^{-/-}SphK2^{-/+}$) did not result in a particular phenotype, although it revealed significantly reduced amounts of blood circulating S1P [27]. However, the

double deficiency of SphK1 and 2 is embryonically lethal due to severe defects in developmental angiogenesis [28, 29]. Although mice express less variants of both kinase isoforms than human cells [30], their functions reflect almost completely the human SphKs and expanded our knowledge about SphK functions enormously.

Both kinase isoforms have been investigated extensively and it became clear that only SphK1 has a conserved function in all tissues. The expression and localization of SphK2 seems to be cell type and cell activation dependent. Thus, more specific experiments will have to identify the process and outcome of SphK2 activation and its localization.

3.1.3 Sphingosine-1-phosphate

S1P was originally considered to be only a product of membrane lipid metabolism without physiological relevance. In the early 1990's, first evidence were found that S1P is able to directly influence cell proliferation and survival, although its signaling pathways remained elusive [31]. Intracellular targets were initially proposed, but only a few direct targets have been described so far. S1P was identified as a required cofactor of TNF receptor-associated factor 2 (TRAF2) to activate the pro-inflammatory transcription factor NF-κB in the cytosol (Figure 2). Furthermore, it was demonstrated that intranuclear S1P inhibits the histone deacetylases 1/2 (HDAC1/2), decreases histone-DNA-binding and affects gene transcription [32]. Soon it turned out that the localization of sphingosine kinases and the rapid export of S1P out of the cell represents an important "inside-out" signaling modus, especially after the identification of highly specific S1P receptors on the surface of almost all cell types [1].

Even though S1P is produced in all tissues, the concentrations of S1P are highly tissue specific. The highest concentrations, about 1 µM, are found in the bloodstream, where it is largely bound to albumin or HDL [33]. Lower concentrations, about 100-300 nM, are found in the lymphatic system, whereas tissue concentrations of S1P are mostly below the limit of quantification or in the low two-digit range. This imbalance of S1P distribution builds up a gradient, directing S1P responsive cell from tissue into the blood and lymph stream [34].

3.1.4 Export of S1P

A long time it was inexplicable how the amphiphile S1P surmounts the plasma membrane and accumulates at the extracellular space. However, it is well known that specific transporters of the ATP-binding cassette (ABC) transporter family are able to export and import a variety of (polar) lipids. The best studied ABC transporter, ABCA1, which transports cholesterol and phospholipids, was found to be involved in the export of intracellular S1P [35]. Similarly, ABCC1, relevant for transport of glucosylceramide and sphingomyelin [36] and ABCG2 were identified as important transporters for S1P. The latter both have been identified as the crucial transporters for MCF-7 breast cancer cell secreted S1P, as their inhibition was able to abrogate S1P secretion from estradiol stimulated MCF-7 completely [37]. Surprisingly, ABC transporter deficient mice revealed only marginally reduced plasma S1P levels, indicating that other pathways have to be involved in the maintenance of high blood S1P concentrations [38]. The analysis of zebrafish cell membrane proteins yielded another S1P specific transporter from the SPNS/Spinster major facilitator superfamily (MFS). The knockout of SPNS2 in mice reduced plasma S1P levels stronger than ABC knockout, but did likewise not completely diminish blood S1P amounts [39]. Most interestingly, SPNS2 is highest expressed in vascular endothelial cells, where it exports S1P in a passive, ATP independent manner [39, 40]. As it was not possible yet to completely block S1P secretion into the blood, other transporters or transporting machineries have to be involved in S1P export and remain to be identified.

Besides the export of intracellular S1P, two pathways of extracellular S1P production have been described. One group could show that SphK1 holds an export sequence and is actively secreted by endothelial cells into the blood, where it contributes to the high S1P concentration [41]. Our group could show a similar process for SphK2, although this export was triggered exclusively in apoptotic cells following the truncation by caspase-1. This cell death specific, extracellular S1P production was linked to immune cell polarization and tumor promoting effects during carcinogenesis [25] (Figure 2).

3.1.5 S1P degradation

To keep the numerous effects of S1P only temporary and to maintain functional S1P gradients, two independent enzymes continuously inactivate S1P. Most of the inactivation is performed by the S1P lyase (SPL) that is predominantly localized in the endoplasmatic reticulum and cleaves S1P irreversibly into phosphoethanolamine and hexadecanal (Figure 2). Due to its high abundance and activity, intracellular S1P levels are generally kept at a low level. The importance of SPL is best illustrated in blood platelets, which do not express SPL and therefore contain large amounts of S1P [42].

Other than the irreversible degradation of S1P, the sphingosine phosphohydrolase (SPP) simply recycles S1P back to sphingosine. Similar to SPL, the expression of SPP is highest in the ER and contributes to intracellular S1P inactivation. Furthermore, SPP has shown to be critically involved in the regulation of S1P secretion, as its inhibition strongly increased the export of S1P [43].

Due to the intracellular localization of both enzymes, S1P cannot be degraded once it is exported. Only the uptake by adjacent cells can reduce S1P in blood and tissue.

Defective S1P degradation, however, frequently results in severe pathologies, as exemplified in SPP or SPL knockout mice. The deficiency of one or both enzymes causes lymphocyte retention in lymphatic organs, defects in organ homeostasis [44] cancer development, cancer growth [45, 46] and might be an additional factor in autoimmune diseases such as atherosclerosis and diabetes.

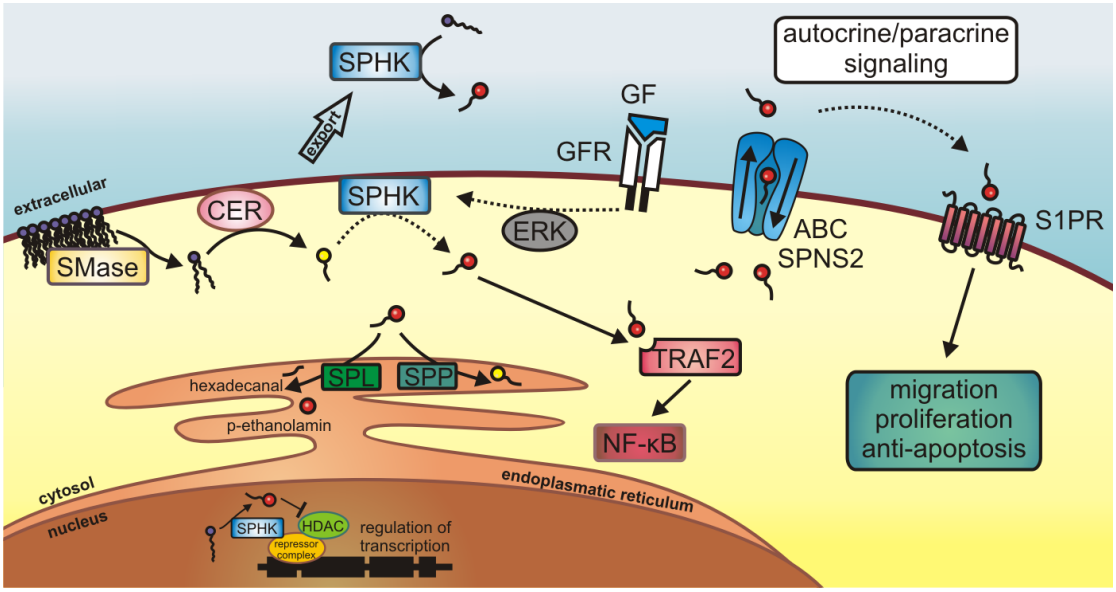

Figure 2. Intra- and extracellular sphingolipid pathways
S1P production starts with the sphingomyelinase (SMase)-mediated hydrolysis of sphingomyelin to ceramide. Ceramidases (CER) convert ceramide into sphingosine which then can be phosphorylated to S1P by sphingosine kinases 1 or 2 (SPHK) after extracellular kinase (ERK)-mediated, growth factor (GF)-induced, SphK activation. S1P inactivation occurs *via* S1P phosphohydrolase (SPP) or S1P lyase (SPL)-mediated dephosphorylation or cleavage to phosphoethanolamine and hexadecanal in the ER. Intracellular S1P activates pathways such as TRAF2-mediated NF-κB activation or is released by ATP binding cassette transporters (ABC) or spinster homologue 2 (SPNS2) to the outside. Extracellular S1P can be produced at the outside by exported SphK1 or 2 and binds in an autocrine or paracrine manner to five individual, highly specific, G-protein coupled, S1P receptors (S1PR). Intranuclear S1P from SphK2 is able to inhibit histone-deacetylases 1/2 (HDAC) and can modulate DNA transcription by increased DNA accessibility.

3.1.6 Sphingosine-1-phosphate receptors

Until today, five S1P specific receptors (S1PR) have been identified, which all belong to the G protein-coupled, seven-transmembrane domain receptor family. Besides their homologies, all S1P receptors differ in their expression at the cell surface, affinity for S1P and their G-Protein coupling within the cell. S1PR1 and 5 have been determined as the S1P receptors with the highest S1P affinity, represented by a K_d in the low nanomolar range (~8 nM S1PR1 / 2-6 nM S1PR5). Opposed by this, the receptors 2 and 3 have a slightly lower affinity with a twofold higher K_d. S1PR4 exhibits the lowest affinity of all identified S1P receptors with a K_d of 12-63 nM and thus, a 2-7 fold lower affinity than

S1PR1/5. If and how these affinities contribute to the functional outcome of S1P signaling remains to be determined.

First attempts with S1PR knockout mice supplied evidence that S1PR1 is the most important S1P receptor during development. Whereas S1PR2,3,4 or 5 knockout mice did not show an obvious phenotype, S1PR1 KO mice die, just as SphK1/2 double-knockout mice, during embryogenesis because of defects in angiogenesis.

Cell specific analyses revealed that S1PR1 and 2 are expressed on almost every cell. Both receptors were identified as critically involved in cell survival, proliferation and directed cell migration, albeit with opposing effects [47]. The activation of S1PR1, and thus G_i signaling, is able to induce JAK2-dependent STAT3 activation [48] that in turn induces pro-survival and proliferation genes, such as MCL-1, BCL-XL and SURVIVIN [49]. Furthermore, S1PR1 induces cell migration along S1P gradients by stimulation of the small GTPase Rac and induces cell motility and mobility (Figure 3). In contrast, S1PR2 commonly inhibits Rac signaling *via* G_q and is able to diminish the pro-migratory input from S1PR1 [50]. This opposing effect is only one of several examples how S1PR are able to influence each other's downstream signaling. Which signaling pathways predominate depends on the balance of S1PR expression, which in turn depends on the cell type and its activation state. However, besides G_q activation, S1PR2 is able to activate G_i and $G_{12/13}$ signaling. This broad spectrum of signaling possibilities makes S1PR2 a versatile receptor whose signaling effects often depend on the G protein expression in the cell.

In contrast to the ubiquitous expression of S1PR1 and 2, the expression of S1PR3 is highest in the cardiovascular system and lower in other organs, such as brain, lung, liver, kidney, pancreas, thymus and the spleen [51]. The signaling pathways of S1PR3 involve G_i, G_q and $G_{12/13}$ and can therefore support all signaling pathways of S1PR1 and 2 (Figure 3). Which pathway prevails, depends on the expressed signaling molecules, which again depends on the cell type and activation state.

S1PR4 can only couple to G_i and $G_{12/13}$ and was found almost exclusively on immune cells, suggesting a role in immune surveillance and maintenance [52]. Despite this, two reports from *in vitro* experiments could demonstrate an involvement of S1PR4 in enhancing the growth of the human breast cancer cell

line MDA-MB-453 *via* interaction with HER2 [53], and migration of CHO cells by stimulating the small GTPase Rac [54]. However, these findings most likely represent mutation-induced S1PR4 expression or aberrantly high receptor expression.

S1PR5 can couple to G_i and $G_{12/13}$ but represents an exception due to its highly restricted expression. Until now, an appreciable expression could only be confirmed for oligodendrocytes in the CNS and for natural killer (NK) cells. A receptor knockout mouse model proved the dispensability for normal organism development but highlighted the importance for correct NK cell homing. One feature of S1PR5 is that it remains active after cell activation, whereas S1PR1 is functionally inactivated by binding to the early activation marker CD69. This interaction is able to prevent S1PR1-dependent T cell migration but not S1PR5-dependent NK cell migration.

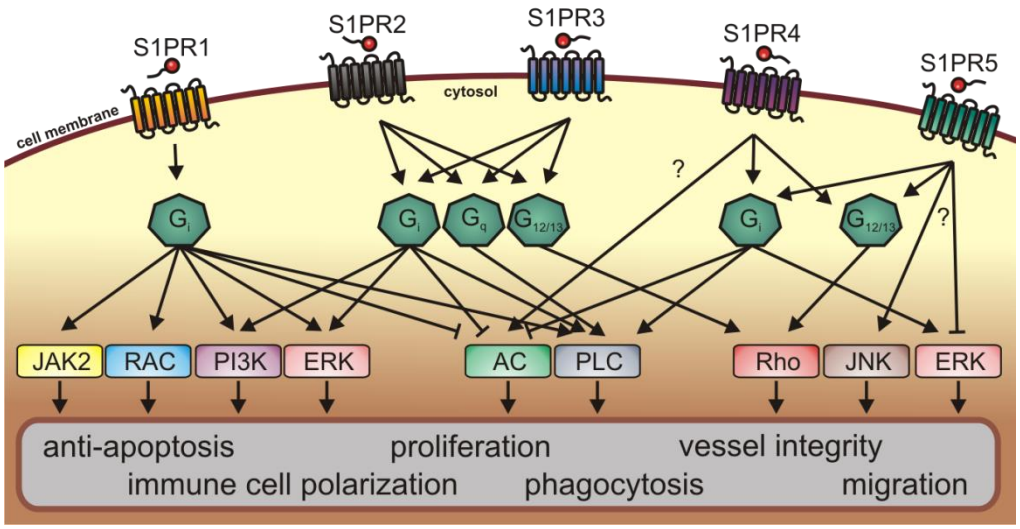

Figure 3. S1P receptor signaling

Tissue or immune cell secreted S1P binds to highly specific, membrane bound, S1PR1-5. Dependent on cell specific G-protein expression, several signaling pathways are activated or inhibited. Except for S1PR1, which exclusively couples to G_i all other receptors are able to activate at least two signaling pathways. G-protein independent effects for S1PR4 and 5 have been postulated, but remain yet undefined. Abbreviations: *Rac* Rho family GTPase, *PI3K* phosphatidylinositol-3 kinase, *ERK* extracellular signal-regulated kinase, *AC* adenylate cyclase, *PLC* phospholipase C, *Rho* Rho GTPase, *JNK* c-Jun N-terminal kinases. Adapted and extended from [1].

3.2 Immune cells, S1P and S1PR signaling

After the first report that S1P modulates T cell trafficking [55], S1P receptors appeared in the focus of immunological research. Shortly after, the S1P-dependent effects on cytokine secretion were discovered [56, 57] and it became apparent that S1P has a considerable impact on the regulation of innate and adaptive immune cells. Throughout the last decade a multitude of effects were discovered that range from initiation and termination of inflammation to the initiation and development of various cancer types.

3.2.1 S1P receptor expression on innate immune cells

Innate immune cells are an excellent example for S1P receptor expression and regulations. The most abundant innate immune cells are monocytes, macrophages, NK cells and granulocytes, whose S1P receptor expressions will be explained in the following passages.

3.2.1.1 Hematopoietic stem and progenitor cells

Hematopoietic stem and progenitor cells (HSPC), the progenitors of all innate and adaptive immune cells, have shown to express all S1P receptor mRNAs except for S1PR5. Although the expression of S1PR1 is lower than on lymphocytes, it is much higher than on innate immune cells. The importance of S1PR1 for HSPC was demonstrated by the finding of a pronounced reduction in blood-circulating HSPC in mice treated with the functional S1PR1 antagonist FTY720. These results indicate the major relevance of HSPC-S1PR1 for circulation and homing, although regulatory effects of S1PRs on cellular processes such as proliferation and differentiation, have not been investigated in depth yet [58].

3.2.1.2 Monocytes

After differentiation from stem- and progenitor-cells, monocytes express the S1P receptors 1, 4 and 5 at a low and S1PR2 at a higher level. However, monocyte attraction is predominantly induced by MCP-1 and other C-C motif chemokines, which is why the inhibition of S1PR1 does not affect monocyte numbers in blood or distribution in tissues [59, 60]. The stimulation of the higher expressed S1PR2 strongly inhibits monocyte migration and the knockout of S1PR2 (in mice) results in a pronounced immigration of monocytes into tumor tissue that give rise to tumor-associated macrophages (TAM) [50]. The outcome

of S1PR4-stimulation is yet unclear and one recent study even doubts its expression on monocytes [61]. The expression of S1PR5 on Ly-6C$^-$ patrolling-monocytes was identified recently and linked to monocyte survival after egress from the bone marrow [62].

3.2.1.3 Macrophages

During the maturation process of monocytes into macrophages, the expression of S1P receptors change and alter the outcome of S1P signaling. Especially the expression of S1PR3 is induced and extends S1P signaling through G_i, G_q and $G_{12/13}$ pathways [59]. The expression and balance of S1PR1, 2 and 3 are dependent on the activation state of the macrophage. The surrounding tissue and cytokine environment can induce S1PR1 expression [63], amplify G_i signaling and induce survival an anti-inflammation [64, 65]. Two independent studies using S1PR2 KO mice could show a reduction of inflammatory cytokine secretion in atherosclerosis, emphasizing the importance of S1PR2 for classical inflammatory macrophages [66, 67]. The expression of S1PR3 is as well induced during alternative-like activation of macrophages, often amplifying S1PR1-G_i-dependent effects. Other than in dendritic cells, S1PR3 seems not be involved in post-inflammatory macrophage migration or regulation of phagocytosis [68, 69]. The effects of S1PR4-stimulation remain yet unclear. As it is expressed on almost all macrophage subsets in various activation states, it might regulate cytokine secretion, as our group could demonstrate recently [70]. Whether these effects are directly mediated by S1PR4 G-Proteins, receptor translocation or because of interfering with other signaling pathways, remains to be determined.

3.2.1.4 Dendritic cells

Although dendritic cells are close relatives to macrophages, their S1PR expression and responses after S1P-stimulation are almost as different as their immunological functions. Dendritic cells are, depending on their maturation state, able to express all 5 S1PRs. Immature DCs (iDC) predominantly express S1PR1 that mediates migration towards S1P, but can be counteracted by S1PR2. During the maturation process, DCs induce the expression of the formerly not expressed S1PR3, which further increases DC migration towards S1P into the lymphatic system. Additionally, S1PR3 activation intensifies

phagocytosis, although the antigen presenting machinery seems not to be affected directly [71]. S1PR4 was identified to be relevant for mature DC (mDC) migration and the induction of T cell responses, resulting in a shift in the Th17/Th2 balance [72] that might influence the termination of inflammation. Although S1PR5 was identified at mRNA level in spleen resident DCs, its functions are not yet specified [73].

3.2.1.5 NK cells

Other than most immune cells, NK cells are restricted to the expression of S1PR4 and 5. Whereas S1PR4 is functionally not assigned, the role of S1PR5 in their biology is well-defined. The deficiency of S1PR5 in mice revealed its importance for proper NK cell emigration from the bone marrow and positioning within organs. The depletion of T-bet, the S1PR5-inducing transcription factor, or direct S1PR5 knockout markedly impaired NK and NKT cell emigration from lymph nodes and the bone marrow [74]. Although S1PR5 signaling resembles that of S1PR1, S1PR5 shows one striking difference; it is insusceptible to CD69-mediated internalization and inactivation. Whereas inflammatory activation of T cells causes the retention in the inflamed area by S1PR1 internalization, S1PR5 remains at the cell surface, maintaining NK cell migration along S1P gradients in inflamed tissues [75].

3.2.1.6 Granulocytes

Inhibition of the S1P-S1PR1 axis is able reduce neutrophil granulocyte-caused hyperalgesia, however, a direct effect *via* S1P receptors on neutrophils seems not to be the case [76]. This reported effect is most likely due to the enhanced vessel permeability and an increase of cell infiltration. Collectively, mast cells seem to be the only receptive granulocytes for extracellular S1P. Besides their high S1PR expression, mast cells are a rich source of S1P after crosslinking of surface IgE and following activation of intracellular SphK1. The rapid export of S1P is able to build up a S1P gradient in the inflamed tissue.

On the receptor side, mast cells express only S1PR1 and 2. Whereas S1PR2 knockout revealed its relevance for mast cell retention and functions such as degranulation, the loss of S1PR1 abrogates mast cell migration along S1P gradients completely [77, 78].

3.2.2 S1P receptor expression on adaptive immune cells

Compared to innate immune cells, adaptive immune cells express only a narrow set of S1PRs. Even though the effects of S1PR1 inhibition are tremendous, the signaling pathways and effects are very limited.

3.2.2.1 T cells

In 2001, Jurkat T cells were the first immune cell type in which S1PR1-induced migration could be identified [55]. After figuring out that the sequestration of T cells to the lymphatic system by FTY720 is mediated by S1PR1 antagonism, the relevance of S1P signaling for immunity was unveiled. Soon the advantages of restricting T cells to lymphoid organs were harnessed, especially for treatment of autoimmune diseases, such as multiple sclerosis [79]. Besides the migratory response, it could be shown that S1PR1 activation inhibits the development of anti-inflammatory Treg cells from $CD4^+$ T cells, instead favoring the development of inflammatory Th1 cells [80]. However, T cells can express S1PR4 as their second S1P receptor. In first attempts S1PR4 overexpression experiments suggested a role for migration of T cells, later experiments proposed its importance for induction of immunosuppression and inhibition of T cell proliferation [52]. However, physiological effects of S1PR4, apart from overexpression, remain elusive. Whether $CD4^+$ or $CD8^+$ T cells or individual subsets, such as Th1 or Th2, regulate their receptor expression individually, remains to be determined.

3.2.2.2 B cells

Depending on the maturation state, B cells express S1PR1, 3 and 4. S1PR1 was identified as crucial for correct shuttling of mature B cells within the spleen, but not for egress back into the blood stream. In contrast, immature B cells egress from the bone marrow after stimulation of S1PR1 and require S1PR3 signaling for proper positioning within the spleen [81]. Similar to most immune cell types, the role of S1PR4 on mature and immature B cells remains elusive.

3.2.3 Anti-inflammatory effects of S1PR signaling

One of the first identified effects that are directly mediated by S1P receptor signaling was the increased barrier function of vascular endothelial cells. Although this S1PR1-mediated effect does not affect inflammatory signaling directly, it reduces edema and secondary inflammatory effects [82]. By using

the S1PR1 agonist KRP-203, a reduced myocardial inflammation could be demonstrated, even though this might as well be due to restraining lymphocytes to the lymphatic system [83]. Albeit the effects of S1P on lymphocytes are mainly restricted to modulation of cell survival and cell migration, a few *in vitro* studies could demonstrate S1P effects on cytokine production and secretion [84]. However, these effects seem to be of minor importance and require further clarification *in vivo*. Finally, the identification of S1P as a mediator for macrophage and DC polarization spurred widespread analysis of immune cell responses after S1PR1-stimulation or inhibition [25, 56, 64, 85].

When iDCs are stimulated with S1P during their maturation process, their ability to induce inflammatory T cell responses is markedly reduced, just as their ability to secrete pro-inflammatory mediators, such as IL-12 or TNFα [56]. Whereas Idzko et al. could not assign these effects to one specific S1PR, Schulze et al. could show that it is mainly dependent on S1PR4 signaling [72]. Similar to iDCs, monocyte S1PR1 or 2-stimulation can reduce inflammatory signaling through inhibition of TLR2-mediated NF-κB and ERK activation [86]. This effect is probably mediated through G_i signaling, when $G_{12/13}$ proteins are not available for S1PR2 signaling. Mature macrophages, however, show opposing effects after S1PR1 or 2 ligation. Signaling through S1PR1 predominantly activates anti-inflammatory effects, such as STAT3-dependent induction of heme-oxygenase 1 and downstream induction of the adenosine A2A receptor (ADORA2A) [63]. Furthermore, it was shown that S1PR1 inhibits NF-κB activation following TLR ligation and the production of TNFα or IL-12 [65]. Contrarily, S1PR2 was related to inflammatory activation, illustrated by two independent studies, demonstrating that S1PR2 KO mice exhibit markedly lower NF-κB activation and inflammatory cytokine secretion [66, 67].

In summary, S1PR signaling effects appear to be highly plastic. The expression of individual S1P receptors, as well as the availability of G proteins varies for every cell type, making it hard to clearly assign S1P signaling to inflammation or immunosuppression.

3.3 Cell death

Cell death is one of the most physiological functions throughout all multicellular organisms to regulate development and homeostasis. Until today, several modes of cell death have been described, which lead to a multitude of different effects within the organism. Besides cell death subtypes such as necroptosis [87] or pyroptosis [88], apoptosis and necrosis are the by far best studied mechanism of cell demise.

3.3.1 Apoptosis

The process of programmed and regulated cell removal was first described in detail in 1972 by Kerr and colleagues. This “counterpart” to mitosis is known to be critically involved in embryonic development and the cell turnover in healthy tissue. After induction of the apoptosis cascade, intrinsically or extrinsically, a tightly regulated cascade is executed, resulting in DNA fragmentation, cell shrinking, the formation of membrane blebs and the release of apoptotic bodies. By exposure of surface markers, so called “eat me” signals, apoptotic cells activate the phagocytosis program of attracted phagocytes.

Extrinsic triggers for the induction of apoptosis bind mostly to surface receptors, so-called death receptors. For example, binding of FasL to its receptor FasR (CD95) induces receptor trimerisation and subsequent adaptor protein binding, leading to the formation of the death-inducing signaling complex (DISC) [89]. The binding of pro-caspase-8 to the death effector domain FADD results in self-activation through autoproteolytic cleavage and the consecutive activation of effector caspases [90]. The extrinsic pathway is the most important instrument for the negative selection of dysfunctional or autoreactive T cells.

Other than the extrinsically-induced pathway, the intrinsic apoptosis cascade represents a response pathway to cell stress, in order to avoid necrosis and inflammation. Deprivation of growth factors, damaging physical stimuli, such as heat or irradiation, or chemotherapeutic compounds that induce DNA damage lead to the release of cytochrome c from the mitochondria into the cytoplasm [91]. This essential part of the respiratory chain represents an intracellular danger associated molecular pattern (DAMP) and triggers the assembly of the apoptosome complex, consisting of apoptotic protease-activating factor-1 (APAF-1) and pro-caspase-9. After autoproteolytic cleavage, caspase-9 is released and activates, similar to caspase-8, the effector caspases 3, 6 or 7,

resulting in protein degradation, DNA fragmentation and morphological changes [90]. Just as cytochrome c, several other proteins can be released from the mitochondria that are able to induce apoptosis. The release of direct IAP-binding protein with low pl (DIABLO) results in the inhibition of IAPs (inhibitor of apoptosis) that under homeostatic conditions consequently inhibit caspase activation. Thus, it is not surprising that overexpression of IAPs is commonly found in cancer tissues [92].

Another family of proteins that is involved in the regulation of apoptosis and survival, is the family of B cell lymphoma 2 (Bcl-2) proteins. It consists of anti-apoptotic proteins (Bcl-2, Bcl-XL, Bcl-W, MCL1, Bcl-B), pro-apoptotic proteins (BAX, BAK, BOK) and a group of regulatory proteins that interfere with anti-apoptotic proteins by binding to their BH3 domain [93].

The activation of pro-apoptotic proteins results in the translocation to mitochondria, the subsequent release of cytochrome c and the initiation of apoptosis. By activation of anti-apoptotic proteins, homodimers of pro- and anti-apoptotic proteins are formed and the activation of effector caspases effectively inhibited. Collectively, the relative expression and localization of apoptosis-regulating proteins determines the fate of the cell.

3.3.2 Primary and secondary necrosis

The unscheduled and rather unorganized cell death type of necrosis is usually induced by external *noxa* such as heat, irradiation, toxins or mechanical overstress. A common feature of all these stimuli is to destroy cell integrity by causing cell membrane rupture and liberation of cytosolic proteins, nuclear proteins, DNA and RNA. Several of these molecules, such as S100 proteins, high-mobility group box 1 (HMGB1), heat shock proteins, RNA, ssDNA and dsDNA serve as extracellular DAMPs for the surrounding cells and induce inflammatory responses after binding to pattern recognition receptors (PRR) (3.4.1) [94].

The same applies if too many cells enter apoptosis at once and outnumber clearing phagocytes. During the process of so called “secondary necrosis”, apoptotic cells or apoptotic cell remnants burst and liberate intracellular molecules that were safely packed during apoptosis [95]. This process often occurs in areas which are poorly supplied with blood, such as hypoxic cancer tissue, or in inflammatory situations with massive apoptosis, such as fulminant hepatitis [96].

3.3.3 Pyroptosis

In the last decade, several studies demonstrated that necrosis-like secretion of intracellular molecules can occur in a regulated manner as well [88]. The immunogenic, programmed cell death “pyroptosis” represents an intermediate between apoptosis and necrosis. Following severe cell damage, such as bacterial toxin uptake, immune cells can assemble their inflammasome (pyroptosome) to activate caspase-1. This activation not only induces inflammatory IL-1β and IL-18 activation, but as well causes membrane pore formation, cell swelling and finally the liberation of intracellular components after cell membrane rupture [88]. Pyroptosis thus represents a tightly regulated and highly inflammatory cell death pathway between apoptosis and necrosis.

3.3.4 Pathophysiological cell death

Many diseases are linked to increased cell death or the absence of correct cell death execution. Defective apoptosis can result in the inefficient depletion of autoreactive T and B cells and cause autoimmune diseases such as multiple sclerosis, rheumatoid arthritis, lupus erythematosus or type I diabetes [97]. Furthermore, the reduced potential of cell apoptosis is one of the major characteristics in carcinomas or lymphomas [98]. On the other hand, cell death beyond the needs can result in degenerative diseases (Arthritis, Parkinson, Alzheimer), immunodeficiency (AIDS) or infertility [99].

However, not only defective apoptosis of cancer or immune cells and their reduction/increase determine pathological conditions. The removal of apoptotic cells is another necessary event to prevent secondary necrosis. Apoptosis and necrosis are both present in tumors or atherosclerotic lesions and are able to induce disease promoting inflammation [100]. Several studies exemplify the correlation between apoptosis, outgrowth of tumors and a poor prognosis for the patient [101-103]. These findings emphasize the complexity of cell death and its influence on tissue development.

3.4 Inflammation

Bacterial, viral or microbial infection and sterile tissue injury are strong inducers of inflammation. The mechanism behind this process was unraveled in 1997, with the identification of the human Toll-like proteins in specific pathogen recognition [104]. However, already in 1994 it was suggested that self and non-self molecular patterns are equally able to induce immunologic self-defense [105].

3.4.1 Pattern recognition receptors

Mammalian cells are well equipped to sense pathogen-associated molecular patterns (PAMPs) and stress-induced DAMPs, for example microbial cell walls components (lipoproteins, peptidoglycans), single or double stranded RNA (ss/dsRNA), DNA fragments (CpG) or endogenous proteins (S100 proteins, HMGB1, HSP). Until today, 4 families of pattern recognition receptors (PRR) have been identified: membrane bound Toll-like receptors (TLR), membrane bound C-type lectin Receptors (CLR), cytosolic NOD-like receptors (NLR) and cytosolic RIG-I-like receptors (RLR). Except for a few NLRs, all PRRs induce pro-inflammatory cytokines, type I interferons (IFNs) and chemokines that contribute to inflammatory responses. These effects are not restricted to professional immune cells but include various non-professional immune cells as well [106].

3.4.1.1 Toll-like receptors

TLR represent the currently best studied family of membrane bound PRRs consisting of 10 human (TLR1-TLR10) and 12 mouse (TLR1-TLR9, TLR11-TLR13) receptors. They are characterized by leucine rich repeats (LRR) at their extracellular N-terminus and a cytoplasmic Toll/IL-1R homology (TIR) domain [107]. Typical ligands for TLRs are components of microbial cell walls and membranes, such as lipoproteins and peptidoglycans (e.g. zymosan A), for TLR1/2/6 [108], double-stranded RNA (dsRNA) for TLR3 [109], lipopolysaccharide (LPS) and flagellin for TLR4 and 5, single-stranded RNA (ssRNA) for TLR 7/8 and unmethylated CpG-DNA for TLR9 [108]. The murine TLR11/12/13 are specialized pathogen receptors that are not expressed in human cells. TLR 11 and 12 are expressed as heterodimers that sense the actin-binding protein profilin secreted by *Toxoplasma gondii [110]*, whereas

TLR12 is specialized to bind bacterial 23S ribosomal RNA [111]. Besides the highly specific ligand binding, the localization of the TLRs differs considerably. Whereas TLR1, 2, 6 and 10 constitutively reside on the cell surface, TLR4 and 5 localize to the plasma membrane whenever it is necessary. The TLR3, 7, 8 and 9 are only expressed in the endosomes where they sense ingested danger molecules [107].

Besides their expression, the signaling cascade differs in their recruitment of adaptor molecules after TLR activation and dimerization. Dependent on the intracellular domain, MyD88, TRIF, TRAM, Mal or SARM can be bound and enable the recruitment of binding partners, such as IRAK, MAPL, NF-κB, AP-1 or IRFs [112]. All TLR signaling pathways have in common to induce pro-inflammatory molecules and cytokines that mediate host defense by inducing acute inflammation. Due to the multitude of binding partners, there are plenty of possibilities where other signaling pathways, e.g. S1PR, can interfere and induce or reduce the outcome of TLR activation.

3.4.1.2 C-type lectin receptors

Similar to the TLR family, CLRs are integral membrane proteins and recognize microbial components. Most ligands for CLRs are carbohydrates, derived from the cell membranes/walls of microorganisms. Dectins on dendritic cells, for example, are able to activate immunoreceptor tyrosine-based activation motif (ITAM) and cause T cell activation against fungi such as *candida albicans* [113]. Just like Dectin on DCs, the mannose receptor (MR) is critically involved in the activation of macrophages [114]. Although CLRs activate other adaptor proteins than TLRs, the signaling outcome, such as NF-κB, AP-1 or NFAT activation can be comparable. However, besides an inflammatory activation, CLRs are equally able to modulate or even inhibit TLR activation and can thus, modulate inflammatory signaling [113].

3.4.1.3 RIG-I like receptors

The RLR family represents a family of PRR that are highly specific for viral pathogens. It consists of 3 members, RIG-I, melanoma differentiation-associated gene 5 (MDA5), and LGP2, which sense genomic RNA and dsRNA. Following their activation, RLRs strongly activate the transcription factors IRF3/7 resulting in a sustained secretion of type-I interferons [115].

3.4.1.4 NOD-like receptors

The family of NOD-like receptors (NLR) consists of at least 22 intracellular proteins, 5 of the NOD subfamily, 14 of the NLRP family, IPAF, NAIP and CIITA. So far best described are the ligands and functions of the NLRP subfamily, in particular, NLRP1 and 3. Both are highest expressed in immune cells, whereas other NLRP subtypes show more tissue specific expression [116]. Especially NLRP and TLR possess an overlapping spectrum of recognized patterns, resulting in a synergistic activation of inflammatory cytokine production. Following the binding of PAMPs or DAMPs (ROS, ATP, insoluble crystals) NLRP3 oligomerizes in an ATP-dependent manner and recruits the adaptor protein ASC by its pyrin domain. ASC in turn recruits inactive pro-caspase-1 through its CARD domain, bringing pro-caspase-1 proteins into close proximity, resulting in autoproteolytic cleavage of caspase-1 (Figure 4). This multi-protein-complex (NLRP-ASC-CASP1) was termed “the inflammasome” because of its ability to activate inflammatory cytokines. Even though other pathways of caspase-1 activation have been described, for example by IPAF activation, the NLRP-ASC-dependent caspase-1 activation has shown to be the most common pathway for caspase-1 activation and cleavage of pro-IL-1β and pro-IL-18 [117].

Although several inflammasome activating mechanisms have been unraveled, the pathways of NLR expression and the distribution of NLRs in various cell types remain more or less rudimentary. Considering the role of chronic and smoldering inflammation in the development and promotion of cancer, it is tempting to assume a role for PRRs in these processes.

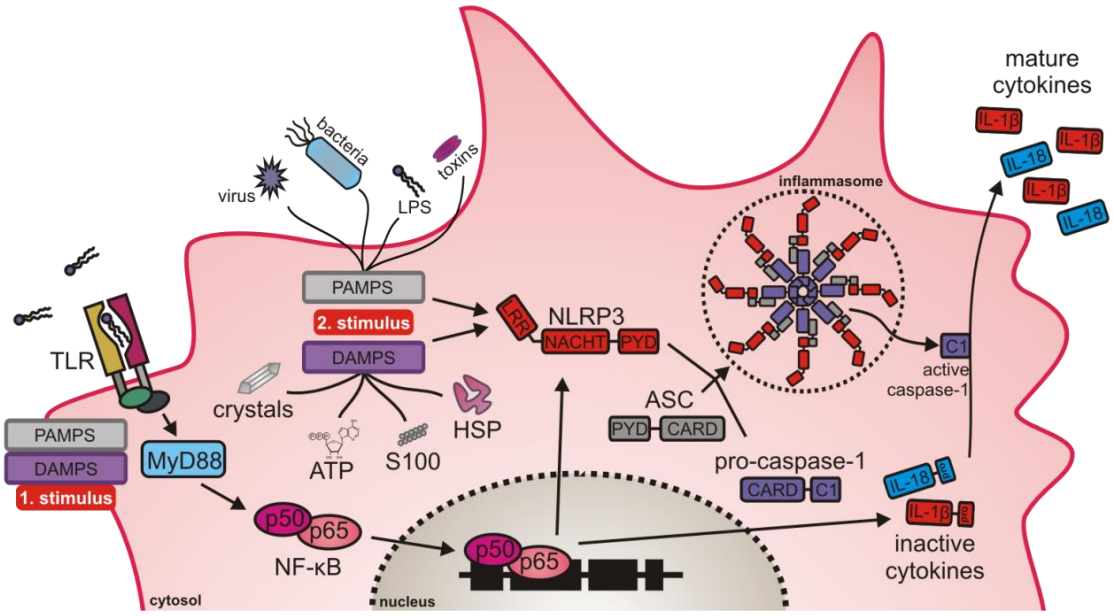

Figure 4. The NLRP3 inflammasome
Inflammasome activation requires two stimuli. First, the activation of receptors, such as TLR, induce NF-κB-mediated NLRP3, pro-IL-1β and pro-IL-18 expression. Second, PAMPs or DAMPs bind to intracellular receptors such as NLRP3 and induce oligomerisation of NLRP3 and ASC *via* its PYR domain. ASC recruits pro-caspase-1 with its CARD domain and brings the pro-caspases into close proximity, resulting in proteolytic cleavage and liberation of active caspase-1 (C1). Caspase-1 then cleaves the pro-forms of IL-1β and IL-18 into their active forms. Their secretion induces paracrine and autocrine inflammatory stimulation of surrounding immune and tissue cells.

3.4.2 The course of inflammation

Tissue damage, infiltration of pathogens or stress-induced liberation of DAMPs are common pathways that trigger acute inflammation. The detection of pattern molecules by tissue-resident sentinel immune cells results in the secretion of inflammatory molecules. These mediators induce the expression of selectins on the vascular endothelium and recruit inflammatory immune cells into the tissue [118, 119]. Rapidly infiltrating polymorphonuclear neutrophils engulf pathogens and danger molecules and secrete a multitude of inflammatory cytokines such as TNFα, IL-1β and PGE_2. This enhanced cytokine secretion attracts further immune cells [120] and accelerates their infiltration by increasing vessel permeability. The TLR-induced maturation of infiltrating iDC under the influence of inflammatory cytokines results in an mDC phenotype that strongly supports inflammation, by secretion of TNFα and IL-12 and the induction of Th1 immune cells [56]. Similarly, attracted monocytes mature

rapidly into classically activated “M1” macrophages, characterized by secretion of IL-1β, TNFα and IL-6, and participate in the acute inflammatory reaction to clear the noxious stimulus. However, the uptake of particles and pathogens by neutrophils and the secretion of TNFα or FAS-Ligand by macrophages are able to induce neutrophil apoptosis and initiate the early resolution phase [121]. During apoptosis, neutrophils secrete several mediators, e.g. Annexin A1 (AnxA1), that mediate neutrophil repellence and phagocyte attraction [121]. By exposing “eat me” signals at the cell surface, apoptotic cells are recognized and engulfed by phagocytes. The uptake of dead cells represents one trigger for macrophages to reduce inflammatory tissue damage and initiate wound healing [122]. This shift from “M1” to alternative-like “M2” activation goes along with an induction of IL-10, VEGF, TGF-β or PGE_2 secretion [123] that suppresses pro-inflammatory signaling of TLRs [124] and actively induces tissue repair [125]. Although it is widely accepted that phagocytosis induces alternative immune cell activation, it is incompletely understood which signaling pathways are involved [123].

In the following resolution phase, macrophages do not only dampen inflammatory signaling, but as well induce the infiltration of T and B cells by secretion of specific chemoattractants (CCL5, CXCL13, XCL1). The maturation of iDCs in this anti-inflammatory cytokine environment induces mDCs with a decreased ability of inflammatory T cell priming, favoring the development of regulatory T and B cells [56]. Furthermore, mDCs exhibit a strong expression of S1PR1 and 3 [59] that directs them along the S1P gradient into the blood or the draining lymphatic system [68, 126].

3.5 Cancer

One of the most accurate definitions of cancer is presumably *“the pathological expansion of a tissue resulting in morbidity”* [127], summarizing the main aspects of cancer.

The inducers of cancer are manifold: physical carcinogens such as UV light, radioactivity or asbestos fibers, chemical carcinogens, such as polycyclic aromatic hydrocarbons, or biological carcinogens, such as viruses, bacteria or parasites. After cell transformation and proliferation, host immune cells recognize mutated cells and exert selective pressure that commonly eliminates the tumor cells. This theory of immune control was originally proposed in 1908

by Paul Ehrlich but could not be verified until the middle of the 20th century, when independent research groups demonstrated the connection of immunodeficiency and increased cancer development [128, 129]. From that time on, the interplay between tumors and host immune system was increasingly characterized as the “immune surveillance of cancer” [130]. During the aforementioned elimination phase, immune cells prevent tumor growth and commonly restore tissue homeostasis. In case that tumor eradication fails and individual tumor cells persist, they can enter the so called equilibrium phase, when as much cells proliferate as cells are killed. This dormant phase can remain for a long time, even a life-time, as often seen in benign thyroid or prostate neoplasm [131]. However, the immune cell exerted selective pressure frequently results in the selection of tumor cells that are able to overcome the immune control or can polarize immune cells into a tumor-promoting phenotype. In that case, tumor cells can escape from the immune surveillance and develop all the characteristics of malignant cancer, such as infiltrative growth or metastasis dissemination [130].

3.5.1 S1P and S1PR in tumor promotion

As mentioned before (3.1.2), SphK1 is involved in several growth factor- and hormone signaling pathways and possesses tumor promoting characteristics. Besides intracellular signaling, S1P strongly affects cell survival, proliferation, migration, angiogenesis and lymphangiogenesis by binding to its receptors on the cell surface (3.5.2). Several mechanisms have been described how S1P can mediate this multiplicity of effects, such as transactivation [9], direct receptor-receptor interactions [53], SphK induction/activation, autocrine signaling loops or the induction of STAT signaling [48]. One hotly debated and probably the most important signaling loop is the recently identified S1P-S1PR1-STAT3-IL-6 feed-forward loop between tumor cells and tumor infiltrating immune cells (Figure 5). Several independent research groups could show that stimulation of S1PR1 induces the activation of the transcription factor STAT3 that in turn induces the production of IL-6, IL-10 and S1PR1 [63]. Whereas IL-6 directly enhances the activation of STAT3 through IL-6R, S1PR1 induction makes the cells more receptive to S1P signaling. However, the presence of inflammatory mediators, especially TNFα, is able to induce the activity of SphK1 and boosts S1P production. This signaling further enhances

S1PR1-mediated STAT3 activation, resulting in increased inflammation and pro-tumorigenic S1P signaling [132] (Figure 5).

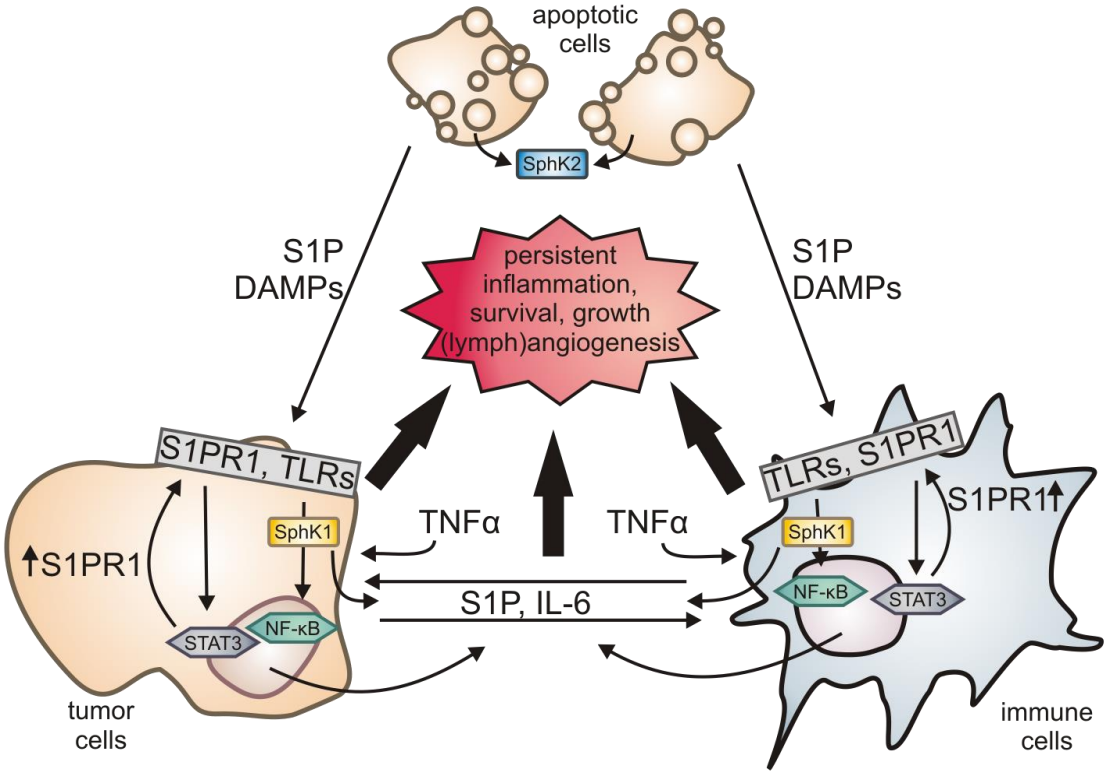

Figure 5. S1P actions in the cancer environment
Apoptotic cell secreted danger associated molecular patterns (DAMPS) such as HMGB or S100 proteins, exported SphK2 and tumor SphK1 derived S1P activate NF-κB *via* Toll-like receptors (TLR) and STAT3 *via* S1PR1. Tumor cells and immune cells thus induce the expression of S1PR1 and secretion of IL-6 through STAT3 and NF-κB. The secreted mediators in turn activate IL-6R, S1PR1 and further induce STAT3 and NF-κB activation in a paracrine and autocrine manner. This interplay is able to induce persistent inflammatory transcription factor activation and cytokine secretion that causes smoldering inflammation, tumor cell and immune cell survival, tumor cell proliferation and incorporation of blood and lymph vessels.

3.5.2 S1P receptors in cancer cells

As cancer cells are malignantly transformed tissue cells, they usually express the same repertoire of S1P receptors as healthy tissue. The expression of S1PR1 is the most common pathway how tumor cells take advantage of S1P and ensure their survival. Surprisingly, both regulations, increase and reduction of S1PR1 have been found in primary tissue samples [31, 133-136]. This clinical evidence once more emphasizes the dependency of S1PR signaling on the affected cell type.

The expression of S1PR2 in cancer cells has mostly been linked to the prevention of cancer formation (lymphoma) [137] and the inhibition of cancer cell migration and metastasis *via* Rac/Rho-stimulation [138]. However, the overexpression of S1PR2 in Wilms' tumor (nephroblastoma) was found to mediate COX-2-induction and strongly elevated PGE_2 levels [139].

The diversity of pathways that can be activated or reduced by activation of S1PR3 makes it a likely target for dysregulations in cancer. However, since S1PR3 is not commonly expressed on epithelial cells, dysregulations are found less frequently and are mostly related to specific cell types. Nevertheless, it was found in several gastric cancer cell lines to stimulate migration and cell survival [140]. The same positive effect on migration, secretion of MMP9 and invasion was identified for breast cancer cells, when the estrogen receptor directly interacts with S1PR3 [136, 141, 142]. However, the most common and most important role of S1PR3 in cancer is certainly the expression on bone marrow derived, tumor infiltrating cells [143, 144].

The even more restricted expression of S1PR4 was so far only identified in human breast cancer cell lines *in vitro.* This expression was found to support cancer cell development, either by preventing inhibitory receptor signaling [145] or by interaction with HER2 and the activation of ERK1/2 [53].

S1PR5 expression was so far only connected to anti-cancer effects by inducing autophagy in PC3 prostate cancer cells [146] and inhibiting migration and proliferation in esophageal cancer cells [147]. Therefore, cancer cells might predominantly benefit from S1PR5 deficiency or inhibition.

3.5.3 Clinical trials on SphK and S1P antagonism

Owing to the role of S1P on cancer cells and the polarization of infiltrating cells, direct targeting of SphK, S1P receptors or the S1P itself sounds promising. Therefore, SphK inhibitors, receptor antagonists or -modulators and even S1P specific antibodies were used extensively in various mouse cancer models [9, 148, 149]. The results from these animal studies appeared so promising that several compounds were tested in humans in clinical trials. Surprisingly, no SphK1 inhibitor was registered at the NIH until today, although several compounds were designated as SphK1 specific [34]. Whether this is due to off-target effects or severe side effects, because of the importance of SphK1, can only be speculated. However, a few drugs that already successfully

entered phase III studies are known to strongly inhibit SphK1 [150], although many other pathways, such as Akt/mTOR inhibition and DNA damage induction, are involved. Collectively, it seems to be more beneficial to interfere upstream and prevent SphK1 activation by blocking tyrosine kinases or growth factor receptors such as EGFR [150, 151].

Other than SphK1 inhibition, the SphK2 inhibitor ABC294640 was used from 2011 on in a Phase-I study to determine its pharmacodynamics and -kinetics in patients with advanced solid tumors. Unfortunately, no further information was provided about the progress of this study (ClinicalTrials.gov, NCT01488513).

Already in 2008, a phase I study on the safety and effect of S1P neutralization in advanced solid tumors, using the humanized S1P-specific antibody sonepcizumab (ASONEP®), was started. Results show that the Phase I trial met its primary endpoint of identifying safe dose levels for further Phase II studies. As the results from the Phase I trial revealed stable disease in the patients, it is encouraging that the same antibody was approved in 2013 for a phase II study to investigate the treatment of unresectable and refractory renal cell carcinoma (NCT01762033).

Surprisingly, no direct S1P receptor antagonist or modulator was or is currently investigated in clinical trials. Not even the promising compound FTY720, which is already approved for multiple sclerosis (Gilenya®). Presumably its immunosuppressive effects impair tumoricidal immune cell functions stronger than the proliferation of cancer cells and would thus assist tumor growth.

3.6 Aims of the studies

Within the last decades it became apparent that immune cells are not only important for protective inflammation, but as well for cancer development and outgrowth. Signaling lipids, such as arachidonic acid derivatives and sphingolipids, came into the focus of inflammation- and cancer research, because of their inflammatory and anti-inflammatory properties. Surprisingly, S1P effects on immune cells appear to be important for both, induction as well as termination of inflammation. In addition, it was found that S1P is able to stimulate survival and proliferation of immune cells, tissue cells and tumor cells. Even though many researchers addressed the question how S1P and S1PR are involved in inflammation and cancer, complex interactions of cells and signaling

pathways have to be considered and require further investigation. Therefore, the first part of my studies concerned the role of S1PR1 expression in the setting of acute inflammation *in vitro* and *in vivo*. The expression of S1PR1 after diverse stimulations of primary macrophages, with apoptotic cells or apoptotic cell supernatants, was analyzed. In the following, I examined the outcome of S1PR1 induction on macrophage responses, such as chemotaxis, chemokinesis and immune cell polarization. To substantiate my *in vitro* findings, I made use of an acute inflammatory mouse model with macrophage-S1PR1 deficient mice to verify the afore-identified S1PR1-dependent effects.

The second part of my studies concerned the role of SphK expression in tissue and immune cells and the effect of macrophage-S1PR1 knockout in carcinogenesis. Therefore, I utilized wildtype mice, SphK1 and 2 KO mice, bone marrow chimeras of wildtype and SphK deficient mice and macrophage-S1PR1 KO mice in an inflammatory fibrosarcoma (MCA) and in a genetic, oncogene-driven, breast cancer model (PyMT). The effects of macrophage-S1PR1 deficiency on macrophage mRNA transcription and intracellular signaling were afterwards analyzed by mRNA array and the obtained data verified and validated *in vitro.*

In summary, I performed my studies to elucidate a part of S1P- and S1PR1-signaling that was so far only poorly described. Especially the role of S1P in carcinogenesis requires further investigations to improve our understanding of cancer and metastasis development, prevention and treatment.

4 Material and Methods

4.1 Material

4.1.1 Cells and cell lines

MCF-7 (human)

MCF-7 human breast adenocarcinoma cells were established in 1970 from pleural effusion of a 69-year-old Caucasian woman with metastatic mammary carcinoma [152].

LLC (mouse)

Lewis lung carcinoma is a cell line established from the lung of a C57BL/6 mouse, bearing a tumor that resulted from implantation of primary Lewis lung carcinoma [153].

E0771 (mouse)

The E0771 medullary breast adenocarcinoma cell line was originally isolated from a spontaneous tumor in a C57BL/6 mouse and adapted for anti-cancer drug testing [154, 155].

Primary human monocytes

Primary human monocytes were isolated from “buffy coats”, obtained from DRK-Blutspendedienst Baden-Württemberg-Hessen.

Primary murine leukocytes

Primary murine leukocytes were isolated from C57BL/6 mice. All procedures performed on these mice followed the guidelines of the Hessian animal care and use committee.

4.1.2 Mouse strains and mouse keeping

All transgenic mice were purchased from Jackson Laboratories, C57Bl/6 wildtypes were obtained from Harlan Laboratories. All used mouse strains were created in C57Bl/6 background or backcrossed for at least 10 generations into C57Bl/6 background. All mice were kept in isolated ventilated cages under sterile and health monitored conditions and followed the guidelines of the Hessian animal care and use committee.

4.1.2.1 mdT/meG double fluorescent reporter mice

Double fluorescent reporter mice were generated by transfection of a double fluorescent vector into (129S6/SvEvTac x C57BL/6NCr) F1-derived G4 embryonic stem cells. The fluorescent construct contains a CMV enhancer/chicken beta-actin core promoter, a loxP-flanked mdT cassette with a STOP codon and a meG cassette, inserted into the Gt(ROSA)26Sor locus. The fluorescent genes were N-terminally modified to achieve cell membrane allocation. Upon expression of the CRE recombinase, the predominant mdTomato gene and its STOP codon are deleted, resulting in expression of the meGFP gene and the switch from PE (mdTomato) fluorescence to FITC (meGFP) fluorescence. Due to the half-life of mdTomato, CRE expressing cells appear double fluorescent for 5-7 days until mdTomato decays [156]. Heterozygous mice were backcrossed with C57Bl/6 mice and inbred for homozygous reporter expression. For analysis of F4/80$^{CRE/+}$ efficiency, mdT/meG mice were crossed into the S1PR1^{plox}-F4/80^{CRE} strain and tissue samples analyzed for cell fluorescence.

4.1.2.2 PyMT mice

PyMT breast cancer mice were originally generated by inserting the polyoma Virus middle T antigen into the expression vector pMMTV-SV40, resulting in a fusion gene of the PyVT oncogene and SV40 poly A and 3' processing signals, driven by the Mouse Mammary Tumor Virus (MMTV) long terminal repeat (LTR). The obtained construct was injected into pronuclei of FVB/N zygotes for recombination [157]. Obtained heterozygous mice were backcrossed into C57Bl/6 background. Female mice show no lactational ability and develop adenocarcinomas from the 5 week of age. Breeding of the transgenic mice was therefore only possible with male heterozygous mice and resulted in heterozygous PyMT^{+} female experiment mice. The PyMT gene was crossed into SphK1KO, SphK2KO, S1PR1^{plox}-F4/80^{CRE} and C57Bl/6 strains for analysis of breast cancer effects.

4.1.2.3 S1PR1^{plox}-F4/80^{CRE} mice

S1PR1 floxed mice were originally generated from modifying 129S6/SvEvTac-derived TC1 embryonic stem cells and backcrossing of heterozygous offspring into C57Bl/6 background. These mice harbor loxP sequences around exon 2 of the S1PR1 gene [158]. F4/80-CRE expressing mice were originally generated by inserting the P1 phage-derived CRE recombinase gene into the F4/80 genomic DNA by homologous recombination in E14.1 C57Bl/6 embryonic stem cells. Heterozygous mice were backcrossed with C57Bl/6 mice [159]. To obtain F4/80 expressing cell specific deletion of S1PR1, I crossed both strains and inbred the offspring to obtain S1PR1$^{plox/plox}$-F4/80$^{CRE/wt}$ knockout and S1PR1$^{wt/wt}$-F4/80$^{CRE/wt}$ corresponding wildtype control mice. During the maturation of F4/80 negative monocytes into F4/80 expressing macrophages, the expression of the CRE recombinase is triggered through the activation of the F4/80 promoter. The subsequent expression of active CRE mediates the deletion of exon 2 from the S1PR1 gene, resulting in disruption of gene and protein function.

4.1.2.4 SphK1KO mice

SphK1 knockout mice were originally generated from modifying 129S6/SvEvTac-derived TC1 embryonic stem cells and backcrossing of heterozygous offspring into C57Bl/6 background. A NEO cassette containing vector was used to replace exons 3-5 and a part of exon 6 disrupting the gene function [160]. SphK1KO mice were bred homozygous transgenic (knockout) and compared with C57Bl/6 wildtype or UbiC$^{GFP/+}$ mice.

4.1.2.5 SphK2KO mice

SphK2 knockout mice were originally generated from modifying 129S6/SvEvTac-derived TC1 embryonic stem cells and backcrossing of heterozygous offspring into C57Bl/6 background. A NEO cassette containing vector was used to replace exons 4 and exons 5-7 disrupting the gene function [29]. SphK2KO mice were bred homozygous transgenic (knockout) and compared with C57Bl/6 wildtype or UbiC$^{GFP/+}$ mice.

4.1.2.6 UbiC$^{GFP/+}$ mice

The UbiC-GFP were generated by microinjection of a construct, containing the enhanced Green Fluorescent Protein (GFP) und the control of the human ubiquitin C promoter, into fertilized C57Bl/6 oocytes. The expression of the

construct was found in all examined tissues, but found highest in hematopoietic cells. Because of this expression pattern, these mice represent an excellent tool to track leucocytes *in vivo* [161]. Heterozygous mice were bred with C57Bl/6 wildtype mice and phenotyped by illumination with UV light and visible detection of green fluorescence.

4.1.3 Agonists and antagonists

Table 1. Agonists, antagonists, solvents

Substance	Target	Supplier
3-methylcholanthrene	PAH carcinogen	Sigma-Aldrich GmbH (Steinheim)
$Al(OH)_3$	Insoluble crystals	Carl Roth GmbH&Co. KG (Karlsruhe)
Corn Oil	3-MCA carrier	Sigma-Aldrich GmbH (Steinheim
Cycloheximide	Protein synthesis inhibitor	Carl Roth GmbH&Co. KG (Karlsruhe)
DMSO	Carrier for most lipids	Carl Roth GmbH&Co. KG (Karlsruhe)
FTY720 phosphate	S1PR1,3-5 super-agonist	Sigma-Aldrich GmbH (Steinheim)
Genistein	Tyrosine kinase inhibitor	Carl Roth GmbH&Co. KG (Karlsruhe)
GM-CSF	CSF2RA agonist	Peprotech (Hamburg)
IFNγ	IFNγ receptor agonist	Roche (Mannheim)
IL-4	IL-4R agonist	Peprotech (Hamburg)
LPS	TLR4 agonist	InvivoGen (San Diego, USA)
M-CSF	CSF1R agonist	Peprotech (Hamburg)
PD98059	MEK inhibitor	Cell Signaling (Danvers, USA)
Poly(I:C)	TLR3 agonist	InvivoGen (San Diego, USA)
Rosiglitazone	PPARγ agonist	Sigma-Aldrich GmbH (Steinheim)
S1P	S1PR1-5 ligand	Biomol GmbH (Hamburg)
Staurosporine (Sts)	Protein kinase Inhibitor	Sigma-Aldrich GmbH (Steinheim)
TNFα	TNFR ligand	Peprotech (Hamburg)
VPC23019	S1PR2/4 antagonist	Avanti Polar Lipids (Alabaster, USA)
W146	S1PR1 antagonist	Sigma-Aldrich GmbH (Steinheim)
T0901317	LXR Agonist	Sigma-Aldrich GmbH (Steinheim)
Tramal® solution	Analgesic	Grünenthal (Aachen)
Zymosan A	TLR2 agonist	Sigma-Aldrich GmbH (Steinheim)
Zymosan A AF488	TLR2 agonist, fluorescent	Invitrogen (Karlsruhe)

4.1.4 Chemicals

Chemicals for animal and laboratory use were purchased in highest grade of purity as commercially available. Common suppliers were Carl Roth GmbH&Co. KG, Merck KGaA, or Sigma-Aldrich GmbH. Cell culture media and media additives were commonly obtained from PAA (Cölbe, Germany). Other reagents, kits and material are listed below (Table 2).

Table 2. Reagents and Kits

Substance	Supplier
Absolute™ qPCR SYBR® Green Fluorescein Mix	Fisher Scientific GmbH (Schwerte)
Accutase	PAA Laboratories GmbH (Cölbe)
Agarose	peqLab Biotechnologie GmbH (Erlangen)
Agilent Small RNA kit	Agilent Technologies (Santa Clara, USA)
Aquatex mounting medium	Merck KGaA (Darmstadt)
Annexin-V (fluorescently labeled)	ImmunoTools GmbH (Friesoythe)
Flow Cytometry Absolute Count Standard	Bangs Laboratories, Inc. (Fishers, USA)
Human serum (AB positive), heat inactivated	DRK-Blutspendedienst Baden-Württemberg-Hessen (Frankfurt)
Human IL-1β Flex Set	BD Biosciences GmbH (Heidelberg)
KAPA Mouse Genotyping Kit	KAPA Biosystems (Wilmington, USA)
JetPEI™ transfection reagent	Biomol GmbH (Hamburg)
Lymphocyte separation medium (Ficoll)	PAA Laboratories GmbH (Cölbe)
Maxima® First Strand cDNA Synthesis Kit	Fermentas GmbH (St. Leon-Rot)
Meyers haemalum	Merck KGaA (Darmstadt)
Mouse IL-1β Flex Set	BD Biosciences GmbH (Heidelberg)
Mouse Inflammation Kit (CBA)	BD Biosciences GmbH (Heidelberg)
Mouse Soluble Protein Master Buffer Kit	BD Biosciences GmbH (Heidelberg)
Mouse Tumor Dissociation Kit	Miltenyi Biotec GmbH (Bergisch Gladbach)
peqGOLD RNAPure™	PeqLab Biotechnologie GmbH (Erlangen)
QIAGEN SensiScript RT	Qiagen N.V. (Venlo, Netherlands)
Vectashield H-1400 mounting medium	Vector Labs (Burlingame, USA)

4.1.5 Antibodies

Antibodies were used for immunologic staining of cell markers for flow cytometry, immunohistochemistry or Western blot.

Table 3. Antibodies

Antibody against	Provider	Application	Dilution
Actin-purified	Cell Signaling Tech. Inc.(Danvers, USA)	Western blot	1:3000
CD3-PE-CF594 (Clone 145-2C11)	BD Biosciences GmbH (Heidelberg)	FACS	1:100
CD4-V500 (Clone RM4-5)	BD Biosciences GmbH (Heidelberg)	FACS	1:50
CD8-eFluor650NC (Clone 53.67)	eBioscience (Frankfurt)	FACS	1:50
CD11b-eFluor605NC (Clone M1/70)	eBioscience (Frankfurt)	FACS	1:200
CD11c-AlexaFluor700 (Clone HL3)	BD Biosciences GmbH (Heidelberg)	FACS	1:200
CD16/32-purified	Miltenyi Biotec GmbH (Bergisch-	FACS (Blocking)	1:50

(Clone 93)	Gladbach)		
CD19-APC-Cy7 (Clone 1D3)	BD Biosciences GmbH (Heidelberg)	FACS	1:100
CD31-purified (Clone ab28364)	Abcam (Cambridge, UK)	IHC-P	1:500
CD45-VioBlue (Clone 30-F11.1)	Miltenyi Biotec GmbH (Bergisch-Gladbach)	FACS	1:50
CD49b-PE (Clone DX5)	Miltenyi Biotec GmbH (Bergisch-Gladbach)	FACS	1:50
FcR-Blocking reagent, mouse	Miltenyi Biotec GmbH (Bergisch-Gladbach)	FACS (Blocking)	1:50
F4/80-purified (Clone ab6640)	Abcam (Cambridge, UK)	IHC-P	1:1000
F4/80-PE-Cy7 (Clone BM8)	BioLegend (San Diego, USA)	FACS	1:200
Ly6C-PerCP-Cy5.5 (Clone AL-21)	BioLegend (San Diego, USA)	FACS	1:200
Ly6G-APC-Cy7 (Clone 1A8)	BioLegend (San Diego, USA)	FACS	1:100
Lyve-1-PE (Clone 223322)	RnD Systems (Minneapolis, USA)	FACS, IHC-P	1:100
MHC-II-APC (Clone M5/114.15.2)	Miltenyi Biotec GmbH (Bergisch-Gladbach)	FACS	1:200
S1PR1-PE (Clone 218713)	RnD Systems (Minneapolis, USA)	FACS, IHC-F	1:100
S1PR1 human	Santa Cruz (Heidelberg)	Western blot	1:3000
S1PR1 mouse	Prosci (Poway, USA)	Western blot	1:3000
Siglec F-PE (Clone E50-2440)	BD Biosciences GmbH (Heidelberg)	FACS	1:100
Siglec H-FITC (Clone 551)	BioLegend (San Diego, USA)	FACS	1:100

4.1.6 Quantitative PCR primer

Primer for qPCR were designed by use of Invitrogen's OligoPerfect™ primer designer and purchased from Biomers GmbH (Ulm) with the indicated primer sequence. Primers purchased from Qiagen GmbH (Hilden) are listed as QuantiTect Primer Assays.

Table 4. qPCR primer

Gene	Forward sequence	Reverse sequence	T_m
CRE recombinase	5-GCCACGACCAAGTGACAGC-3	5-TGCACGTTCACCGGCATC-3	60 °C
human IL-4	QuantiTect Primer Assays	QuantiTect Primer Assays	60 °C
human NLRP3	QuantiTect Primer Assays	QuantiTect Primer Assays	60 °C
human S1PR1	QuantiTect Primer Assays	QuantiTect Primer Assays	60 °C
human S1PR2	5-AGTTGCACTATTTGGGGCAC-3	5-GGTGGCTGTTTTTGAAAGGA-3	60 °C

human S1PR3	5-GCTTCAGGAAATGGAAGCTG-3	5-TCAGGATGCTGTGAAACTGC-3	60 °C
human 18S	5-GTAACCCGTTGAACCCCATT-3	5-CCATCCAATCGGTAGTAGCG-3	60 °C
mouse β-actin	5-CAGCTTCTTTGCAGCTCCTT-3	5-CACGATGGAGGGGAATACAG-3	60 °C
mouse ARG1	5-GTGAAGAACCCACGGTCTGT-3	5-CTGGTTGTCAGGGGAGTGTT-3	60 °C
mouse B2M	5-TGACCCTGGTCTTTCTGGTG-3	5-CGGGTGGAACTGTGTTACG-3	60 °C
mouse Casp1	5-CGGGTGGAACTGTGTTACG-3	5-GGCCTTCTTAATGCCATCAT-3	60 °C
mouse ERDR1	5-ACAGTGATGTCACCCACGAA-3	5-ACAGTGATGTCACCCACGAA-3	60 °C
mouse FIZZ1	5-CCCTTCTCATCTGCATCTCC-3	5-CAGTAGCAGTCATCCCAGCA-3	60 °C
mouse IL-1β	5-TGAAATGCCACCTTTTGACA-3	5-TGAAATGCCACCTTTTGACA-3	60 °C
mouse IL-6	5-CCGGAGAGGAGACTTCACAG-3	5-CCGGAGAGGAGACTTCACAG-3	60 °C
mouse IL-18	5-CCGGAGAGGAGACTTCACAG-3	5-CCGGAGAGGAGACTTCACAG-3	60 °C
mouse iNOS	5-GTGGTGACAAGCACATTTGG-3	5-GGCTGGACTTTTCACTCTGC-3	60 °C
mouse NLRP3	5-ATTGCTGTGTGTGGGACTGA-3	5-AACCAATGCGAGATCCTGAC-3	60 °C
mouse NRP2	5-CCGGAGAGGAGACTTCACAG-3	5-CCGGAGAGGAGACTTCACAG-3	60 °C
mouse PPARδ	5-TCCAGAAGAAGAACCGCAAC-3	5-GGCCTTCTTTTTGGTCATGT-3	60 °C
mouse Pycard	5-CCGGAGAGGAGACTTCACAG-3	5-GCTGGTCCACAAAGTGTCCT-3	60 °C
mouse S1PR1	QuantiTect Primer Assays	QuantiTect Primer Assays	60 °C
mouse SLC44A2	5-CAACTCGCCATGCAGATATT-3	5-AGCAGGACGATGAACAGGAG-3	60 °C
mouse TBP	5-CTGACCACTGCACCGTTGCCA-3	5-GACTGCAGCAAATCGCTTGGGA-3	60 °C
mouse TNFα	5-CCATTCCTGAGTTCTGCAAAGG-3	5-AGGTAGGAAGGCCTGAGATCTTATC-3	60 °C
mouse TSP1	5-CATCCAGAGCATCTTCACCA-3	5-AGCAGCCTTTGTTCCTGAGA-3	60 °C
mouse VCAM-1	5-ACTACGGGCTGCGAGTCACCA-3	5-ACTACGGGCTGCGAGTCACCA-3	60 °C
mouse XPR1	5-TCAAGATGGACTGGGGTCTC-3	5-GCTCGGAATTCACCACAGTT-3	60 °C
mouse YM-1	5-CTGGAATTGGTGCCCCTACAA-3	5-TCATAACCAACCCACTCATTACC-3	60 °C

4.1.7 Mouse genotyping primers

All mouse genotyping primers were taken over from the creator of the knockout strain or supplier (The Jackson Laboratory, Maine, USA) and used as required for the genotyping mix (KAPA Mouse Genotyping Kit). UbiC-GFP mice were phenotyped by presence of green fluorescence.

Table 5. Mouse genotyping primers

Gene	Forward sequence	Reverse sequence	T_m
F4/80 wt	5-AGAGGAGCAGCCAAAAGCCCC-3	5-CTGATGGTGGCAACTCAGC-3	60 °C
F4/80 CRE	5-AGAGGAGCAGCCAAAAGCCCC-3	5-GCATGCACCGGTAATGCAGGC-3	60 °C
mT/mG wt	5-CTCTGCTGCCTCCTGGCTTCT-3	5-CGAGGCGGATCACAAGCAATA-3	60 °C
mT/mG gene	5-CTCTGCTGCCTCCTGGCTTCT-3	5-TCAATGGGCGGGGGTCGTT-3	60 °C
PyMT	5-GGAAGCAAGTACTTCACAAGGG-3	5-GGAAAGTCACTAGGAGCAGGG-3	60 °C
SphK1 wt	5-ATGTGAAGCTGTGCAGGGCC-3	5-GCGAAGTGCCCAACACCAGC-3	60 °C
SphK1KO	5-TCGTGCTTTACGGTATCGCCGCTCCCGATT-3	5-GCGAAGTGCCCAACACCAGC-3	60 °C
SphK2 wt	5-AGGCATTGTCACTGTGTCTGG-3	5-AGGTCAACACCGACAACCTGCTC-3	60 °C
SphK2KO	5-GGCCGGAGAACCTGC-3	5-AGGTCAACACCGACAACCTGCTC-3	60 °C
S1PR1 loxP	5-GAGCGGAGGAAGTTAAAAGTG-3	5-CCTCCTAAGAGATTGCAGCAA-3	60 °C

4.1.8 Consumables

Table 6. Consumables

Material	Supplier
BZO Seal Film	Biozym Scientific GmbH (Hessisch Oldendorf)
Cell strainer (70 µm)	BD Biosciences GmbH (Heidelberg)
Cover slips	Menzel GmbH (Braunschweig)
Hard-Shell® Full-Height 96-Well Semi-Skirted PCR Plates	Bio-Rad Laboratories GmbH (Munich)
FACS tubes	Sarstedt AG & Co. (Nürnbrecht)
FACS tubes with 30 µm cell strainer	BD Biosciences GmbH (Heidelberg)
Filcon (70 µm)	BD Biosciences GmbH (Heidelberg)
Filter paper	Whatman GmbH (Dassel)
Gentle MACS C Tubes	Miltenyi Biotec GmbH (Bergisch-Gladbach)
Histosette II	VWR International GmbH (Darmstadt)
Leucosep tubes	Greiner Bio-One GmbH (Frickenhausen)
Medicons	BD Biosciences GmbH (Heidelberg)
Microscope slides	Süsse Labortechnik (Gudensberg)
NaCl 0.9 %	B. Braun Melsungen AG (Melsungen)
Pipets (10 µL; 100 µL; 1000 µL; 5000 µL)	Eppendorf GmbH (Hamburg)
Pipette tips (10 µL; 100 µL; 1000 µL; 5000 µL)	Eppendorf GmbH (Hamburg)
Plastic material (cell culture)	Greiner Bio-One GmbH (Frickenhausen)
Reaction tubes (0.5 mL, 1.5 mL, 2 mL)	Eppendorf GmbH (Hamburg)
RNeasy Micro Kit	Qiagen GmbH (Hilden)
Steril filters (0.22 µm, 0.45 µm)	Millipore GmbH (Schwalbach)
Syringes and injection needles	BD Medical (Franklin Lakes, USA)
Tissue culture dishes	Sarstedt AG & Co. (Nürnbrecht)
Whatman PROTRAN® nitrocellulose membrane	Whatman GmbH (Dassel)
xCELLigence E-Plates	Roche Deutschland Holding GmbH (Mannheim)
xCELLigence CIM-Plates	Roche Deutschland Holding GmbH (Mannheim)

4.1.9 Instruments

Instrument	Supplier
Agilent 2100 Bioanalyzer	Agilent Technologies (Santa Clara, USA)
Apollo-1 LB 911 photometer	Berthold Technologies GmbH & Co. KG (Bad Wildbad)
Autoclave HV 85	BPW GmbH (Süssen)
AxioCam MRm	Carl Zeiss MicroImaging GmbH (Jena)
B250 Sonifier	Branson Ultrasonics (Danbury, USA)
CASY®	Schärfe System GmbH (Reutlingen)
Centrifuge 5415 R and 5810 R	Eppendorf GmbH (Hamburg)
CFX 96 qPCR system	Bio-Rad Laboratories GmbH (Munich)
FACS Aria III	BD Biosciences GmbH (Heidelberg)
Galaxy Mini	VWR International GmbH (Darmstadt)
Hera cell 150 (Lamina)	Fisher Scientific GmbH (Schwerte)
LabLine Orbit Shaker	Uniequip GmbH (Martinsried)
LSRII/Fortessa	BD Biosciences GmbH (Heidelberg)
Leica Paraffin Embedding Station EG1140H	Leica Biosystems Nussloch GmbH (Nussloch)
Leica EG1150 C Cold Plate	Leica Biosystems Nussloch GmbH (Nussloch)

Leica RM2235 Microtome	Leica Biosystems Nussloch GmbH (Nussloch)
Magnetic stirrer Combimag RCH	IKA Labortechnik GmbH & Co. KG (Staufen)
Mastercycler®	Eppendorf GmbH (Hamburg)
Medimachine	Keul GmbH (Steinfurt)
MyiQ iCycler system	Bio-Rad Laboratories GmbH (Munich)
NanoDrop ND-1000	Peqlab Biotechnologie GmbH (Erlangen)
Neubauer improved counting chamber	Labor Optik GmbH (Friedrichsdorf)
Odyssey infrared imaging system	Li-COR Biosciences GmbH (Bad Homburg)
Optima L-90K Ultracentrifuge	Beckman Coulter (Krefeld)
Pure water system Purelab Plus	ELGA LabWater GmbH (Siershahn)
Reax Top	Heidolph Instruments GmbH & Co. KG (Schwabach)
Roller Mixer SRT1	Bibby Scientific Ltd. (Staffordshire, UK)
Thermomixer compact	Eppendorf GmbH (Hamburg)
Trans-Blot SD blotting machine	Bio-Rad Laboratories GmbH (Munich)
xCELLigence RTCA DP Analyzer	Roche Deutschland Holding GmbH (Mannheim)

4.1.10 Software

Software	Provider
AutoStitch v2.2 (Demo)	CloudBurst Research Inc. (Vancouver, Canada)
AxioVision Release 4.7	Carl Zeiss MicroImaging GmbH (Jena)
BD Bioscience FCAP software	BD Biosciences GmbH (Heidelberg)
CorelDRAW Graphics Suite X4	Corel Cooperation (Ottawa, Canada)
EndNote X3	Thomson Reuters Endnote (Carlsbad, USA)
FlowJo V7.6 / V10	FlowJo (Ashland, USA)
GraphPad 5.03	GraphPad Software (La Jolla, USA)
Ingenuity pathway analysis	Qiagen GmbH (Hilden)
Microsoft Office 2007	Microsoft Deutschland GmbH (Unterschleißheim)
MyiQ Optical Systems, Software 1.0	Bio-Rad Laboratories GmbH (Munich)
ND-1000 V3.2.1	Peqlab Biotechnologie GmbH (Erlangen)
Odyssey 2.1	Li-COR Biosciences GmbH (Bad Homburg)
Partek Genomics Suite	Partek (St. Louis, USA)
RTCA Software 1.2.1	Roche Deutschland Holding GmbH (Mannheim)
Photo Read V1.2.0.0	Berthold Technologies GmbH & Co. KG (Bad Wildbad)

4.2 Methods

4.2.1 Cancer cell culture

MCF-7 breast cancer cells were cultured in RPMI 1640 with supplementation of 10 % heat inactivated fetal calf serum (FCS), 10 µg/mL bovine insulin, non-essential amino acids, 100 U/mL penicillin and 100 µg/mL streptomycin. Lewis lung carcinoma and E0771 breast cancer cells were cultured in RPMI 1640 supplemented with 10 % heat inactivated fetal calf serum, 100 U/mL penicillin and 100 µg/mL streptomycin. Primary human monocytes and

macrophages were cultured in RPMI 1640 supplemented with 2.5 % heat-inactivated AB^+ human serum, 100 U/mL penicillin and 100 µg/mL streptomycin. Mouse primary bone marrow, bone marrow derived macrophages and peritoneal macrophages were cultured in DMEM high glucose with addition of 10 % heat inactivated fetal calf serum, 100 U/mL penicillin and 100 µg/mL streptomycin.

All cells were cultured in a humidified atmosphere of 5 % CO_2 at 37 °C and were splitted two or three times per week, depending on cell growth. Cell numbers were determined for FACS analysis with the CASY® cell counting system, otherwise with Neubauer improved counting chambers.

4.2.2 Human monocyte isolation

Each peripheral blood sample (~30 mL) was divided into two 50 mL Leucosep® tubes, diluted with PBS + 2 mM EDTA and gradient centrifuged (440 x g, 35 min, break off, RT) with Ficoll-Hypaque gradients by addition of 15 mL lymphocyte separation medium. The leucocyte ring (buffy-coat) was collected, washed twice with PBS-EDTA and seeded in human macrophage culture medium on tissue culture dishes. After 2 h of cell adherence in the incubator, cells were washed once with culture medium to remove non-adherent cells [162]. Afterwards, cell medium was renewed three times a week and differentiated macrophages were used from 1 week until 3 weeks after isolation at cell densities of 75 % up to 100 % confluency.

4.2.3 Mouse bone marrow isolation

Mice of the appropriate genotype were killed by cervical dislocation in narcosis by isoflurane inhalation. Hind legs were removed and fleshed, taking care not to open the medullary cavity. The upper and lower bones were separated at the knee joint, sterilized and cut opened under sterile conditions in a laminar air flow. The bone marrow was flushed out of the medullary cavity with sterile PBS with syringe and 26G injection needles. The dissolved bone marrow was separated into single cells by filtering through a 70 µm Filcon and suspended in culture medium afterwards. Whole bone marrow samples were either seeded on tissue culture plates with the addition of 20 ng/mL M-CSF or GM-CSF to differentiate macrophages or used in sterile PBS immediately without additions for bone marrow transfer.

4.2.4 Mouse bone marrow transfer

Bone marrow transfer was performed with SphK1KO, SphK2KO and UbiC$^{GFP/+}$ mice at least 6 weeks before 3-MCA injection. 7 weeks old recipient mice were irradiated with 9 Gy to eradicate host bone marrow, using a ^{60}Co radiation source. Irradiated mice were grafted intravenously with isolated sterile bone marrow (4.2.3) in a ratio of 1 donor mouse to 3 recipient mice. The engraftment was verified by appearance or disappearance of UbiC$^{GFP/+}$ positive cells, measured by FACS, in the peripheral blood 6 weeks after bone marrow transplantation. According to the animal experiment proposal, all irradiated mice were weighted and controlled daily until the day of 3-MCA injection.

4.2.5 Induction of mouse peritonitis and peritoneal lavage

To reduce inflammation-induced pain, all experiment mice were pretreated 1 day before till the end of the experiment with Tramadol® supplied drinking water (25 mg/L). At day 0 mice were injected with 10 mg/kg zymosan A (75 % zymosan A, 25 % zymosan A AlexaFluor488 coupled biospheres) in sterile PBS. All mice were monitored after 3 h, 8 h, 24 h, 48 h, 72 h, 96 h, 120 h and 144 h for apparent changes in behavior according to the animal experiment proposal. After 72 h or 144 h mice were sacrificed by cervical dislocation in Isoflurane inhalation narcosis. Afterwards, each mouse peritoneum was rinsed with 5 mL ice cold PBS and the lavage subjected to the following experiment. 1 mL of the lavage was centrifuged (500 x g, 5 min, 4 °C), stained for FACS analysis and cells quantified by use of counting beads. 100 µL of peritoneal lavage was snap-frozen for later inflammatory cytokine CBA analysis. The remaining lavage was centrifuged (500 x g, 5 min, 4 °C), the pelleted cells were suspended in culture medium and seeded on cell culture dishes for cell attachment. After attachment, non-adherent cells were removed by washing 3 times with ice-cold PBS and remaining attached cells were subjected to mRNA isolation and subsequent analysis.

4.2.6 Cancer induction by 3-methylcholanthrene injection

UbiC$^{GFP/+}$, SphK1KO, UbiC$^{GFP/+}$-BM-SphK1KO, SphK2KO, UbiC$^{GFP/+}$-BM-SphK2KO, SphK1KO-BM-UbiC$^{GFP/+}$, SphK2KO-BM-UbiC$^{GFP/+}$, S1PR1$^{wt/wt}$-F4/80$^{CRE/+}$, S1PR1$^{plox/plox}$-F4/80$^{CRE/+}$ were narcotized by Isoflurane inhalation, shaved at their right flank and subcutaneously injected with 100 µL corn oil containing 100 µg of 3-methylcholanthrene with a 26G injection needle and a 1 mL syringe.

4.2.7 Monitoring of cancer development and growth

PyMT breast cancer and 3-MCA fibrosarcoma mice were monitored at least two times a week. The body weight was determined by weighing, cancer development was determined by palpating all 10 breast glands or the 3-MCA injection site. The tumor size was measured with sliding calipers in the largest diameter and the orthogonal diameter and assigned to 4 categories: no tumor, 0-0.5 cm, 0.5-1 cm, 1-1.5 cm, 1.5-2 cm. PyMT mice were sacrificed as soon as the tumor reached a size of >1 cm or met one of the defined criteria (loss of 20 % body weight, skin ulcerations, apathy, abnormal behavior). 3-MCA mice were sacrificed as soon as the tumor reached a size of 2 cm or met one of the defined criteria (loss of 20 % body weight, skin ulcerations, apathy, abnormal behavior). After sacrifice, mice were cardially perfused with 0.9 % NaCl solution and the tumors were removed. The weight of every single tumor was determined for calculation of tumor mass and tumor burden [mouse body weight/tumor weight] x 100. For immunohistochemistry, one representative (part of the) tumor was fixed with a zinc-fixative (4.2.16.1). Tumor draining lymph nodes, control lymph nodes and other tissue were isolated likewise.

4.2.8 Mouse leukocyte isolation from tumor tissue

After mouse sacrifice, mice were cardially perfused with 0.9 % NaCl solution to reduce remaining blood in the tumor. All isolated tumors were minced with a scalpel and the tumor mass was pooled. Out of this, 0.75 g for flow cytometric analysis or 1.4 g for FACSorting were digested with the tumor dissociation kit mouse (Miltenyi Biotech) for 40 min at 37 °C, according to the manufacturer's instruction. The obtained digest was passed through a 70 µm nylon mesh to singularize the cells and centrifuged afterwards (500 x g, 5 min, 4 °C). The cell pellet was resuspended in 10 mL erythrocyte lysis buffer (135 mM NH_4Cl,

10 mM $NaHCO_3$, 0.1 mM Na_4EDTA, pH 7.4) and incubated for 4 min at room temperature. After stopping the lysis and centrifugation, cells were suspended in 10 mL PBS+0.5 % BSA for flow cytometry analysis (4.2.9), or PBS+3 % FCS for FACSorting (4.2.10).

4.2.9 Multicolor FACS analysis

Single cell suspensions were counted with the CASY® counting system and 3 million cells were added to each FACS tube in 100 µL PBS-0.5 % BSA. To avoid Fc-receptor binding, cells were incubated at 4 °C for 15 min with CD16/32 Fc-receptor blocking antibodies, followed by staining with the indicated antibodies for further 15 min at 4 °C. Before measuring, cells were washed once to remove unbound antibodies and for cell quantification supplemented with 30 µL of Flow Cytometry Absolute Count Standard beads (BangsLab). All samples were acquired on a BD LSRII/Fortessa flow cytometer and analyzed with FlowJo (Treestar) afterwards.

4.2.10 Multicolor FACS sorting

Whole tumor cell samples were transferred into FACS tubes and cells were resuspended in 100 µL PBS-3 % FCS. To avoid Fc-receptor binding, cells were incubated at 4 °C for 15 min with CD16/32 Fc-receptor blocking antibodies, followed by staining with the indicated antibodies for further 15 min at 4 °C. Before measuring, cells were washed once to remove unbound antibodies, filtered through a 70 µm Filcon, followed by filtering through a 30 µm cell strainer to avoid clogging of the FACSorter nozzle. The sample was diluted to the ideal concentration for cell sorting, and the identified cell populations were sorted into medium-prefilled FACS tubes and centrifuged afterwards. The obtained cells were used for cell culture or RNA isolation.

4.2.10.1 Tumor-associated macrophage sorting

TAMs from primary mouse tumor tissue were isolated by identification of surface markers. Dead cells, doublets and cell debris were excluded by FSC-H/FSC-W/FSC-A and SSC-H/SSC-W/SSC-A gating strategies. TAM were identified as $CD45^{+}CD11b^{+}CD11c^{+/-}Ly6G^{-}Ly6C^{+/-}F4/80^{high}$ cells and sorted into culture medium.

4.2.11 Preparation of apoptotic cell conditioned medium (ACM)

For the generation of apoptotic cell conditioned medium, MCF-7 cells were cultured in FCS-free medium and stimulated for 2 h with 0.5 µg/mL staurosporine (STS). Afterwards, cells were washed two times to remove STS and incubated over-night in fresh culture medium, supplemented with 10 % FCS, at a density of approximately 2.5E6 cells/mL. For ensuring apoptotic cell death, cells were detached with Accutase, stained with propidium iodide and annexin-V-antibodies and measured on a BD LSRII/Fortessa cytometer. When the MCF-7 cells showed apoptotic cell death in more than 35 % of cells, the conditioned medium was collected. The harvested ACM was centrifuged at 1000 x g for 10 min at 4 °C and filtered through a 0.22 µm filter to remove cell fragments. The ratio of apoptotic cells to stimulated cells was roughly 1:5. ACM was aliquoted and stored at -80 °C for further experiments.

4.2.11.1 Preparation of microparticle-free ACM

To generate microparticle-free ACM, normal ACM was ultracentrifuged for 24 h, 30000 x g at 4 °C. The supernatant was taken off and the pelletized fraction suspended in normal cell culture medium for stimulation purposes. Both media were aliquoted and stored at -80 °C for further experiments.

4.2.12 Transient cell transfection

Knockdown of IL-4 receptor in primary human macrophages was performed by using HiPerFect® (Qiagen) according to the manufacturer's instructions. Cells were incubated for 6 h with 16.8 µL HiPerFect and 150 µM siRNA (si_IL-4R or si_ctrl) in 500 µL RPMI 1640. Afterwards, 1 mL RPMI 1640 was added and incubation was continued over-night. The next day, transfected cells were stimulated as indicated. Efficiency of the knockdown was controlled by qPCR in control cells.

4.2.13 Isolation and analysis of mRNA

Depending on the cell number, RNA extraction was performed with peqGold (for more than 500000 cells) or RNEasy micro kit (Quiagen)(less than 500000 cells).

4.2.13.1 mRNA isolation peqGold

Total cell RNA isolation with peqGold RNAPure™ was performed according to the manufacturer's instruction. 1 mL peqGold was added to the culture plate or pelleted cells for lysis of the cells. After 5 min of incubation, cells were mixed with 200 µL of chloroform, vortexed, incubated for 5 min and centrifuged at 4 °C for 10 min, 12000 x g. The RNA containing aqueous phase was added to 500 µL 2-propanol and incubated for 20 min at 4 °C. After RNA precipitation and centrifugation at 4 °C for 10 min, 12000 x g, pelleted RNA was washed twice with 75 % ethanol in ultra-pure water and dried for 5 min at 70 °C. The purified, dried RNA was dissolved in ultra-pure water for 30 min at 60 °C and quantified using the NanoDrop ND-1000 and optical density at 260 nm.

4.2.13.2 mRNA isolation RNEasy micro kit

Low amounts of cells were pelleted in a 1.5 mL reaction tube for 5 min, 500 x g at 4 °C and suspended in the RNEasy micro kit RLT buffer, according to the manufacturer's instruction. Directly before RNA isolation, the sample was supplemented with 1:100 β-mercaptoethanol to reduce disulfide bonds. Cell samples were diluted with RLT buffer to 350 µL and homogenized by using Qiagen Shredder Spin-columns (2 min, full speed, RT). The obtained homogenate was mixed with 350 µL 70 % ethanol, loaded on the microRNA filter column, quickspinned (15 s, >8000 x g, RT), washed with Buffer RW1 and quickspinned again. DNA was digested with 80 µL DNAse Mix for 15 min, diluted with 350 µL buffer RW1 and quickspinned. Remaining bound RNA was washed with 500 µL buffer RPE and 500 µL 80 % ethanol followed by quickspinning each time. Afterwards, the microRNA spin columns were dried by centrifugation for 10 min, full speed, RT. Pure RNA was eluted with 14 µL ultra-pure water, using the centrifuge at full speed for 1 min at RT.

4.2.13.3 mRNA quantification with the Agilent 2100 Bioanalyzer

Low amounts of RNA, obtained from <500000 cells were quantified using the Agilent 2100 Bioanalyzer® according to the manufacturer's instructions. In brief, the pico RNA chips were loaded with 9 µL of gel-dye mix and all gel reservoirs were filled with 9 µL of remaining gel mixture. All sample and ladder wells were filled with 5 µL RNA dye-solution and 1 µL of prepared RNA solution or ladder was added. After adding conditioning solution, electrode cleaning with RNAse away® and ultra-pure water, the Eukaryote Total RNA Pico program was

executed. Only RNA with a RNA integrity number (RIN) of >6 was used for Qiagen SensiScript® reverse transcription.

4.2.13.4 mRNA reverse transcription Fermentas

The Fermentas Maxima® cDNA Synthesis Kit was used for RNA amounts >50 µg RNA according to the manufacturer's instructions. 1 µg of RNA (if less, total RNA) was mixed with 4 µL 5X reaction mix, 2 µL provided reverse transcriptase and filled up to 20 µL with ultra-pure water. The final mixture was incubated for 10 min at 25 °C, 15 min at 50 °C followed by 5 min at 85 °C for enzyme inactivation. The transcribed cDNA was diluted 1:10.

4.2.13.5 mRNA reverse transcription SensiScript

The Qiagen SensiScript® was used for RNA amounts <50 ng RNA. 50 ng of RNA (if less, total RNA) was mixed with 2 µL 10X buffer, 2 µL dNTP mix, 0.4 µL oligo dT primer (50 µM), 0.25 µL RNAse inhibitor (40 U/µL), 1 µL SensiScript reverse transcriptase and filled up to 20 µL with ultra-pure water. The final mixture was incubated for 1 h at 37 °C and diluted 1:5 afterwards.

4.2.13.6 Quantitative real-time PCR (qPCR)

For cDNA analysis by qPCR, 4 µL of obtained cDNA solution was mixed with 5 µL Absolute™ qPCR SYBR® Green Fluorescein Mix and 1 µL QuantiTect Primer Assay or 0.2 µL forward and reverse primer plus 0.6 µL ultra-pure water. The final mixture was transferred into a qPCR compatible plate and sealed with a BZO Seal Film. qPCR was performed on a CFX96 qPCR system with the following thermal cycling program:

1) Enzyme activation, 95 °C, 15 min
2) cDNA denaturation, 95 °C, 15 s
3) Annealing, 60 °C, 30 s
4) Extension, 72 °C, 30 s
5) Denaturation, 95 °C, 30 s
6) Starting temperature melting curve, 60 °C, 30 s
7) Melting steps, 60 °C, 10 s, +0.5 °C per cycle, 80 cycles

The program steps 2-4 were repeated for 45 cycles for Fermentas obtained cDNA and 60 cycles for SensiScript obtained cDNA. The steps 5-7 were performed to record a melt curve and confirm the specificity of cDNA amplification.

4.2.14 Protein identification and quantification

4.2.14.1 Protein quantification (Lowry)

Protein quantification, prior to Western blotting, was carried out using the Lowry method and the DC Protein Assay Kit. 2 µL of each sample and a prepared BSA standard dilution (0.625-10 mg/mL) were mixed with 20 µL solution A, in duplicates, in a 96 well plate. The colorimetric reaction was started by addition of 160 µL of solution B. After incubation for 15 min, optical absorption was determined at 750 nm on an Apollo-8 LB 912 photometer.

4.2.14.2 Western blot procedure

SDS-PAGE Western blot analysis was performed with protein mixtures obtained from cell cultures, lysed in adequate urea lysis solution. 100 µg protein were mixed with 4x SDS sample buffer and heat denatured for 10 min at 95 °C. Proteins were separated on 5-15 % SDS-polyacrylamide gels in 1x SDS-glycine-running buffer. Separated proteins were blotted on nitrocellulose membranes by semi-dry blotting and unspecific binding of proteins to the membrane was blocked by incubation with PBS-5 % BSA for 1 h, RT. Membranes were incubated with the according primary antibody in TTBS-5 % BSA over night at 4 °C, washed three times with TTBS for 15 min and incubated with IRDye secondary antibodies in TTBS-5 % BSA for 1 h. After washing the membrane three times with TTBS for 15 min each, staining of proteins was detected and quantified, using an Odyssey infrared imaging system.

4.2.15 Cytokine quantification by cytometric bead array (CBA)

Cytokine quantification in cell culture supernatants was performed by use of cytometric bead arrays (mouse inflammatory cytokine kit [IL-6, IL-10, MCP-1, IFNγ, TNFα, IL-12p70], human IL-1β Flex Set, mouse IL-1β Flex Set). 25 µL of sample were incubated with 25 µL of cytokine specific beads or bead mixtures in provided master buffer. After one hour, cytokine specific PE-labeled antibodies were added in 25 µL master buffer and incubated for one hour (mouse), two hours (human). Following washing with FACS Flow® (200 x g, 5 min, RT) samples were suspended in 250 µL FACS Flow, acquired on a LSRII/Fortessa flow cytometer and evaluated with BD Bioscience FCAP software.

4.2.16 Immunohistochemistry

4.2.16.1 Fixation

Primary tissue, obtained from experiment mice (tumor, lung, lymph nodes), was fixed in Zn-fixation solution (0.5 % $ZnCl_2$, 0.5 % ZnAcetate, 0.05 % CaAcetate in 0.1 M Tris base buffer, pH 7.4) for at least 8 h at 4 °C [163]. Fixed tissues were transferred to pencil-labeled Histosettes and dehydrated over-night.

4.2.16.2 Dehydration, paraffining

Tissues were dehydrated by incubation in increasing concentrations of Ethanol for 1.5 h each (70 %, 80 %, 85 %, 90 %, 95 %, 100 %). Following ethanol incubation, tissues were incubated for 1.5 h in Xylene and 1.5 h in liquid paraffin. After end of the program, paraffined tissue was embedded in liquid paraffin and cooled for hardening. Paraffin blocks were stored at RT, protected from light.

4.2.16.3 Tissue preparation and staining

Paraffined tissues were pre-cooled and sliced in 4 µm thick sections. Two consecutive sections per tumor and 4 consecutive sections per lung were sliced from 4 levels of the tissue, mounted on glass slides and dried at 37 °C over-night. Deparaffinization was carried out using successive Xylene-Ethanol dilutions (3x 100 % Xylene, 5 min, 2x 100 % ethanol, 2x 95 % ethanol, 2x 90 % ethanol, 2x 80 % ethanol, 2x 75 % ethanol [2 min each], tap water). Rehydrated sections were stored at 4 °C or used immediately for tissue staining. For staining with Mayer's hemalum solution, hydrated sections were incubated for 5 min in hemalum solution and developed for 5 min in running tap water. Stained sections were mounted in Aquatex Mounting Medium and covered with a glass cover slip.

4.2.16.4 Lung metastasis quantification

Hemalum stained lung sections were examined on a light microscope and all metastatic cell nodules in each section were counted. At least 10 sections from 4 different organ levels were analyzed and the average of metastasis per section was calculated. Panorama pictures from mouse lungs were obtained from stitching single pictures together with the Autostitch software v2.2 after color adjusting with Corel Photo-Paint x4.

4.2.17 mRNA array analysis of tumor-associated macrophages

mRNA array analysis from primary tumor-associated macrophages was performed by the Deutsche Krebsforschungszentrum (DKFZ, Heidelberg). Cells were isolated as described under 4.2.10 and RNA was isolated as described under 4.2.13.2. Because of the small RNA quantities, the total RNA was amplified by use of the µMACS SuperAmp Kit (Miltenyi) and analyzed with mouseWG-6 v2 BeadChip® afterwards. Array data were provided statistically evaluated and pathway analysis was carried out using Ingenuity Pathway Analysis (IPA) and Partek Genomics Suite.

4.2.17.1 Statistical data analysis

All experiments were performed at least three times with independent blood donors or experiment mice. Presented data graphs show arithmetic mean values ± standard error of the mean (SEM). Statistical analysis were performed, as indicated in the figure legends, by one-sample t-test, paired or unpaired two-tailed student's t-test, one-way or two-way analysis of variance (ANOVA) followed by Bonferroni's post-test with GraphPad Prism 5.03. Differences were considered as significant at $p \leq 0.05$ (*), $p \leq 0.01$ (**) or $p \leq 0.001$ (***).

5 Results

In previous experiments our group could show that ACM contains substantial amounts of S1P, secreted during cell death [63, 64]. By means of secreted mediators and S1P, apoptotic cells are able to polarize macrophages towards an anti-inflammatory phenotype, leading to restoration of tissue integrity and homeostasis [164]. Hence, my aim was to determine the effect of the S1PR1 on the functional outcome of macrophages, but also the regulation of its expression in two different experimental settings.

First, I investigated the regulation of S1PR1 expression on human peripheral blood derived macrophages *in vitro,* after stimulation with inflammatory and anti-inflammatory stimuli. To verify the *in vivo* relevance, I investigated the effect of macrophage-S1PR1 deficiency in an acute but self-resolving peritonitis mouse model. Second, I sought to determine the roles and functions of sphingosine kinases and macrophage-S1PR1 in cancer development and tumor growth. Therefore, I utilized two different mouse cancer settings, an inflammatory cancer model, elicited by injection of the carcinogen 3-methylcholanthrene (3-MCA) and a genetic breast cancer model, driven by endogenous expression of a viral oncogene (PyMT) specifically in the mammary epithelium.

5.1 Alternative activation of primary human macrophages *in vitro*

Within the first set of experiments, I followed up previous findings in our lab [63] to show that stimulation of primary human macrophages with supernatants of apoptotic cells *in vitro* was sufficient to induce the transcription and translation of S1PR1 and 3. Whereas the induction of S1PR1 and S1PR3 was most pronounced after 3 hours (Figure 6A), the expression of S1PR2 remained unchanged throughout the analyzed time-span [165, 166]. However, since the Cq levels of S1PR3 were mostly close to the negative control, indicating a low transcript level, I focused on the induction of S1PR1. As I identified the maximum induction after 3 hours for mRNA (Figure 6A) and 6 hours for protein (Figure 6B), I chose these time points for my further investigations.

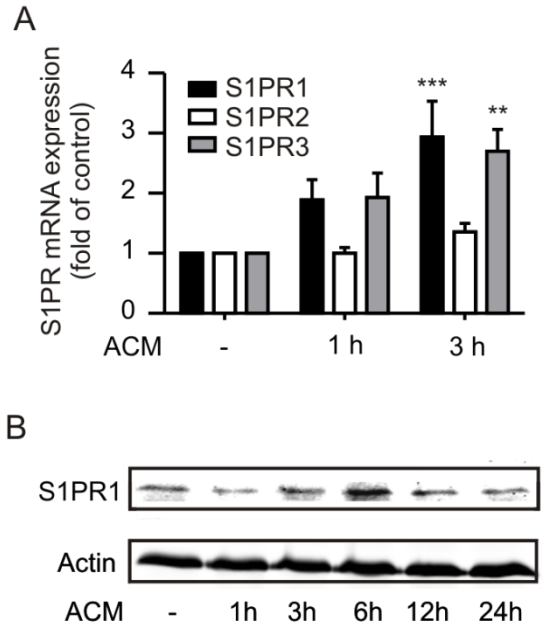

Figure 6. Regulation of S1PR by ACM

(A) S1P receptor mRNA was analyzed by qPCR after treatment with ACM for the indicated time. Data are mean values ± SEM of at least 5 experiments. (B) S1PR1 protein concentration was determined by Western blot after stimulation with ACM for the indicated time. One representative blot of 3 independent experiments is shown. Statistics were performed with two-way-ANOVA with Bonferroni's correction.*$p \leq 0.05$, **$p \leq 0.01$, ***$p \leq 0.001$ (Figure adopted from Nicole Weis and modified).

5.1.1 Alternative activation induces macrophage-S1PR1 expression

During the process of cell death, apoptotic cells do not only secrete cytokines, but are as well able to form membrane blebs and secrete these as microparticles, containing lipids in the membrane and intact or degraded proteins in their lumen. To investigate whether cell derived particles are involved in shaping the macrophage-S1PR1 response, I decided to pellet the particle fraction by ultracentrifugation (30000 x g, 24 h at 4 °C). However, neither the vesicle free soluble fraction, nor the pelleted particle fraction alone were able to induce S1PR1 expression (Figure 7). These data indicate that the mechanism of S1PR1 induction requires more than one signaling element and that the interplay of mediators from different compartments determines the final outcome.

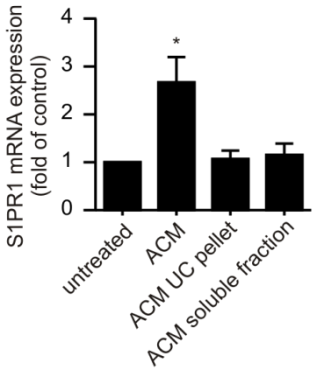

Figure 7. Ultracentrifugation abrogates ACM effects on S1PR1
Primary human macrophages were treated for 3 h with ACM, RPMI with the ultracentrifuge-pelleted particle fraction or the particle-free ACM. S1PR1-mRNA expression was analyzed by qPCR, the ratio of S1PR1 to 18S RNA in unstimulated control was set to 1. All data are mean ± SEM of four independent experiments. Statistics were performed using one-way ANOVA. Significant differences to the control group are marked by asterisks. *p ≤ 0.05.

Knowing that ACM, as an inducer of an "alternative-like" phenotype in macrophages, is able to induce the increase of S1PR1, I hypothesized that S1PR1 upregulation might generally occur during alternative activation. To test this hypothesis, I compared the regulatory effects of typical *in vitro* stimuli on S1PR1 expression. Whereas LPS and IFNγ, inducing classical 'M1' activation, were unable to induce the transcription and translation of S1PR1, IL-4 led to a sustained and significant induction of S1PR1 mRNA (Figure 8A) and protein (Figure 8B).

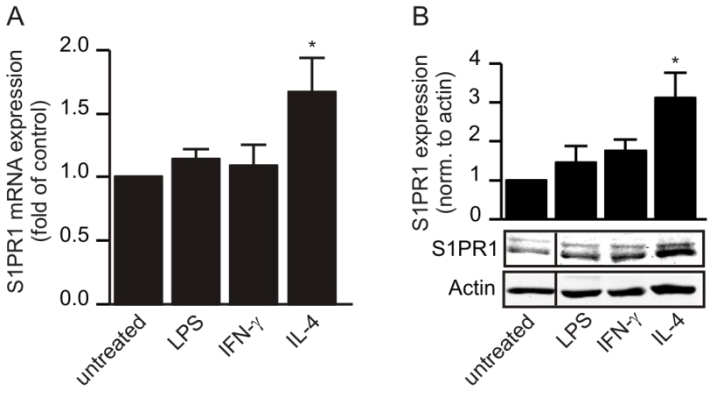

Figure 8. Alternative activation of macrophages induces S1PR1 expression
Primary human macrophages were treated with 1 µg/mL LPS, 100 U/mL IFNγ or 10 ng/mL IL-4. (A) S1PR1-mRNA expression was analyzed after 3 h by qPCR, the ratio of S1PR1 to 18S RNA in untreated control was set to 1. Protein expression was analyzed after 6 h by Western blot. Data are shown as mean ± SEM of (A) five (B) four experiments, one representative blot is shown. All data are mean ± SEM. Statistics were performed using one-way ANOVA. *p ≤ 0.05.

5.1.2 IL-4R is dispensable for S1PR1 mRNA induction by ACM

The finding that IL-4 is able to induce transcription and translation of S1PR1 raises the question whether IL-4R signaling is involved in the macrophage response. Although previous experiments could show that ACM does not contain IL-4 [167], other IL-4R binding cytokines, such as IL-13 or paracrine/autocrine signaling loops could shape the cell response. In order to analyze a possible involvement of IL-4R, I used primary human macrophages with an IL-4R knock-down. However, the transfection of IL-4R siRNA resulted in an unaltered S1PR1 mRNA profile (Figure 9), ruling out direct effects of IL-4 or IL-13 within the ACM and the macrophage response as S1PR1-inducing factors.

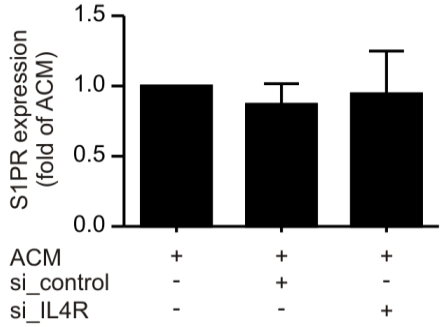

Figure 9. IL-4 receptor in macrophage ACM response
Macrophages were transfected with scrambled siRNA (si_control) or IL-4R-specific siRNA (as described in [70] and incubated for 48 h prior to treatment with ACM for 3 h. S1PR1 expression was determined by qPCR. Ratio of S1PR1 to 18S RNA of ACM stimulated control macrophages was set to 1. Data are mean ± SEM of four independent experiments.

5.1.3 M-CSF differentiation but not GM-CSF induces S1PR1

Given that the differentiation process of monocytes to macrophages favors “classical” or “alternative” phenotypes, dependent on the cytokine environment, I compared the macrophages differentiated under diverse stimuli. M-CSF is described as a stimulus favoring “alternative phenotype” whereas GM-CSF favors the “classical” macrophage activation [168, 169]. Indeed, M-CSF stimulation led to a substantial increase of S1PR1 mRNA over GM-CSF (Figure 10). This finding provides further evidence that alternative activation of macrophages in general induces S1PR1 expression.

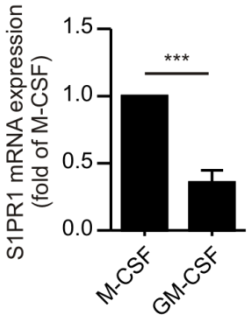

Figure 10. M-CSF differentiation leads to higher S1PR1 levels than GM-CSF
Human monocytes were differentiated for 7 days in either 20 ng/mL M-CSF or GM-CSF. Expression of S1PR1 mRNA analyzed by qPCR is shown. The ratio of S1PR1 to 18S RNA from M-CSF-treated macrophages is set to 1. Data shown are mean values ± SEM of seven independent experiments. Statistics were performed with one-sample Students t-test. ***p ≤ 0.001.

5.1.4 LXR activation but not PPARγ activation induces S1PR1

To identify further alternative activation stimuli that are able to trigger S1PR1 induction, I decided to analyze its expression level after stimulation with two well-known stimulators of alternative activation patterns. The PPARγ agonist rosiglitazone as well as the liver X receptor (LXR) agonist T0901317 have been identified as potent anti-inflammatory agents, especially for monocytes and macrophages [170-172]. To my surprise, exclusively the LXR agonist resulted in a substantial induction of S1PR1 mRNA, whereas PPARγ activation left S1PR1 mRNA expression unaltered (Figure 11). Although both compounds induce non-inflammatory macrophage activation, the mechanism behind seems to be more sophisticated than I previously expected.

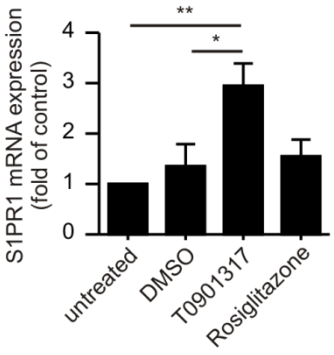

Figure 11. LXR but not PPARγ mediate S1PR1 induction
Human macrophages were stimulated with 1 µM Rosiglitazone or 1 µM T0901317 for 3 h. mRNA expression was analyzed by qPCR. The ratio of S1PR1 to 18S from untreated macrophages was set to 1. Data shown are mean values ± SEM of five independent experiments. Statistics were performed with one-way ANOVA. *p ≤ 0.05 **p ≤ 0.01.

5.2 The functional role of ACM-induced S1PR1

After providing evidence for a regulatory link between alternative macrophage activation and the induction of S1PR1 by various stimuli (see 5.1 *et seq.*), I questioned whether the elevated receptor expression results in an increase of S1P signal transduction. Preceding experiments from our group could show an increased localization of S1PR1 in the pseudopodia-like structures at the macrophage surface following ACM-stimulation [165]. As surface expression of S1PR1 is known to induce migration in several cell types, such as endothelial cells, cancer cells and leucocytes [71, 173-175], I hypothesized that macrophage migration is likewise induced by the increase of surface S1PR1.

In a first set of *in vitro* experiments, I utilized a random migration scratch assay to analyze macrophage motility [165]. After inflicting a scratch into a confluent macrophage population, I stimulated macrophages for 16 h with ACM, with or without the addition of the S1PR1/3 specific inhibitor VPC23019. Whereas ACM-stimulated macrophages were able to close the scratch almost completely, VPC23019 addition was able to reduce the random macrophage migration significantly, resulting in an increased remaining scratch width (Figure 12).

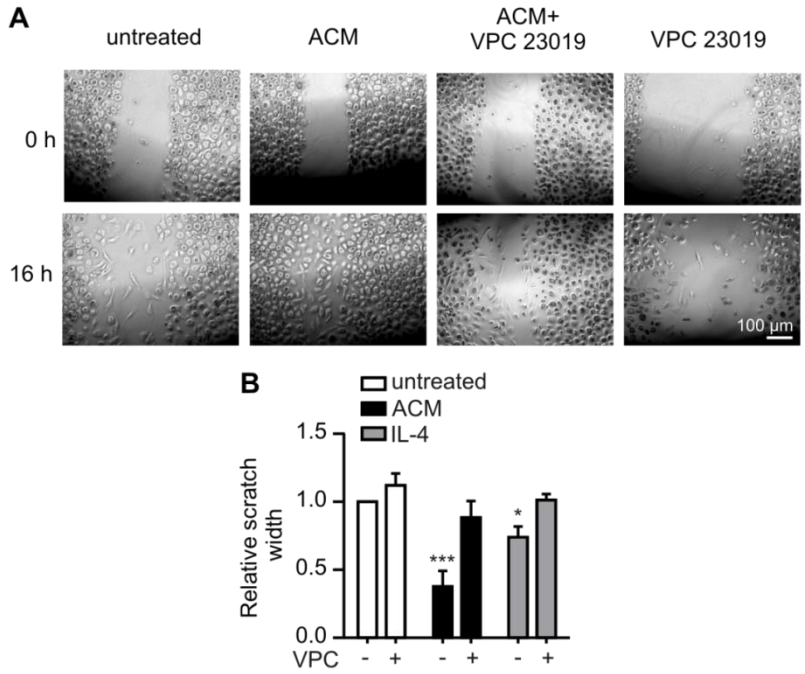

Figure 12. S1PR1 induces random migration in ACM stimulated human macrophages

Scratches were inflicted into confluent macrophage populations. For 16 h cells were treated with (A) ACM ± 1 µM VPC23019 or (A, B) ACM 10 ng/mL IL-4 ± 1 µM VPC23019 and left migrating. Evaluation of scratch closure was performed by light microscopy and measurement of the cell free area. (A) Representative microscopy images of the scratch area are shown. (B) The quantification of scratch closure is shown. The ratio between untreated at 0 h and 16 h was set to 1. Statistics were performed with two-way-ANOVA with Bonferroni's correction. *p ≤ 0.05 ***p ≤ 0.001. (Figure adopted and modified from Nicole Weis).

To unambiguously prove the role of S1PR1 in migration, I repeated the scratch closure experiment with S1PR1 knockout mouse macrophages. Indeed, similar to human macrophages, S1PR1 deficient macrophages were unable to close the scratch after stimulation with ACM (data not shown). These *in vitro* data provide evidence for the first time that S1PR1 is necessary for macrophage motility and migration [165].

5.2.1 Elevated macrophage-S1PR1 expression increases directed migration

Whereas random migration, the so called chemokinesis, is induced by ACM (see 5.2), I wondered whether directed migration of macrophages, the so called chemotaxis, is increased likewise. To investigate the directed migration *in vitro,* I made use of a modified, automated Boyden chamber assay (xCELLigence migration system) to obtain real-time data on macrophage chemotaxis.

Therefore, I stimulated macrophages for 6 h with either ACM or IL-4, detached and reseeded them in the upper well of xCELLigence CIM-plates and allowed them to migrate towards 100 nM S1P in the lower well, until the migration reached its maximum and came to rest.

The addition of 100 nM S1P into the upper compartment again increased the undirected chemokinesis, whereas addition into both wells completely abrogated directed macrophage migration (Figure 13A). To prove the dependency on S1PR1 signaling, I repeated the experiment with addition of the S1PR1/3 inhibitor VPC23019 to the macrophages, which again completely abolished macrophage migration towards 100 nM S1P in the lower well (Figure 13B).

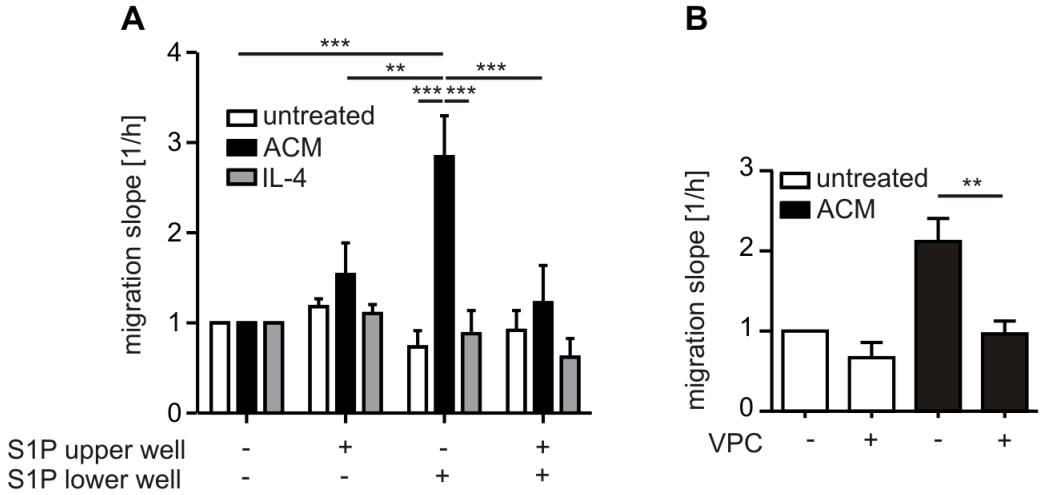

Figure 13. ACM-induced S1PR1 increases directed migration

Human macrophages were stimulated for 6 h with ACM or 10 ng/mL IL-4. Cells were detached and reseeded in the upper well of the modified xCELLigence Boyden chamber. (A) Macrophage migration in a checkerboard setup with addition of S1P into upper/lower or both wells. (B) Macrophages were left migrating towards 100 nM S1P in the lower well, with or without addition of the S1PR1/3 inhibitor VPC23019. The migration was normalized to (A) the control of each treatment (B) the untreated S1P stimulated control. Data are shown as mean ± SEM of five independent experiments. Statistics were performed with two-way ANOVA with Bonferroni's correction. **p ≤ 0.01 ***p ≤ 0.001.

Whereas stimulation with ACM led to an increase in macrophage migration towards S1P in the lower well, pretreatment with IL-4 did not affect macrophage migration (Figure 13A). This might be explained by the fact that IL-4 treatment indeed increased S1PR1 mRNA and protein, but not S1PR1 density on the cell surface (Figure 14).

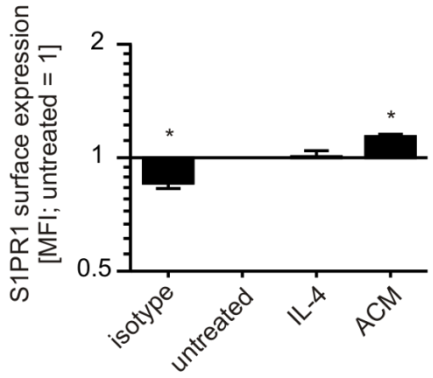

Figure 14. Surface expression of S1PR1 after alternative stimulation
Human macrophages were stimulated for 6 h with ACM or 10 ng/mL IL-4. Cells were detached and stained for S1PR1. Data are shown as mean ± SEM of four independent experiments. Statistics were performed with one-way ANOVA with Bonferroni's correction. *p ≤ 0.05.

This effect might be explained by macrophage secreted factors that result in paracrine or autocrine signaling. The long term stimulation of macrophages with S1P in ACM, for example, results in secretion of VEGF [63] and other factors that can regulate S1PR1 expression through receptor transactivation. To determine whether transactivating receptor tyrosine kinases (RTK) are involved in IL-4-mediated S1PR1 regulation, I performed the aforementioned random migration scratch assay (see 5.2) with supplementation of the RTK inhibitor genistein. As supposed, the scratch closure of IL-4-stimulated macrophages, just as S1P-treated macrophages, was entirely prevented in the presence of genistein (Figure 15).

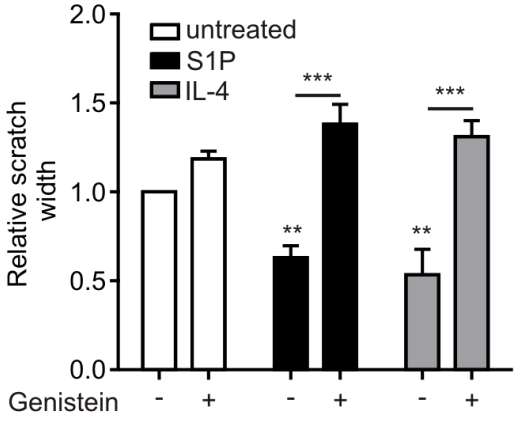

Figure 15. Inhibition of RTK inhibits macrophage migration towards S1P
Scratches were inflicted into confluent macrophage populations as described under Figure 12. These populations were left migrating for 16 h with the addition of 100 nM S1P or 10 ng/mL IL-4 ± 25 µM genistein. Scratch width was determined by measuring the cell free area under the light microscope. Data are mean values ± SEM of five independent experiments. Statistics were performed with two-way-ANOVA with Bonferroni's correction. **p ≤ 0.01 ***p ≤ 0.001.

To expand the conclusions from the *in vitro* experiments to physiological or even pathophysiological situations, I decided to introduce a more physiological macrophage stimulation protocol. In contrast to apoptotic tumor cell supernatants, which do not exist *in vivo* in such a pure form, the confrontation of macrophages with apoptotic neutrophils is a common situation in almost every inflammatory event. To determine whether apoptotic neutrophils are equally potent to induce macrophage-S1PR1 expression and migration, I generated apoptotic neutrophils from primary human blood. After induction of apoptosis, I used the whole mixture of apoptotic neutrophils and their secretions (AN) to stimulate the primary human macrophages. After this incubation I subjected the macrophages to mRNA quantification by qPCR (Figure 16A) or migration assay in the modified Boyden chamber (Figure 16B). In accordance with my earlier ACM findings, AN were able to induce S1PR1 expression and resulted in an identical chemokinetic response as apoptotic cell supernatants (compare Figure 13).

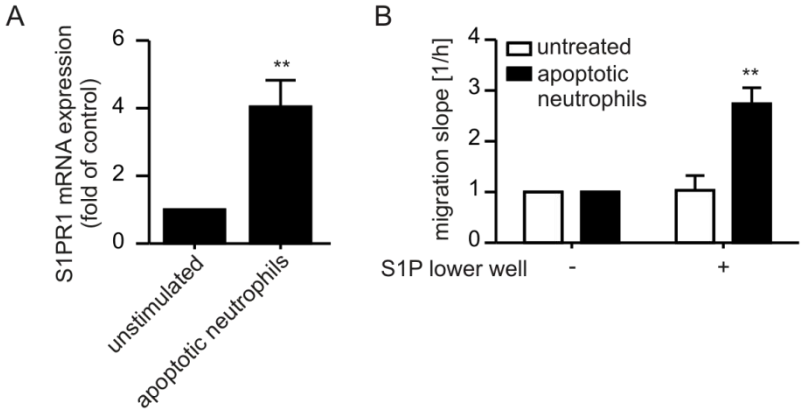

Figure 16. Apoptotic neutrophils increase S1PR1 mRNA and migration

Human macrophages were stimulated with apoptotic neutrophils for (A) 3 h (B) 6 h. (A) S1PR1 mRNA expression was analyzed by qPCR. Data are mean ± SEM of five independent experiments. (B) Stimulated macrophages were detached and seeded in the upper well of the modified Boyden chamber and allowed to migrate towards 100 nM S1P. Data are mean ± SEM of at least 3 independent experiments. Statistics were performed with (A) Student's t-test (B) two-way-ANOVA with Bonferroni's correction. **$p \leq 0.01$.

5.3 Post-inflammatory migration of mouse macrophages is S1PR1-dependent *in vivo*

From the results I obtained in the first set of *in vitro* experiments, I concluded that apoptotic cells are able to induce macrophage-S1PR1 expression in general. To determine whether this regulation also occurs *in vivo*, I decided to transfer the *in vitro* experiments to an acute inflammatory mouse model of self-resolving peritonitis.

5.3.1 The suitability of the conditional knockout system

To analyze the changes on macrophage polarization and migration in absence of S1PR1, I made use of a conditional (CRE-loxP) S1PR1 knockout mouse model as described in 4.1.2.3. In brief, the promoter of the membrane receptor F4/80 triggers the expression of the CRE recombinase and causes the deletion of the loxP flanked S1PR1. Since F4/80 is highly specific for mouse macrophages, the deletion of the S1PR1 occurs exclusively in macrophages [158, 159].

To verify the specificity and efficiency of the knockout system, I used a double fluorescent reporter mouse harboring two fluorescences, separated by a stop codon, flanked by loxP sites, resulting in the expression of only one fluorescence per time (Figure 17) [156].

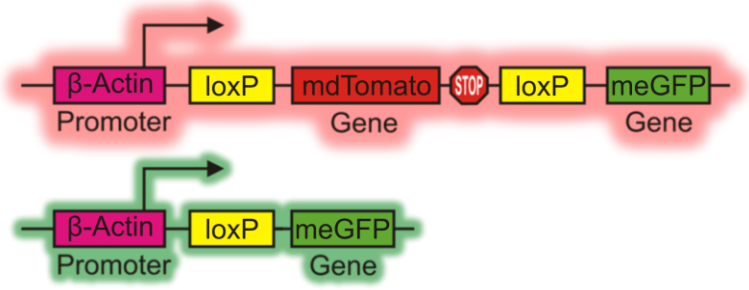

Figure 17. mdT/meG double fluorescence reporter construct
Reporter mice were constitutively expressing the shown construct under an additional β-Actin promoter. Expression of active CRE recombinase results in the deletion of the mdTomato gene and the terminating stop codon, thereby allowing expression of meGFP.

In order to determine the active efficiency of the CRE-loxP-mediated conditional knockout, I analyzed the mdT/meG reporter expression in peritoneal macrophages and splenocytes from F4/80$^{CRE/wt}$mdT/meG$^{+/wt}$ mice by flow

cytometry. The expression was highest in $CD45^+CD11b^+F4/80^+$ resident peritoneal macrophages (Figure 18A), whereas $CD45^+CD11c^+F4/80^{+/-}$ peritoneal dendritic cells (Figure 18B), $SSC^{int/high}CD45^+CD11b^+SiglecF^+$ peritoneal eosinophils (Figure 18C) or $CD45^+CD11b^+Ly6G^+$ peritoneal neutrophils (Figure 18D) were devoid of meGFP expression. Hence, the reporter mice provide an indication about the high specificity of the F4/80 triggered CRE expression in macrophages.

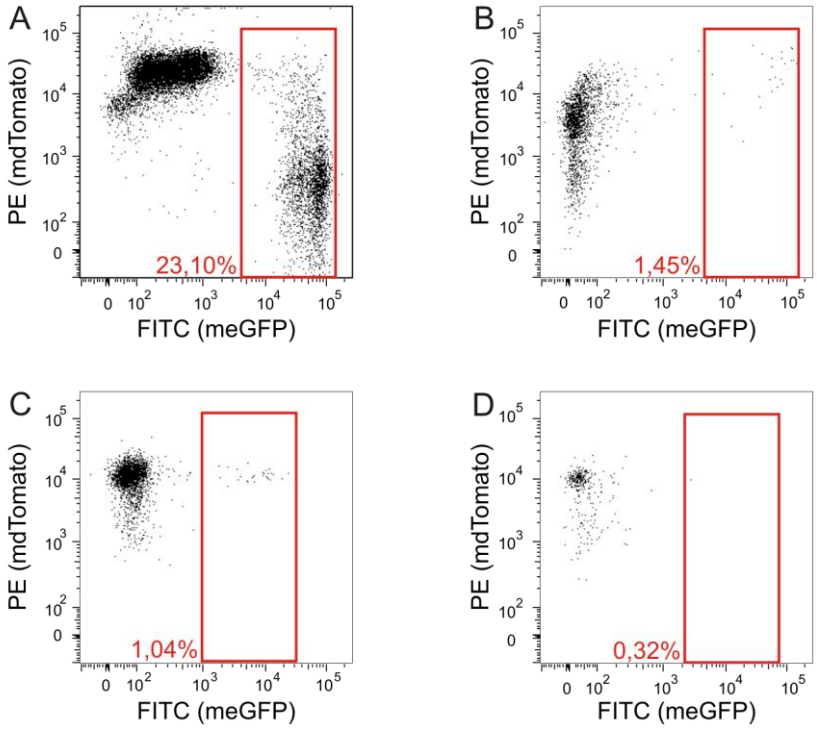

Figure 18. Expression of meGFP in various cell types
Peritoneal macrophages from healthy mice were isolated by lavage and stained for surface markers (see Figure 20). (A) peritoneal macrophages, (B) peritoneal DCs, (C) peritoneal eosinophils, (D) peritoneal neutrophils. One representative blot is shown.

To analyze the effect of S1PR1 deficiency on resolving inflammation, I injected $S1PR1^{fl/fl}$-$F4/80^{CRE/+}$ mice and their corresponding wildtype $S1PR1^{wt/wt}$-$F4/80^{CRE/+}$ with 10 mg/kg zymosan A, which provokes an acute but transient inflammation peaking around day 3 and slowly resolving afterwards. This inflammation is characterized by a rapid infiltration of neutrophil granulocytes within 12 hours, followed by infiltration of $Ly6C^+$ monocytes, which subsequently differentiate into macrophages. The macrophage numbers peak around day 3 after the induction of inflammation and emigrate in the following days [176]. Six days post-induction, when the acute inflammation is resolved, neutrophil

numbers reach the homeostatic amount, whereas infiltrated macrophages can remain in the peritoneal cavity up to several weeks.

However, to verify the functionality of the S1PR1 knockout, I first isolated mRNA from macrophages and quantified the reduction of S1PR1 expression. Indeed, as indicated by the reporter system, the mRNA expression of peritoneal macrophages 6 days post-induction was about 3 to 4 times higher in the corresponding wildtype, compared to the knockout mice (Figure 19). Approximately 30 % of the macrophages in the peritoneal cavity retained the receptor expression. This discrepancy to the reporter mice, where about 20 % achieved a switch in the reporter fluorescence, indicates how variable the CRE-loxP system works and that it has to be verified for every knockout system individually.

However, this reduction was sufficient for my *in vivo* demonstration, but it explains in part why the F4/80-CRE model is not commonly used, especially for experimental systems where 100 % knockout efficiency is required.

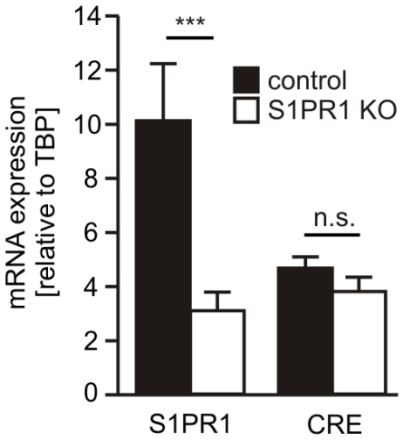

Figure 19. Macrophage-S1PR1 expression in corresponding wt and KO
S1PR1 and CRE recombinase mRNA were quantified by qPCR 6 days after induction of peritonitis with zymosan A. Expression levels were calculated as $2^{(-\Delta Cq)}$ relative to TBP. Statistics were performed with two-way-ANOVA with Bonferroni's correction. ***p ≤ 0.001.

5.3.2 FACS identification of peritoneal immune cells

To examine phagocytosis of zymosan A particles and furthermore, to directly identify the macrophages that remain in the peritoneum after the resolution of inflammation, I injected AlexaFluor488 (AF488)-labeled zymosan A particles. Whereas FITC-conjugates lose their fluorescence rapidly, AlexaFluor488 remains stable for the whole experimental period.

To analyze the peritoneal immune cell composition in detail, I established a multicolor antibody panel and a gating strategy, suitable for the unambiguous identification of the most relevant immune cell subsets as depicted in Figure 20. The used antibodies are listed in Table 3. By addition of fluorescent counting beads, I was able to quantify the absolute amount of immune cells within the peritoneal cavity.

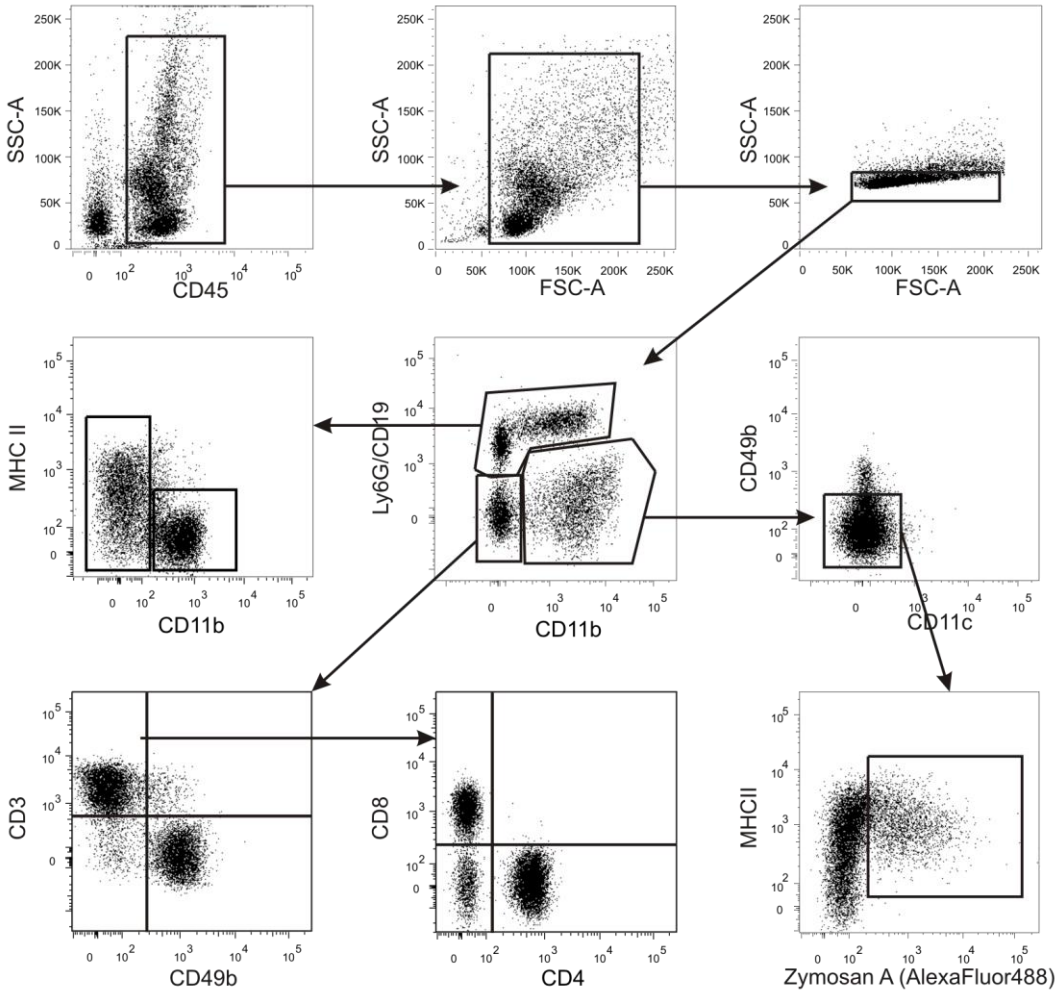

Figure 20. Gating strategy of peritoneal immune cells

First, $CD45^+$ single cells were identified. Dead and doublet cells were excluded by their FSC and SSC characteristics. Of all living single immune cells the following populations were defined: macrophages ($CD11b^+Ly6G^-CD19^-CD49b^-CD11c^-F4/80^+$), B cells ($CD11b^-Ly6G^-CD19^+MHCII^{+/-}$), neutrophils ($CD11b^+Ly6G^+CD19^-MHCII^-$), $CD4^+$ T cells ($CD11b^-Ly6G^-CD19^-CD3^+CD4^+CD8^-$), $CD8^+$ T cells ($CD11b^-Ly6G^-CD19^-CD3^+CD49b^-CD4^-CD8^+$), NK cells ($CD11b^-Ly6G^-CD19^-CD3^-CD49b^+$). In AlexaFluor488-coupled-zymosan A injected mice, macrophages were analyzed for their AlexaFluor488 fluorescence as the marker for zymosan A phagocytosis. The data shown are representative of three independent experiments with at least 3 mice each.

With the established FACS panel, I was able to discriminate the different immune cell subsets within the peritoneal cavity before, during and after the acute inflammation. The use of fluorescent zymosan A biospheres revealed that neutrophils and macrophages engulf the particles during inflammation to a comparable extent (Figure 21), although neutrophils predominantly take up free particles, whereas macrophages take up free particles as well as zymosan A containing apoptotic neutrophils.

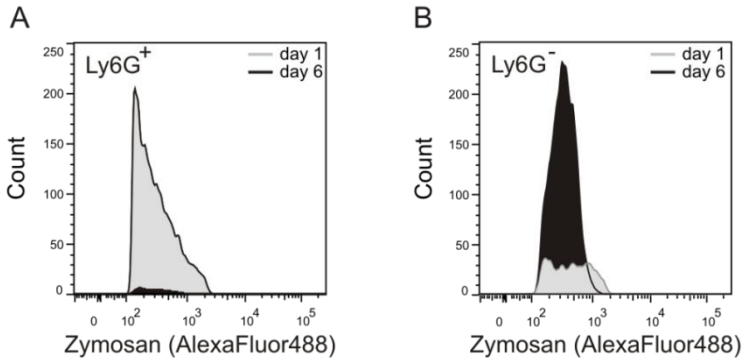

Figure 21. Zymosan A phagocytosis by neutrophils and macrophages *in vivo*
Zymosan A was injected intraperitoneally at day 0. Peritoneal immune cells were harvested by lavage at day 1 or day 6 after peritonitis induction. Immune cells were analyzed as indicated in Figure 20. (A) AF488 positive $CD11b^+Ly6G^+$ neutrophils (B) AF488 positive $CD11b^+Ly6G^-$ macrophages. One representative histogram each is shown.

5.3.3 F4/80-mediated S1PR1 KO increases post-inflammatory macrophage counts

With these experimental options, I investigated the general immune cell composition at day 0 (before) and at day 6 after induction of peritonitis. Six days post-induction I observed a significant increase in the $CD11b^+$ immune cell fraction, which comprised mainly granulocytes, monocytes and macrophages. To analyze this subset in more depth, I gated on the F4/80 positive population that consisted to more than 95 % of macrophages (data not shown). Within this population I examined the AF488 positive cell fraction, which had ingested zymosan A particles. Not only the ($F4/80^+$) macrophage population was significantly increased in the S1PR1 knockout mice (Figure 22A), but especially the AF488 positive fraction within the $CD11b^+F4/80^+$ parent population (Figure 22B). Whether this increase was due to an increased uptake of zymosan could not be determined in the FACS analysis and was investigated in the following experiments.

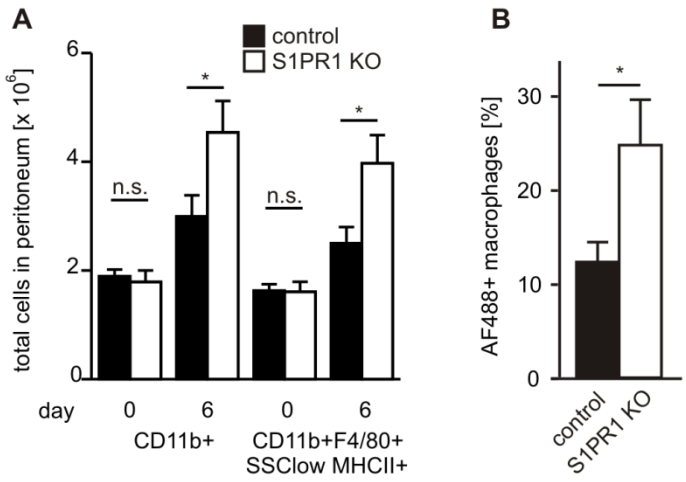

Figure 22. CD11b$^+$ immune cell subsets before and after inflammation
Zymosan A was injected intraperitoneally at day 0. Peritoneal immune cells were harvested before (day 0) or after (day 6) inflammation by peritoneal lavage and analyzed by flow cytometry as depicted in Figure 20. (B) Bone marrow derived macrophages that ingested zymosan A were identified by within the macrophage population. Data are mean ± SEM of nine mice per group and pooled from four independent experiments. Statistics were performed with (A) two-way-ANOVA with Bonferroni's correction (B) Student's t-test. n.s.: not significant, *p ≤ 0.05.

5.3.4 F4/80-mediated S1PR1 KO does not alter general immune cell counts

To verify that S1PR1 deficiency does not generally affect the immune cell composition in naïve mice or after the inflammatory process, I quantified the total immune cell amount in the peritoneum at both time points. As the most abundant and relevant cell types in inflammation, I chose B cells, neutrophil granulocytes, CD3$^+$ T cells and NK cells for FACS analysis. Although the knockout mice revealed a slight increase in the neutrophil numbers at day 6 after induction of inflammation, I found no significant alterations in the analyzed immune cell subset, except for the macrophages (Figure 23). These data provide evidence that macrophage-S1PR1 is dispensable for tissue homeostasis in untreated mice. Likewise, the deficiency of S1PR1 does not alter the recruitment of immune cells into the peritoneal cavity throughout the inflammatory process.

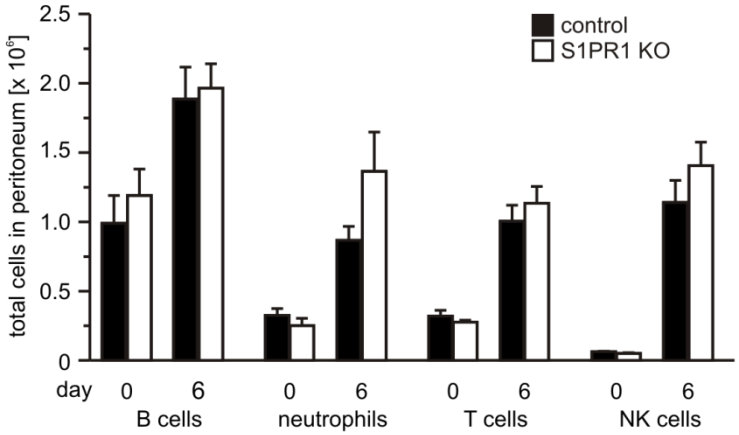

Figure 23. Cell subsets before and after inflammation in the peritoneal cavity
Immune cell populations were quantified as displayed in Figure 20, before the induction of peritonitis (day 0) or in the resolution phase of inflammation (day 6). Data are mean ± SEM from 5-9 individual mice per group.

5.3.5 Macrophage counts are not elevated due to infiltration or differentiation

To determine whether the infiltration of macrophages or monocytes respectively, accounts for the macrophage increase after 6 days, I decided to quantify the monocyte incidence at day 3, the peak point of monocyte infiltration. As proposed, I observed neither a change in the quantity of infiltrated monocytes, nor in the number of already differentiated macrophages (Figure 24).

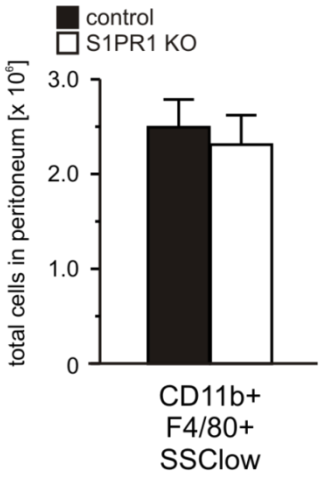

Figure 24. Macrophage counts at day 3 post inflammation are equal
Peritoneal cells were isolated by peritoneal lavage at day 3 after injection of zymosan A and identified by flow cytometry as depicted in Figure 20. Data are mean ± SEM of at least 6 individual mice per group.

As the deficiency of S1PR1 apparently does not affect the infiltration and differentiation of monocytes, I addressed the question if other events than emigration, such as proliferation or reduced apoptosis, might explain the macrophage excess in the peritoneum.

5.3.6 Macrophage proliferation and survival are not affected by S1PR1 knockout

Although the infiltration and differentiation were not affected in S1PR1 KO mice, emigration is not the sole reported functional effect of S1PR1 expression. Several experiments could demonstrate the role of S1P on cell survival and proliferation [64, 85]. Additionally, it could be shown that proliferation is one important process in peritoneal inflammation models, especially for peritoneal resident macrophages [177]. Therefore, I determined macrophage proliferation and apoptosis with the automated xCELLigence system after stimulation with typical cytokine combinations. In both experiments, bone marrow differentiated macrophages from both genotypes behaved identically (Figure 25). These experiments clearly rule out a decreased survival or increased proliferation of knockout macrophages as the reason for increased macrophage numbers following inflammation.

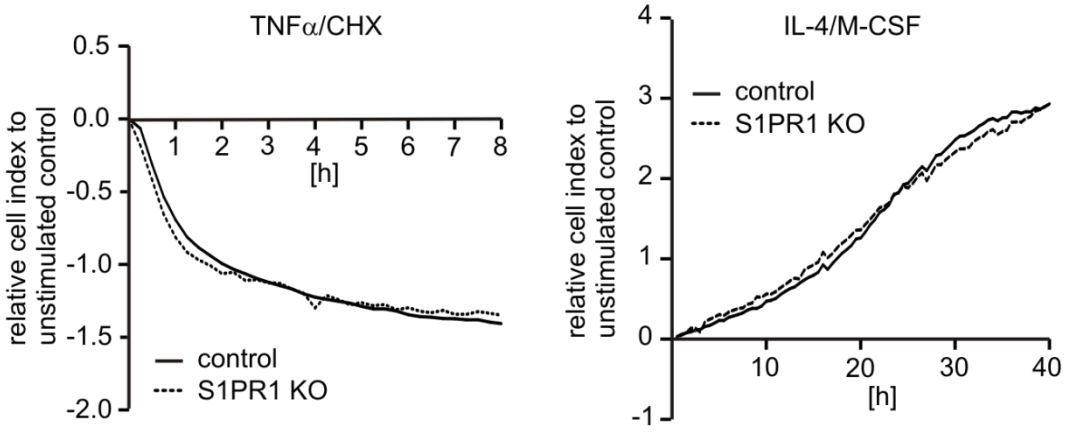

Figure 25. Macrophage survival and proliferation are not affected by S1PR1 KO
Primary bone marrow derived macrophages were generated as described in 4.2.3. Cells were detached and seeded at 5E4 cells/well on xCELLigence E-Plates and stimulated with (A) TNFα (10 ng/mL) / CHX (10 µg/mL) to induce cell death (B) or IL-4 (10 ng/mL) / M-CSF (20 ng/mL) to induce proliferation for the indicated times. Cell indices were calculated as relative to the recorded baseline. The curves shown are mean of four individual experiments each.

5.3.7 Phagocytosis of zymosan A is not regulated by S1PR1

To prove that the increase of AlexaFluor488 positive macrophages is not due to increased phagocytosis, I analyzed the ability of zymosan A uptake by bone marrow derived macrophages *in vitro.* Therefore, I incubated primary bone marrow derived macrophages for 1 hour with a ratio of 10 AlexaFluor488-labeled particles per cell and analyzed AF488 fluorescence afterwards by flow cytometry. Again, both genotypes did not differ in their behavior, resulting in an identical uptake of AF488-labeled zymosan A particles (Figure 26). These data prove that the loss of S1PR1 does not affect the phagocytosis capability of bone marrow derived macrophages, which are most abundant during peritoneal inflammation.

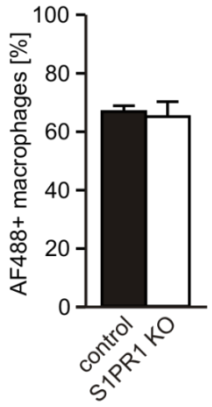

Figure 26. S1PR1 knockout does not influence zymosan A phagocytosis
Bone marrow derived mouse macrophages were incubated with 10 AlexaFluor488-labeled zymosan A particles per cell for 1 h, followed by flow cytometric analysis. Data are mean ± SEM of 4 individual mice per group.

5.4 The effect of S1PR1 on macrophage polarization in resolution of acute inflammation

In 2009 our group could show the relevance of apoptotic cell derived S1P on the expression of M2 polarization markers in macrophages [25]. To explore if this regulation is of relevance in S1PR1 deficiency during acute inflammation, I used the RNA and primary peritoneal lavage to determine the polarization state of resolution phase macrophages from the zymosan A inflammation model.

5.4.1 Inflammatory cytokines are not altered in S1PR1 knockout macrophages

In a first set of experiments I used the primary peritoneal lavage after 6 days and the RNA from overnight cultured macrophages from the lavage. Within the lavage I quantified the most relevant inflammatory cytokines (IL-6, MCP-1, TNFα, IFNγ) by cytometric bead array (CBA) (Figure 27). Although S1P signaling has been proven to be relevant for alternative macrophage activation and termination of inflammation, I did not observe alterations in the amount of secreted inflammatory cytokines.

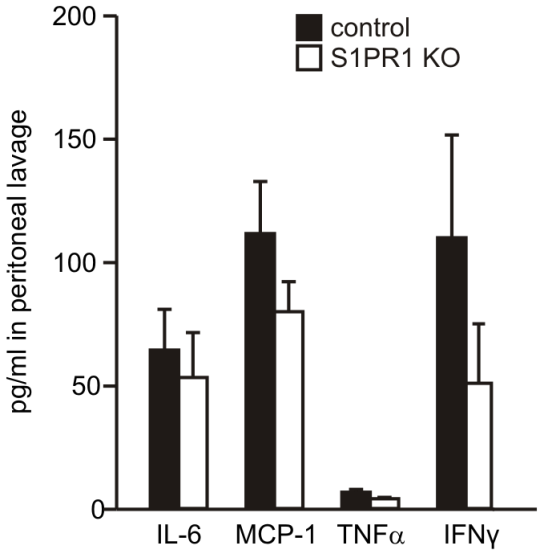

Figure 27. Peritoneal cytokine secretion
Peritoneal lavage, 6 days after peritonitis induction, was analyzed by CBA as described in 4.2.15. Data are mean ± SEM of 9 individual mice per group.

However, the absence of alterations in cytokine secretion raises the question if the activation state is changed in general. Therefore, I analyzed the macrophage RNA for typical “M1” and “M2” polarization markers. The most commonly used markers for M2 polarization, YM-1, ARG1, Fizz1, as well as the typical M1 markers IL-1β, iNOS and TNFα revealed no evident changes in macrophage polarization between S1PR1 KO and wildtype (Figure 28). Even though S1P could be demonstrated as a relevant mediator for immune cell polarization, it is apparently not involved in M2-polarization of macrophages through S1PR1 in the resolving phase of peritonitis.

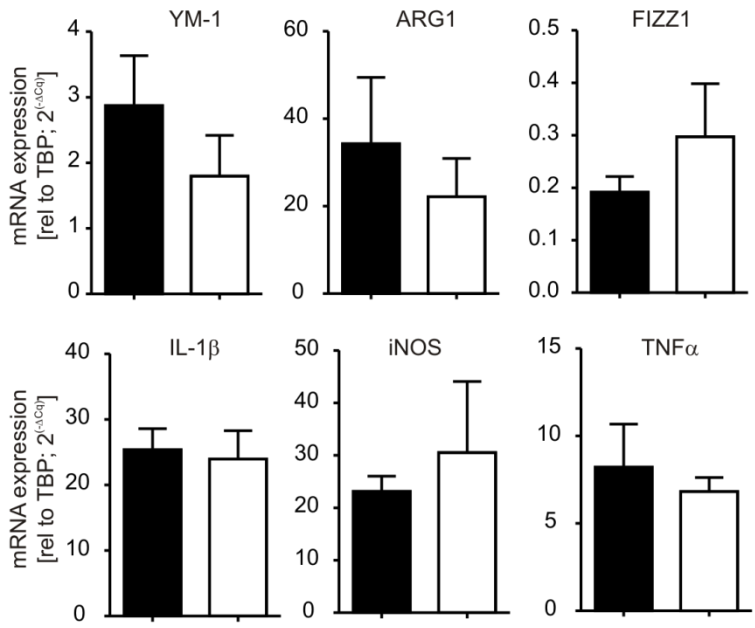

Figure 28. RNA expression patterns of polarization markers
Adhesion selected macrophages from peritoneal lavage were subjected to mRNA isolation and analyzed by qPCR for the indicated mRNAs. Data are mean ± SEM of 9 individual mice per group.

5.5 Sphingosine kinases and macrophage-S1PR1 in tumor growth and development

My second experimental topic concerned the role and relevance of SphK1, SphK2 and macrophage-S1PR1 in cancer development and tumor growth. It is widely accepted, that the intracellular enzyme SphK1 exerts tumor promoting properties, which are involved in signaling of many growth factor pathways [150, 178]. In line with this, several studies could prove an aberrantly high expression and activity of SphK1 in diverse cancer types [179-181].

However, not only SphK1 plays a critical role in cancer development. Recently one study provided evidence that SphK2 might as well be involved in tumor development and could serve as a prognostic marker for cancer patients [182]. Additionally, earlier experiments of our group demonstrated that SphK2-dependent S1P production during apoptosis results in alternative immune cell activation and tumor growth [25], as well as increasing chemoresistance by interfering with other signaling pathways [183].

To figure out the roles of sphingosine kinases and macrophage-S1PR1, I chose a carcinogen-induced inflammatory cancer model, the 3-methylcholanthrene (MCA) cancer model and an endogenous breast cancer

model, the polyoma middle T oncogene knock-in breast cancer model (PyMT) for my investigations (see 4.1.2.2).

To discriminate between the relevance of sphingosine kinases in hematopoietic and tissue cells, I created bone marrow chimeras from SphK1KO, SphK2KO and UbiC$^{GFP/+}$ mice. Unfortunately, PyMT breast carcinogenesis starts already after 4 to 6 weeks of life [184], which is before the possibility to perform a bone marrow transfer. Therefore I used the bone marrow chimera system only for the MCA cancer model.

In contrast to the germ-line knockout mice, the macrophage-S1PR1 knockout model (S1PR1 KO) affects almost exclusively macrophages, due to the F4/80-promoter triggered CRE expression (4.1.2.3). Accordingly, these mice were not subjected to a bone marrow transfer and directly used in comparison to their corresponding wildtype animals, lacking the loxP sequences in the S1PR1 gene.

5.5.1 Generation of bone marrow chimeras

The role of sphingosine kinases in cancer cells was analyzed thoroughly in the last decade. Especially the role of SphK1 derived S1P for migration, survival and proliferation was shown in various experiments [34, 185, 186]. Further research found SphK1 involved in inflammatory signaling, especially in the signal transduction towards NF-κB [187, 188]. Hence, SphK1 might be involved in tumorigenic inflammation, as well as in protective, tumor rejecting inflammation. Other than SphK1, SphK2 is expressed in the nucleus and the mitochondria, where it regulates HDACs [21, 189] and mitochondrial integrity [26, 190]. However, its role in tumor cells and tumor-infiltrating cells remains elusive up to date.

To identify the cell type specific effect of SphK deficiency, I created bone marrow chimeras as described in 4.2.4. In brief, mice were irradiated with a sub-lethal dose of 9 Gy, which is sufficient to eradicate the host bone marrow. Afterwards, bone marrow from donor mice was grafted intravenously to the irradiated recipient mice. The engraftment was verified by appearance or disappearance of UbiC$^{GFP/+}$ positive cells in the peripheral blood 6 weeks after transplantation (Figure 29B). Collectively, the bone marrow engraftment worked in 100 % of transplanted mice after 6 weeks, along with the absence of host bone marrow recovery within 190 days follow-up (Figure 29).

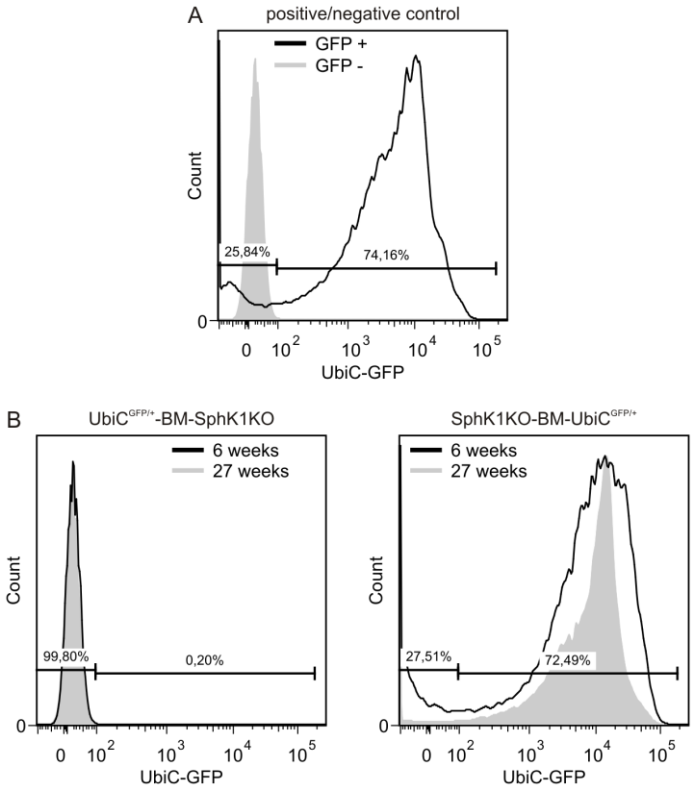

Figure 29. Efficiency of the bone marrow transfer

Mice were irradiated with 9 Gy, followed by injection of donor bone marrow. 6 weeks after the transfer, a blood sample was taken from each mouse and analyzed by FACS for GFP expression. 27 weeks after the transfer, the experiment was ended and the mouse sacrificed. Data shown are representative plots of all mice used in the experiment. Percents shown are data from (A) the positive control or (B) week 27.

5.5.2 Tumor incidence and growth in chronic inflammatory cancer mice

For carcinogenesis experiments, knockout and chimeric mice were anesthetized, subcutaneously injected with 100 µg MCA in 100 µL corn oil into the right flank and monitored for 150 days. Tumor mass, tumor burden and the development of metastases were analyzed after sacrifice. During the experimental time course, all mice were monitored at least twice a week and the tumor diameter was determined using a sliding caliper. When the tumor reached the size of 2 cm, showed visible lesions (ulceration), or the mouse was potentially suffering, it was sacrificed and cardially perfused with 0.9 % NaCl solution. Afterwards, the tumor was excised and its size and weight were determined. Lung and liver were removed for immunohistochemical analysis of metastasis (4.2.16).

Surprisingly, all genotypes and chimeras exhibited a tumor incidence of more than 80 % (Figure 30), although Swann et al. demonstrated a tumor incidence of about 60 % for C57BL/6 wildtype mice with a MCA dose of 100 µg [191]. Thus, my model was limited in the possibility to prove an increase in tumor incidence. Albeit this, I found no obvious difference in the tumor occurrence, although SphK1KO mice exhibited the lowest rate of tumor occurrence. Solely the reduction of tumor formation in SphK2KO mice with UbiC$^{GFP/+}$ bone marrow (SphK2-BM-UbiC$^{GFP/+}$) was remarkable, as the opposing chimera (UbiC$^{GFP/+}$-BM-SphK2KO) revealed 100 % tumor incidence, similar to the SphK2KO mice (Figure 30).

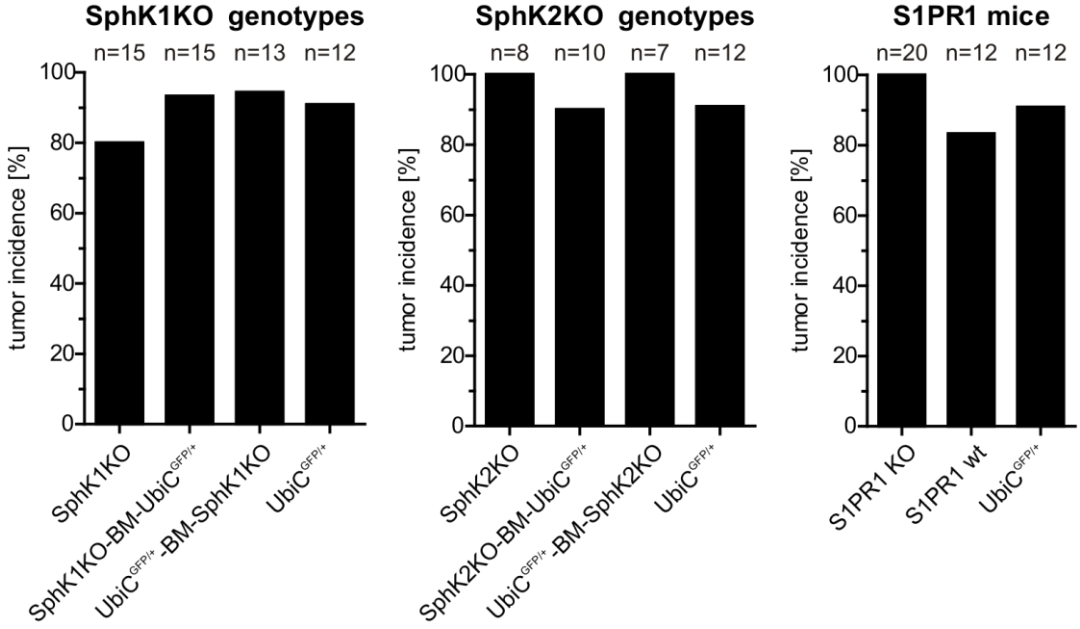

Figure 30. Tumor incidence in all MCA injected knockouts and chimeras
Tumor incidence in all genotypes was calculated at the end of the experiments. UbiC$^{GFP/+}$ mice serve as control mice for SphK1 and SphK2 chimeras. S1PR1 wt serves as corresponding wildtype to macrophage-S1PR1 KO mice.

As further parameters for the analysis of tumor development I chose the time point when the tumor was first palpable and when it reached a diameter of 1 cm. These two time points designate the steps of tumor initiation (palpable) and tumor outgrowth without immune control (1 cm). Except for SphK2-BM-UbiC$^{GFP/+}$, compared to UbiC$^{GFP/+}$ mice, I found no statistical significant changes between the genotypes (Figure 31A, B). This finding is in line with previous data, demonstrating that SphK2 deficiency hampers tumor growth by reducing the ability to polarize immune cells into a tumor promoting phenotype [25]. Furthermore, the presumably reduced tumor incidence in

SphK2KO-BM-UbiC$^{GFP/+}$ mice (Figure 30) emphasizes an involvement of SphK2 in cancer development and outgrowth.

However, the lack of effects in the SphK1 genotypes was unexpected, as most SphK related cancer effects were attributed to SphK1 so far. The only effect I could determine in my experimental setup was a slight but not significant reduction in the time span until tumor formation in UbiC$^{GFP/+}$-BM-SphK1KO mice (Figure 31A). This effect might be explained by the pro-inflammatory role of SphK1 signaling within immune cells [192, 193] and hence, a reduced tumor control in SphK1 deficient mice.

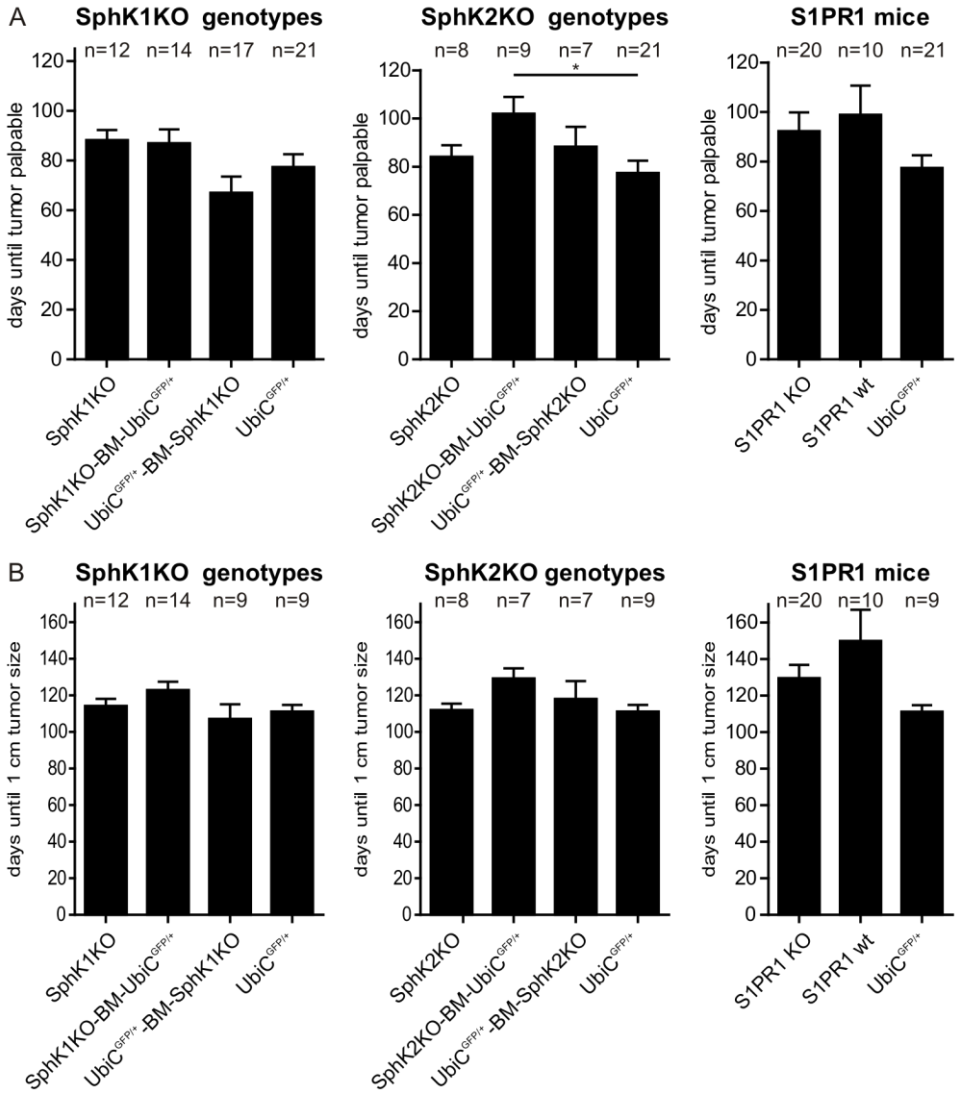

Figure 31. MCA tumor onset and outgrowth

All mice were examined for tumor development twice weekly. Tumor outgrowth was monitored by measuring with sliding calipers for the largest diameter (A, B). Data are mean ± SEM of the number of mice stated above, UbiC$^{GFP/+}$ mice served as reference. Significances were determined by one-way ANOVA. *p ≤ 0.05.

As the measure for the overall tumor outgrowth, I quantified the days until the mice had to be sacrificed due to their tumor size. Although there were no significant changes in this time span – regardless of the genotype – I observed apparent changes in the tumor burden. Even though it was not significant compared to the UbiC$^{GFP/+}$ control animals, SphK1KO exhibited the strongest tumor outgrowth of all genotypes. Together with the finding of reduced tumor initiation by inflammation, this can be explained by the involvement of SphK1/S1P signaling in inflammation, but here due to reduced tumoricidal responses.

In contrast to the SphK1 chimeras, SphK2KO-BM-UbiC$^{GFP/+}$ mice showed an almost significantly delayed tumor outgrowth, indicated by a reduced tumor burden at the end of the experiment (Figure 32A), concomitant with an increased time span until sacrifice (Figure 32B). This finding is in line with the aforementioned delay of tumor formation in this genotype.

Finally, the significant increase of the tumor burden in S1PR1 KO mice, together with an increased lifetime until sacrifice in the wildtype, is counterintuitive, as recent publications propose a tumor promoting feed forward signaling loop *via* the S1P-S1PR1-STAT3 axis [49, 132, 194-196]. According to this hypothesis, S1PR1 deficiency should reduce the tumor burden instead of promoting tumor outgrowth (Figure 32A).

However, the almost significant difference in tumor growth and tumor burden between UbiC$^{GFP/+}$ wildtype and the S1PR1 corresponding wildtype was likewise surprising (Figure 32A). Both strains origin from the same C57Bl/6 background and differ only in the heterozygous loss of F4/80. Whether these genetic changes, minor variations in the genetic background, or a potential underpower of the study account for the difference remains arguable.

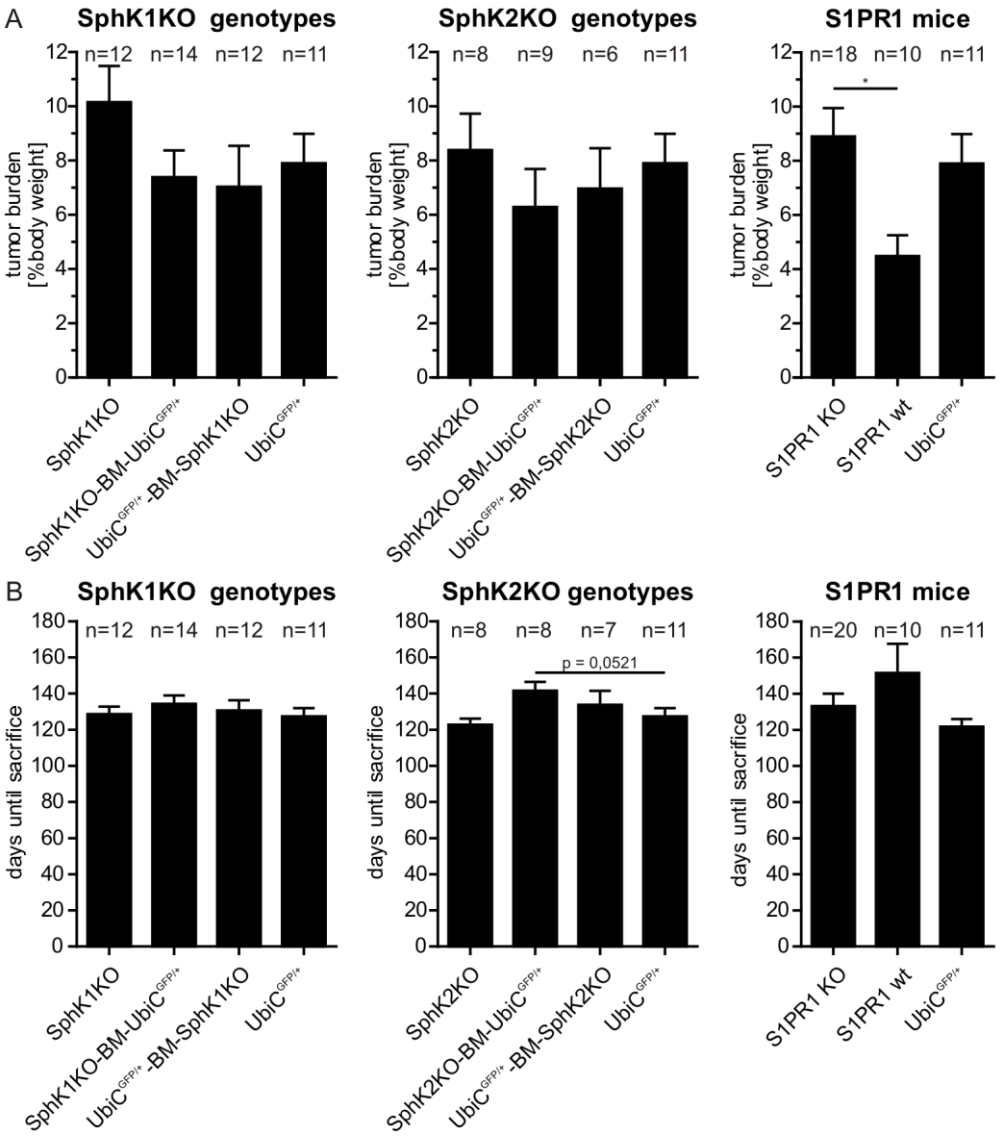

Figure 32. MCA tumor burden and days until sacrifice

At the end of the experiment (A) tumor mass was determined and divided by the mouse mass for tumor burden [%]. (B) Days since injection of 3-MCA. Data are mean ± SEM of the number of mice stated above, UbiC$^{GFP/+}$ mice served as reference. Significances were determined by one-way ANOVA.*p ≤ 0.05.

5.5.3 Metastasis formation in 3-MCA-induced fibrosarcomas

As metastasis is one of the most frequent fatal characteristics in cancer patients, I evaluated the frequency of metastases to lung and liver in all MCA-treated genotypes. Although almost all tumor bearing mice developed late stage carcinomas within the experimental period, no mouse developed detectable lung or liver metastases. However, only very few publications address the frequency of metastasis development in the MCA system. From the existing publications I conclude that metastasis is not a frequent or reproducible event in MCA elicited carcinogenesis [197].

5.5.4 Tumor incidence and growth in PyMT mice

As the MCA cancer model clearly represents a system of strong and chronic inflammation, I wondered about the relevance of SphK or S1PR1 deficiency in a different cancer model that depends on oncogene-driven tumorigenesis. Therefore, I chose a genetic breast cancer mouse model as my second mouse cancer model (see 4.1.2.2). In brief, the PyMT mice harbor the middle T oncogene of a mouse polyoma virus under the control of the mouse mammary tumor virus LTR (MMTV LTR). Thus, the tumorigenic process is restricted to the mammary epithelium. Due to the expression of the viral proteins, several growth-signaling pathways, such as src, ras and PI3K, are exploited and commonly overexpressed [198]. Cancer development and cell characteristics – loss of estrogen and progesterone receptors, overexpression of ErbB2/Neu and cyclin D1 – are comparable to human breast cancer and equally linked to a poor prognosis [184]. Hence, the PyMT mice represent an excellent model to replicate the MCA experiments and simultaneously link it to human breast cancer development. Therefore, I crossed the PyMT gene into SphK1KO, SphK2KO and macrophage-S1PR1 KO strains and used the PyMT-heterozygous female offspring for my experiments. However, as PyMT mice develop tumors as early as 4-6 weeks of life, it was not possible for me to determine the onset of tumor growth (due to external breeding). Thus, I chose the commonly used growth stages 0.5 cm and 1 cm as indicators for tumor onset and late stage carcinoma with presumable metastatic dissemination. However, I could not observe differences in the tumor onset (Figure 33A) and outgrowth (Figure 33B) in SphK1KO and SphK2KO mice compared to the wildtype. Contrary to this, the macrophage-S1PR1 KO mice showed a remarkable and highly significant delay in tumor onset and outgrowth (Figure 33A, B).

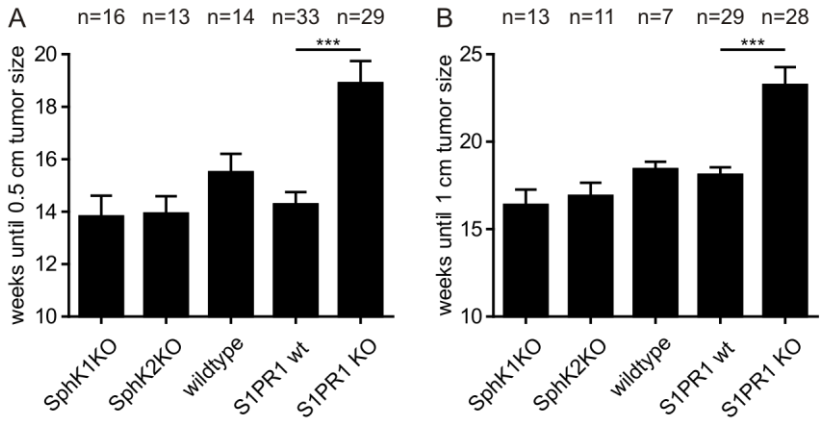

Figure 33. PyMT tumor development

All mice were examined for tumor development twice weekly. Tumor onset (A) and tumor outgrowth (B) were monitored by measuring with sliding calipers for the largest diameter. Data are mean ± SEM of the number of mice stated above, wildtype mice served as reference for SphK1KO/SphK2KO, S1PR1 wt served as reference for S1PR1 KO. Significances were determined by one-way ANOVA. ***p ≤ 0.0001.

Similar to the tumor onset, the lifetime of SphK1KO, SphK2KO, wildtype and S1PR1 corresponding wildtype were not altered, whereas S1PR1 KO mice lived significantly longer until they had to be sacrificed (Figure 34A). However, there was no relevant change in the measured tumor burden at the day of sacrifice detectable (Figure 34B), indicating a delayed but not reduced tumor formation.

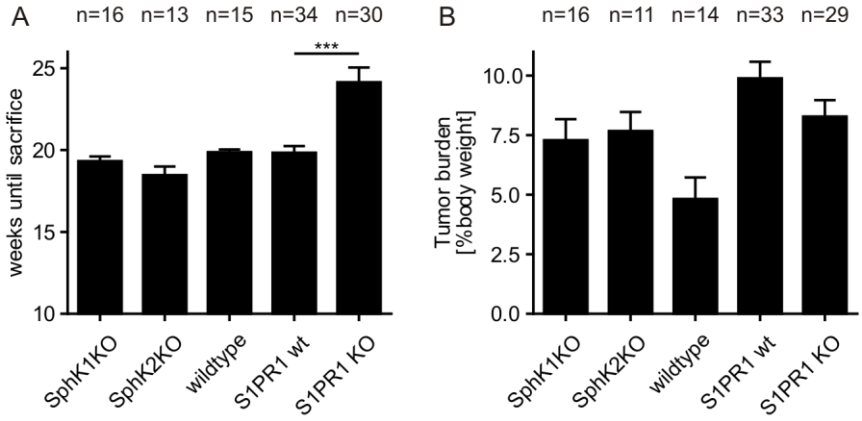

Figure 34. PyMT weeks until sacrifice and tumor burden

(A) The weeks until sacrifice were determined as the time span between birth and sacrifice. (B) At the end of the experiment tumor weight was determined and divided by the mouse weight for tumor burden [%]. Data are mean ± SEM of the number of mice stated above, wildtype mice served as reference for SphK1KO/SphK2KO, S1PR1 wt served as reference for S1PR1 KO. Significances were determined by one-way ANOVA. ***p ≤ 0.001.

5.5.5 PyMT breast cancer metastasis formation

Metastasis formation is a frequent and typical feature of malignant breast carcinomas and the leading cause of death in breast cancer patients [199]. To identify distant metastasis formation, I performed immunohistochemistry of the lung, as the most common organ for metastasis formation. Therefore, all mice were cardially perfused with 0.9 % NaCl to reduce erythrocyte contamination of the tissues. Afterwards the whole lung was fixed with a zinc-fixative and embedded in paraffin blocks (4.2.16.2). The analysis and quantification of metastasis was performed in 4 µm thick sections after staining with Mayer's haemalum as explained in 4.2.16.3.

When I observed a significant reduction of lung metastasis formation in S1PR1 KO mice after 20 weeks of life (Figure 35), I wondered whether this was due to the reduced tumor burden at this time point, or because of the macrophage-S1PR1 deficiency. To avoid a bias because of the tumor load, I sacrificed the mice henceforward at the same tumor burden.

However, compared to the wildtype PyMT mice, SphK1KO mice developed significantly more lung metastases, whereas SphK2KO mice exhibited a minor and not significant increase in metastasis formation (Figure 35). Contrary to this, the S1PR1 KO mice developed significantly less metastases than their corresponding wildtype, even though they developed the same tumor burden.

With regard to this exciting outcome, I decided to further focus on the S1PR1 KO mice and their corresponding wildtype for mechanistic studies.

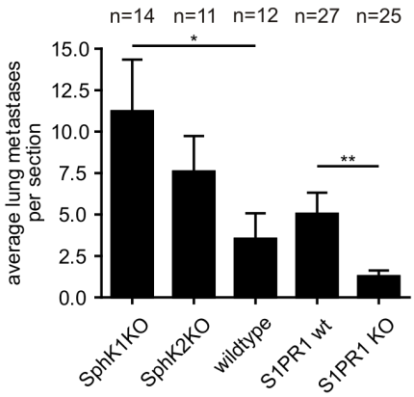

Figure 35. Metastasis formation in PyMT mice
At least nine sections of the largest lung lobe per mouse were stained and examined under the light microscope. Metastases were manually counted in the whole section. Data are mean ± SEM of the number of mice stated above, wildtype mice served as reference for SphK1KO/SphK2KO, S1PR1 wt served as reference for S1PR1 KO. Significances were determined by one-way ANOVA with Bonferroni's correction. *p ≤ 0.05,**p ≤ 0.01.

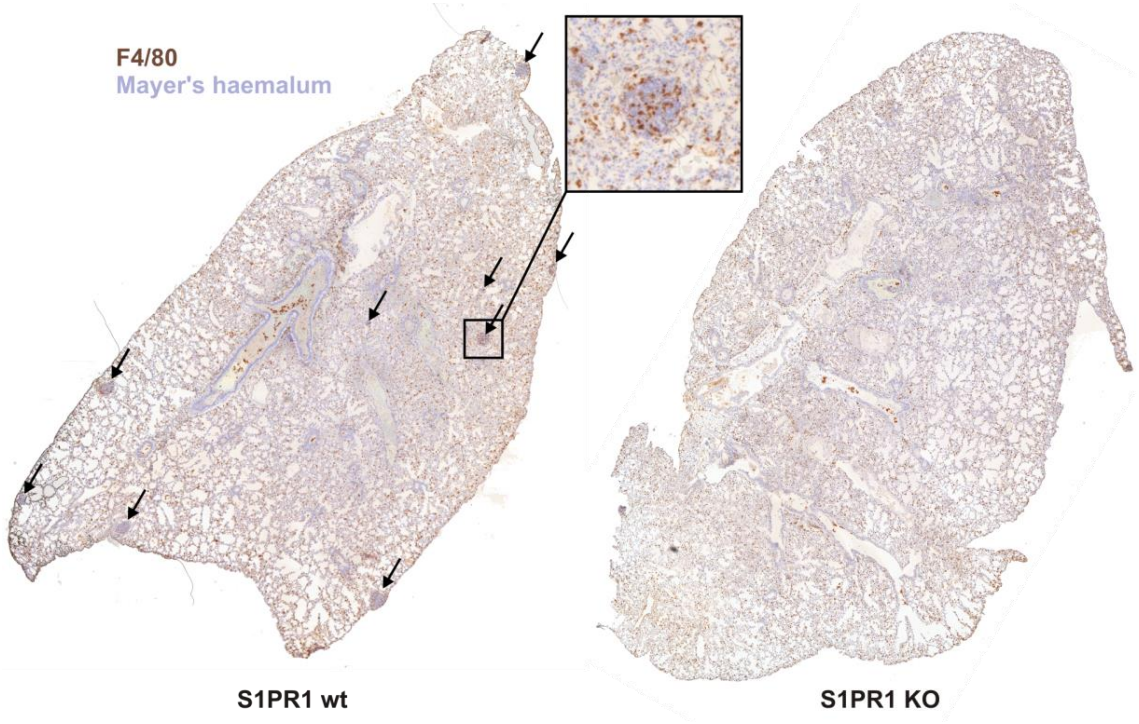

Figure 36. Lung metastasis formation in PyMT mice
Lung sections were stained with anti-F4/80 antibody with horseradish peroxidase and counterstained with Mayer's haemalum. Metastases are observable as compact cell agglomeration, infiltrated by F4/80 positive cells. Arrows indicate metastasis. All PyMT mice were analyzed for lung metastases. One representative image for each genotype is shown.

5.5.6 The role of macrophage-S1PR1 in (lymph-) angiogenesis

Besides matrix degradation, epithelial-mesenchymal-transition (EMT) and tumor cell extravasation, the existence of a functional draining vessel system is a prerequisite for metastasis formation [199, 200]. Blood and lymph vessels are the common way how tumor cells exit the primary tumor site and settle as a metastasis in distant organs. To identify whether blood vessels or lymphatic vessels are involved in PyMT metastasis, I chose immunofluorescence as the means to visualize the vessel density in the primary tumors. However, by staining for the blood vessel endothelium marker CD31 (Figure 37A) I found no significant changes within the blood vessel density, although there was a tendency to a reduction within the MCA S1PR1 KO mice. In contrast, the lymph vessel density was significantly reduced in S1PR1 KO PyMT mice, as well as in the MCA cancer mice (Figure 37B). This result was exciting, as macrophage-S1PR1 was not yet known to impact on tumor lymphangiogenesis.

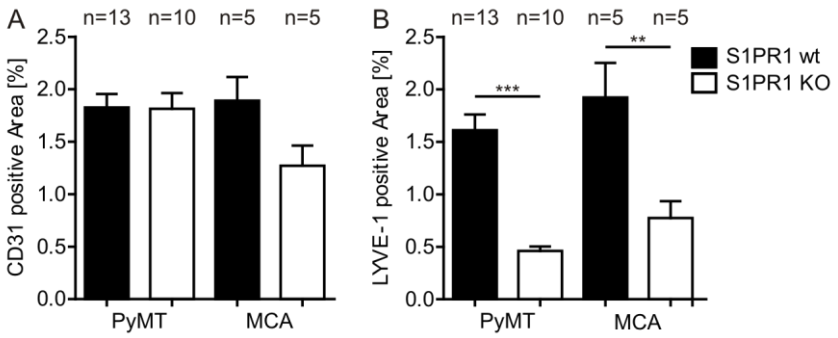

Figure 37. Angiogenesis and lymphangiogenesis in MCA and PyMT mice
Zink-fixed primary tumor samples were stained with antibodies against (A) CD31, (B) LYVE-1 and counterstained with DAPI. Pictures were taken with a fluorescence microscope. The fluorescence positive area was quantified with the AxioVision software and calculated as positive area. 3 areas of each tumor were analyzed of the number of mice stated above. Data are mean ± SEM, significances were calculated by one-way ANOVA. **p ≤ 0.01, ***p ≤ 0.001.

5.5.7 Metastatic niche preparation in S1PR1 wt and KO

The observation of a strongly reduced lymph vessel density in S1PR1 KO mice suggested lymph vessel-dependent tumor cell dissemination. However, tumor cell emigration is only one of many steps in tumor metastasis. Increasing numbers of publications emphasize the importance of the so called “pre-metastatic niche” for metastasis formation. Recently, it was suggested that simultaneous S1PR1-STAT3 signaling in tumor cells and myeloid cells together contributes to the formation of a pre-metastatic niche, especially in the lung [195]. To examine the role of S1PR1 in my experimental model, I analyzed the lungs of corresponding wildtype and S1PR1 knockout mice from both cancer models. By use of the aforementioned FACS panel (5.3.2), I quantified the so called “myeloid derived suppressor cell” (MDSC) fraction, which are presumably the most important cell type for establishing the metastatic niche. Secondary, I analyzed the immune cell composition in the lung for myeloid derived cells, as all of these might be involved in supporting metastasis growth. Although the lungs of tumor bearing mice generally held a higher amount of immune cells, only the MDSC subsets showed relevant differences. Both genotypes from both cancer models revealed a significant enrichment of granulocytic MDSCs ($Ly6G^+$) in the lungs of tumor bearing mice (Figure 38). Monocytic MDSCs ($Ly6C^+$) were likewise enriched, but significantly less than their granulocytic counterpart.

Surprisingly, all tumor bearing mice revealed this obvious accumulation of MDSC within the lung, irrespective of the cancer model or the genotype. Although I found a reduction of lung metastases in S1PR1 KO mice, it was accompanied by an increase of MDSCs in S1PR1 KO lungs, which is in contrast to the current understanding of the metastatic niche function.

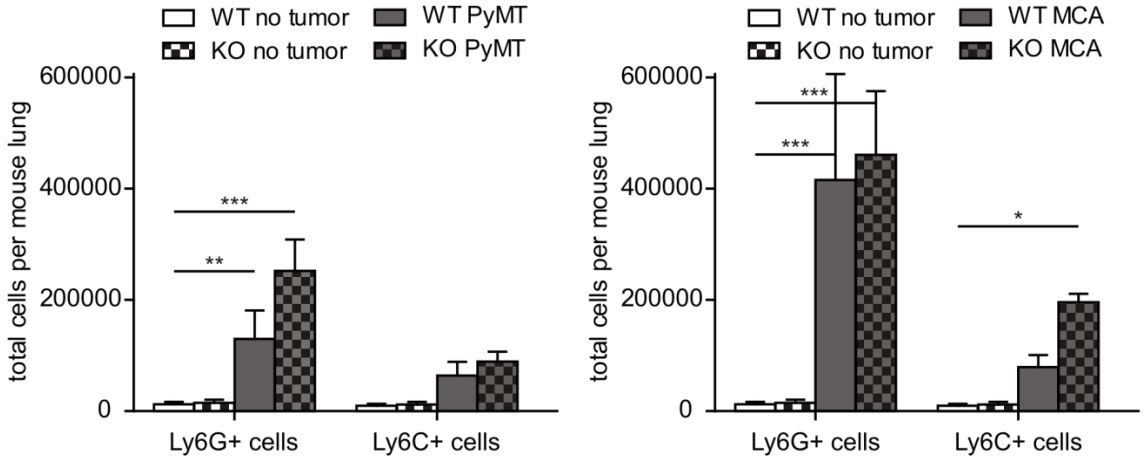

Figure 38. The lung metastatic niche in PyMT and MCA mice
Lung metastatic niche was analyzed by FACS analyzing the 4 smaller lung lobes for $CD45^{+}CD11b^{+}Ly6G^{high}Ly6C^{low}$ and $CD45^{+}CD11b^{+}Ly6G^{low}Ly6C^{high}$ cells and quantified by counting beads. Data are mean ± SEM of at least 4 mice per group, significances were calculated by two-way ANOVA. *p ≤ 0.05, **p ≤ 0.01, ***p ≤ 0.001.

To verify whether the metastatic niche formation is comparable in wildtype and S1PR1 KO mice, I designed further experiments with a more reproducible system of “conditioned medium-induced metastatic niche formation”. Therefore, mice are injected with hypoxic tumor cell conditioned medium for 5 days, which induces the formation of metastatic niches in all organs [201]. The following intravenous injection of mouse cancer cells then will result in tumor cell settling into the prepared pre-metastatic niche and growth of metastases. After the experimental time span of 35 days, the development of lung metastases can be visualized, analogous to PyMT metastasis, by use of immunohistochemistry and counting of metastatic nodules.

5.5.8 Tumor immune cell composition

To investigate whether the immune cell composition within the tumor microenvironment is affected similar to the lung, I analyzed the whole tumor immune cell composition by flow cytometry. All experiment mice were perfused intracardially to reduce remaining blood and circulating immune cells. Afterwards, the excised tumors were enzymatically digested and the achieved single cell suspension FcγR blocked and stained for immune cell markers, as described in 4.2.9.

However, as many effects of tumor promotion are assigned to tumor-resident immune cells, I expected an increase in typical, tumor-promoting immune cell subsets, such as myeloid derived immune cells (MDSCs) or tumor-associated macrophages (TAM). However, the analysis of the FACS measurement revealed no relevant alterations in the tumor-resident immune cell composition. Neither the total immune cell fraction ($CD45^+$), nor the specific immune cell subsets, such as MDSCs or lymphocytes, were relevantly altered in their frequencies (Figure 39). This finding emphasizes that rather the activation state of tumor-infiltrating immune cells than the sole abundance affects the outcome for the tumor development. Given that alterations in the activation state of TAM should result in an altered immune cell profile or immune cell attraction, I conclude from my experiments, that the deficiency of S1PR1 rather affects the direct macrophage effector function than shaping the tumor immune infiltrate.

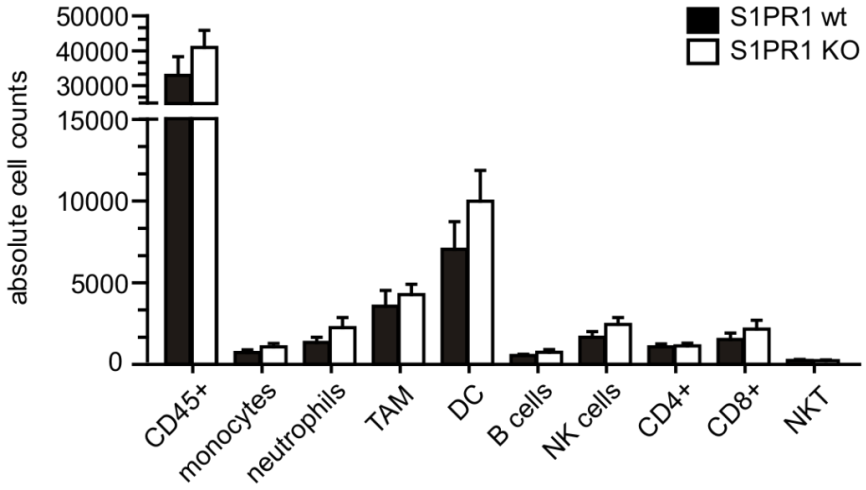

Figure 39. Immune cell composition in S1PR1 wt and KO mice tumors
Tumors from wildtype and macrophage-S1PR1 KO mice were isolated following cardial perfusion. Tumors from all mammary glands were pooled within each mouse and enzymatically digested. The achieved single cell suspension was blocked, stained, analyzed by flow cytometry and the absolute immune cell number within the tumor quantified. Data are mean ± SEM of 22 wt and 18 S1PR1 KO mice.

5.5.9 TAM mRNA array

As addressed under 5.5.8, the relative immune cell composition within the tumor is one of multiple essential factors in cancer progression and secondary events, such as metastasis or vessel development. However, my analysis revealed that the depletion of macrophage-S1PR1 does not result in an altered immune cell composition within the tumor. Thus, I decided to investigate the transcriptomic changes in S1PR1 deficient macrophages, compared to their corresponding wildtype. Therefore, I isolated the TAM fraction ($CD45^{+}CD11b^{+}CD11c^{+/-}Ly6G^{-}Ly6C^{+/-}F4/80^{high}$) from PyMT and MCA tumors by FACS sorting. To increase the robustness of the results and the amount of the RNA, always two mice were pooled before RNA isolation. Still the amount of RNA per sample was exceptionally low, so it had to be amplified by µMACS SuperAmp® to achieve the required amount of RNA for the expression analysis.

Following amplification, mouseWG-6 v2 BeadChip® were used to perform a genomewide transcriptomic analysis. Out of the genomic analysis of 45281 transcripts, I obtained 8587 significant changes for MCA and 22519 significant changes for the PyMT groupings. I decided to take only these genes into consideration that are similarly regulated in both MCA and PyMT tumors to identify those genes that are relevant for the alteration in lymphangiogenesis I observed in both cancer models. Hence, I could identify 5936 genes that were equally regulated in both cancer models. By use of routine pathway analysis software [“Partek Genomics Suite” and “Ingenuity Pathway Analysis” (IPA)] I was able to group and classify the regulated genes. Within the equally regulated genes I discarded all genes that were regulated less than 1.2 fold. This analysis yielded 160 regulated genes, thereof 102 genes that were down-regulated and 52 genes that were upregulated in S1PR1 KO (Table 7).

Table 7. Significantly regulated genes, S1PR1 KO *vs.* wildtype TAM

From all analyzed 45281 genes the most significantly and relevantly regulated genes were identified by clustering together wildtypes and S1PR1 KO from both cancer modes and following pathway analysis. The genes are shown in their regulation from S1PR1 KO compared to the corresponding wildtype. The analysis consists of 3 wildtype PyMT & 3 S1PR1 KO PyMT samples and 3 wt MCA & 3 S1PR1 KO MCA, each pooled from TAMS sorted out of 2 individual mice.

Gene	Regulation	Gene	Regulation	Gene	Regulation	Gene	Regulation
SLC44A2	-2,019	TGFBI	-1,408	MGP	-1,244	SLC27A1	1,309
LOC623121	-1,973	GCNT2	-1,400	PLEKHA5	-1,242	SBF2	1,310
AGL	-1,884	OAS3	-1,400	CSF2RA	-1,241	IDH1	1,372
PLAC8	-1,869	FNBP4	-1,399	ATP8B4	-1,238	DYNLT3	1,387
OLFML3	-1,835	KARS	-1,395	TCOF1	-1,236	SLC37A1	1,397
HELB	-1,807	LY6C1	-1,394	TBCEL	-1,233	ADAM17	1,399
MAD	-1,795	GRASP	-1,392	CIAS1	-1,231	LOH11CR2A	1,404
IFIT2	-1,773	CD72	-1,389	IQGAP1	-1,231	SRD5A3	1,415
DAXX	-1,748	GTPBP1	-1,381	DNAHC17	-1,200	MSI2	1,419
ABCD3	-1,712	MLSTD2	-1,378	TMEM184B	-1,195	PMEPA1	1,420
KLRB1B	-1,679	BACH1	-1,374	TRPS1	-1,192	GAS7	1,440
VRK1	-1,650	DUSP2	-1,370	SELPLG	-1,191	DHDH	1,458
GLS	-1,621	TFPT	-1,368	EDG5	-1,189	FN1	1,464
RSAD2	-1,570	ZNFX1	-1,340	FHOD1	-1,188	ADAM8	1,474
CNOT3	-1,554	NLRP3	-1,335	LMTK2	-1,188	TIMP2	1,478
IFITM1	-1,553	DOCK10	-1,333	IFITM3	-1,188	CDK5R1	1,480
CHD1	-1,532	PVR	-1,328	CCDC109B	-1,187	COX7A2L	1,487
THBS1	-1,531	IHPK1	-1,327	STAT2	-1,184	GAS6	1,505
ITGAM	-1,527	STAT4	-1,326	FCGR1	-1,181	ST6GAL1	1,514
TMEM119	-1,523	PIK3AP1	-1,321	CSF2RB	-1,180	INPP4B	1,538
PSCDBP	-1,522	PXN	-1,318	SESN2	-1,179	TIMP1	1,553
UPF2	-1,511	CD300LF	-1,314	SLPI	-1,178	ZHX1	1,565
MLL5	-1,510	AI451617	-1,310	MOV10	-1,177	VCAM1	1,597
LRRK1	-1,497	DDX24	-1,300	GPR137B-PS	1,217	MAG	1,633
SLC35C2	-1,493	FBXO39	-1,295	COX5A	1,225	BIRC5	1,648
VPS4A	-1,478	IL1R2	-1,295	GLB1	1,230	EMP1	1,677
AB124611	-1,475	IL21R	-1,295	SCL0001187.1_2	1,237	XPR1	1,680
TNFSF9	-1,468	SELPL	-1,292	CUEDC2	1,244	LMNA	1,697
TRPC4AP	-1,462	OAS1G	-1,285	LSM2	1,247	PDGFA	1,709
B3GNT8	-1,462	CLM3	-1,283	GHITM	1,253	HIST1H1C	1,717
EMILIN2	-1,460	PPARD	-1,280	RPPH1	1,266	BCL2L1	1,780
GIG2	-1,450	IFIT3	-1,276	P2RY12	1,272	CANT1	1,780
ARHGAP22	-1,446	STAP1	-1,265	ALG14	1,272	NRP2	1,862
ESM1	-1,435	CD69	-1,263	OXCT1	1,273	MITF	1,925
RCSD1	-1,423	DHX58	-1,260	CLEC4N	1,276	RNF121	1,966
CHI3L3	-1,417	VAV3	-1,259	MAP3K7IP1	1,288	AGTRAP	1,997
CDKN1B	-1,416	FOSL2	-1,258	WWP1	1,288	PMP22	2,000
TMEM49	-1,414	HDAC4	-1,257	LIN7C	1,291	FOLR2	2,030
NAPSA	-1,410	ARHGAP24	-1,256	SMARCA5	1,301	SERPINB6A	2,183
APBA3	-1,409	HIST2H2AA1	-1,245	IGH-VJ558	1,306	ERDR1	2,655

Of all these significantly and relevantly regulated genes, I chose those genes that were associated with matrix regulation, immune cell polarization or immune cell activation. I subjected the identified genes to detailed literature research to identify genes that were previously described to be regulated in cancer or cancer associated immune cells. Finally, from all 45281 tested genes, I compiled a list of 13 candidates (Table 8) that might be involved in shaping the lymphangiogenesis and metastasis phenotype I observed in my experimental mice. The most interesting genes to verify were ERDR1, NLRP3, NRP2,

PPARδ, SCL44A2, VCAM, XPR1 and YM-1, since all of them were found to be regulated in mouse cancer tissue or tissue-resident cells.

Table 8. S1PR1 wt and KO mRNA array results

From the identified 160 regulated genes, the most interesting genes were identified by literature research. *ERDR1* erythroid differentiation regulator 1, *NRP2* neuropilin 2, *XPR1* xenotropic and polytropic retrovirus receptor 1, *VCAM* vascular cell adhesion molecule, *IFITM3* interferon-induced transmembrane protein 3, *CD69* cluster of differentiation 69, *PPARδ* peroxisome proliferator-activated receptor delta, *NLRP3* NACHT, LRR and PYD domains-containing protein 3, *IFITM1* interferon-induced transmembrane protein 1, *CHI3L3* chitinase-like 3 (YM-1), *ITGAM* integrin alpha M, *IFIT2* interferon-induced protein with tetratricopeptide repeats 2, *SLC44A2* solute carrier family 44, member 2.

2,655	ERDR1
1,862	NRP2
1,680	XPR1
1,597	VCAM
-1,188	IFITM3
-1,263	CD69
-1,280	PPARδ
-1,335	NLRP3
-1,417	CHI3L3
-1,527	ITGAM
-1,553	IFITM1
-1,773	IFIT2
-2,019	SLC44A2

While verifying the array results with primary TAM mRNA, I found only the inflammasome component “nucleotide-binding oligomerization domain receptors-like receptor family, pyrin domain containing 3” (NLRP3) significantly downregulated in the S1PR1 KO TAM, whereas the other potential target genes were not or only marginally regulated (Figure 40, Figure 41). To verify the functionality of the S1PR1 knockout, I simultaneously quantified the S1PR1 mRNA expression, which was reduced to approximately 50 % in both cancer models.

However, the finding of relevant NLRP3 expression, which is one prerequisite for the secretion of the functional inflammatory cytokine IL-1β, was a surprise as the PyMT cancer model is not characterized as an acute inflammatory cancer model. The MCA fibrosarcoma, on the other hand, is known to be elicited by inflammatory factors. From this finding I conclude that a persistent secretion of

IL-1β within the tumor causes a persistent, smoldering inflammation that was described for various cancer types before [202, 203].

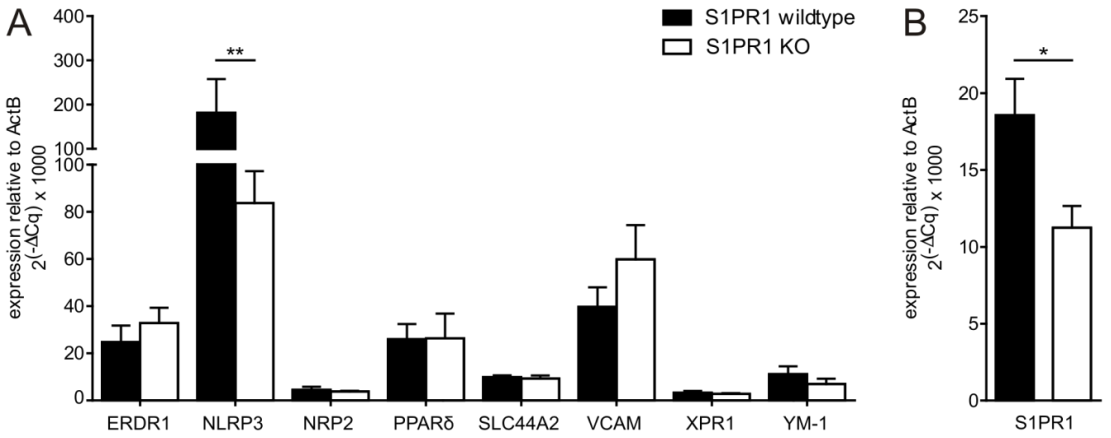

Figure 40. Validation and verification of PyMT array hits

TAMs from PyMT tumors were isolated and cDNA from RNA generated. qPCR of the transcripts indicated was performed. Data are mean ± SEM of 9 individual mice. Significances were calculated by (A) two-way ANOVA,**p ≤ 0.01 (B) student's t-test. *p ≤ 0.05.

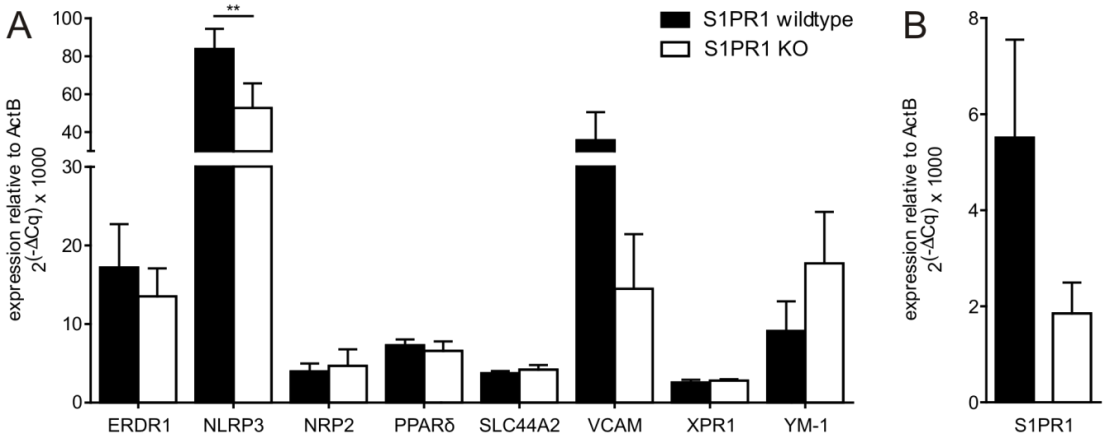

Figure 41. Validation and verification of MCA array hits

TAMs from MCA tumors were isolated and cDNA from RNA generated. qPCR of the indicated mRNA was performed. Data are mean ± SEM of 5 individual mice. Significances were calculated by two-way ANOVA. **p ≤ 0.01.

5.5.10 S1PR1 deficiency reduces NLRP3 expression and IL-1β secretion

To prove a functional relevance of the reduced NLRP3 mRNA I observed in the array and the following validation, I transferred the tumor model into the cell culture. Therefore, I used mouse peritoneal macrophages, mouse bone marrow derived macrophages and primary human macrophages for my *in vitro* verification experiments. By use of these 3 different cell types, I aimed to identify the signaling role of S1PR1 in the context of inflammasome activation.

In 2008 and 2012 two independent groups could prove a functional interaction of LPS signaling with S1P through its receptor S1PR1 on endothelial and epithelial cells. This signaling cooperation led to an increase of the secretion of inflammatory mediators by activation of MAPK and NF-κB signaling; signaling pathways that are well known to induce NLRP3 and pro-IL-1β [204, 205]. Results from an inducible IL-1β overexpression model revealed that IL-1β is able to selectively stimulate lymphangiogenesis in mouse airways by activating infiltrating macrophages to induce lymphangiogenesis [206]. These discoveries suggest TAM as contributors to tumor remodeling and vessel growth due to increased inflammatory signaling. The function of S1P as the co-factor for TNF-α receptor-associated factor 2 (TRAF2), activating its E3 ligase activity, the degradation of IκBα and thereby NF-κB activation, is well known and could be one part in S1P signaling during inflammation. However, this intracellular S1P effect is not mediated by S1PR1 signaling, but commonly triggered through an increased activity of SphK1. However, the stimulation of S1PR1 by extracellular S1P can induce the activation of ERK1/2 by G_i signaling and activate activator protein 1 (AP-1) through pERK1/2.

The activation of TLR4 with LPS is able to activate NF-κB by recruiting the adapter protein MyD88 and subsequently inducing the transcription of NLRP3 [207]. Besides the NF-κB binding site it could be shown that AP-1 has its own binding site in the promoter region of NLRP3, suggesting an involvement of ERK1/2 signaling in the NLRP3 inducing pathway [207].

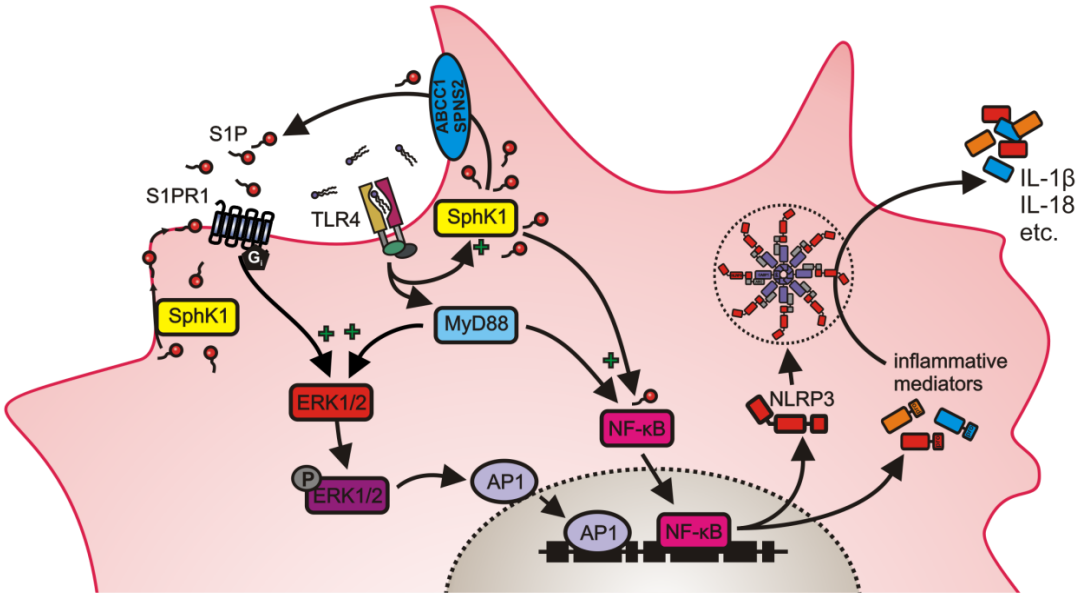

Figure 42. Hypothesis: S1PR1 TLR4 co-signaling
The stimulation of TLR can induce S1P production *via* SphK1 and S1P export through ABC transporters or SPNS2. TLR-dependent activation of MyD88 can activate ERK1/2 activation and NF-κB-dependent production of NLRP3 and proinflammatory mediators, such as pro-IL-1β and pro-IL-18. Simultaneous activation of S1PR1 by S1P can further increase ERK1/2 activation through G_i protein signaling. pERK1/2 is able to activate AP1 that in turn binds to the promoter region of the NLRP3 gene. Cooperation of TLR and S1PR1 signaling pathways thus can result in increased inflammasome assembly and enhanced inflammatory cytokine activation.

To test my hypothesis, I incubated human peripheral blood monocyte derived macrophages and mouse bone marrow derived macrophages with the TLR4 ligand LPS or the TLR3 ligand poly(I:C) to activate inflammatory signaling. To analyze the effect of S1PR1 signaling, I added either the S1PR1 antagonists VPC23019, W146 or the ERK-kinase inhibitor PD98059 and analyzed the secretion of cleaved (active) IL-1β by CBA (Figure 43). To induce a sustained activation of the inflammasome, macrophages require an additional stimulus, such as ATP, nigericin or crystals. Thus, I incubated macrophages with $Al(OH)_3$ crystals to fully activate the inflammasome.

Whereas LPS strongly induced the secretion of IL-1β, poly(I:C) did not induce an inflammatory macrophage response. As proposed, inhibition of S1PR1 with the antagonist W146, as well as the pERK inhibition with PD98059, resulted in a pronounced decrease of IL-1β secretion. Interestingly, VPC23019 was unable to reduce IL-1β cytokine secretion following LPS-stimulation. This might be explained by additional blocking of S1PR3, which is also able to stimulate multiple signaling pathways through diverse G proteins. Unlike S1PR1, S1PR3

is able to couple to various G proteins that might abolish the effect of S1PR1 inhibition in this case (Figure 43).

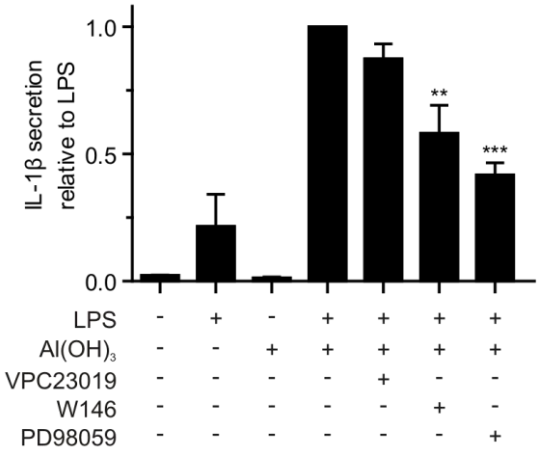

Figure 43. S1PR1 influence on IL-1β secretion

Primary human macrophages were incubated for 24 h with 100 ng/mL LPS, 100 µg/mL $Al(OH)_3$, 1 µM VPC23019, 10 µM W146 or 50 µM PD98059 as indicated. Secreted IL-1β was quantified by CBA. LPS and $Al(OH)_3$-treated cells were set to 1. Data shown are mean values ± SEM of five independent experiments. Statistics were performed with one-way ANOVA. **p ≤ 0.01 ***p ≤ 0.001.

Further experiments will have to prove whether the regulation of IL-1β is mediated by the reduction of NLRP3 expression or dependent on other S1PR1 signaling pathways that were not tested to date.

In summary, I was able to show the relevance of S1PR1 in varying inflammatory conditions. During acute peritoneal inflammation S1PR1 is upregulated following exposure to apoptotic cells. Although several studies demonstrated its relevance in the process of alternative immune cell activation, I did not observe a shift in macrophage polarization. However, I could provide evidence for the first time that the induction of S1PR1 mediates macrophage emigration from the inflammatory site in the resolution phase.

In contrast, the role of S1PR1 in cancer development and outgrowth is controversial. Although I observed a reduction in tumor growth in the PyMT breast cancer model and lymph vessel development in both cancer models, I did not observe a regulation on STAT3 or IL-6 signaling that was proposed by other researchers. However, I could demonstrate a role for S1PR1 in the modulation of IL-1β secretion, which in turn can result in a persistent, pro-tumor inflammation. The report that IL-1β can selectively induce lymphangiogenesis suggests a role for macrophage-S1PR1 in modulation of inflammatory signaling, the promotion of cancer development, and metastasis formation through lymphatic vessel growth.

6 Discussion

Within the last 20 years great efforts were made to elucidate the role and function of sphingosine-1-phosphate (S1P) and its receptors (S1PR1-5) in physiology and pathophysiology. Whereas ceramide and sphingosine act in a pro-apoptotic manner, it was first discovered that S1P generally results in enhanced cell survival and proliferation. The discovery of specific S1P receptors accelerated the findings of how S1P induces its effects and allowed a multitude of further, often cell type specific, discoveries.

The finding that lymphocytes are restrained to the lymphatic compartment after the administration of the functional S1PR antagonist FTY720, emphasized its importance for immune cells and pointed to beneficial effects of S1PR inhibition during inflammatory disorders. More and more researchers identified the relevance of S1P signaling on immune cell maturation and trafficking. The reports of dendritic cell polarization and chemoattraction by S1P extended once more the area of research. In line with these findings, our group identified apoptotic cell secreted S1P as one important mediator for macrophage survival and alternative activation. These alternative activation properties raised the question of the role and importance of S1PR1 signaling for termination of acute inflammation and restoration of tissue homeostasis.

1] Therefore I first analyzed the expression patterns of S1PR1 on macrophages following various stimulations to characterize the circumstances of S1PR1 signaling

2] Observing S1PR1 induction following non-classical activation, I examined its functional role on stimulated macrophages *in vitro*

3] To estimate the relevance of S1PR1 regulations *in vivo*, I utilized macrophage specific S1PR1 knockout mice in an inflammatory peritonitis mouse model.

Along with inflammatory diseases, such as atherosclerosis or multiple sclerosis, cancer is well known to be involved in inflammation. Some cancer types can even be induced by excessive inflammation and so it is widely accepted that inflammation possesses the ability to promote tumor (out)growth.

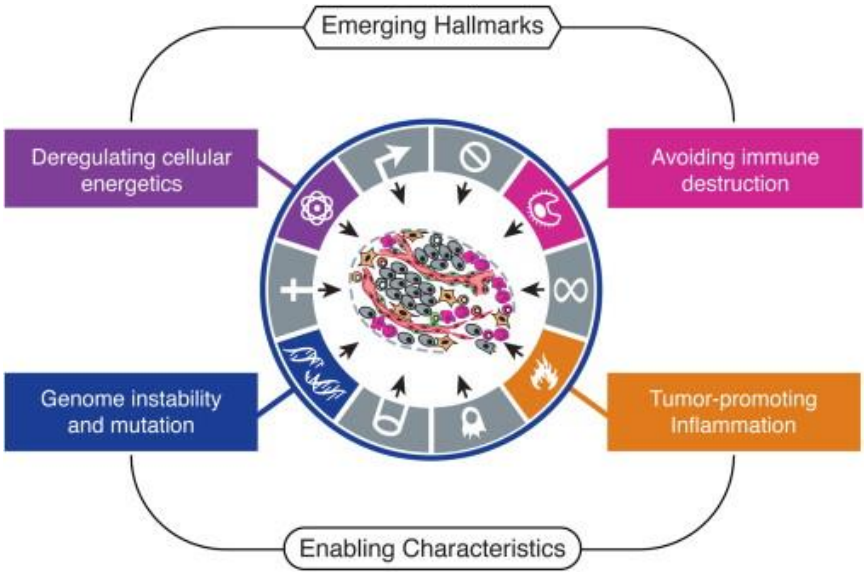

Figure 44. The hallmarks of cancer
Adopted from [100]

Since the finding of sphingosine kinases (SphK) and S1P to be involved in inflammatory signaling [208], a multitude of further pathways and effects have been discovered and investigated. Today we know that SphK1 is activated downstream of several growth factor receptors. This activation causes sphingosine phosphorylation, subsequent S1P-mediated cell proliferation and resistance to apoptotic stimuli. Consequently, SphK1 came into the focus of cancer research. The finding that transfection of non-malignant NIH3T3 fibroblasts with a constitutively active form of SphK1 results in a malignant cell-type strengthened the perception of SphK1 as a tumor promoter [209]. To this day, several transcriptomic screenings established SphK1 expression levels as a predictive marker for patient prognosis.

In contrast to SphK1, the influences of SphK2 on cancer incidence, growth and prognosis are yet largely unexplored. Several studies illustrate the relevance of intranuclear SphK2 expression for transcription, demonstrating that any manipulation, knockdown or overexpression, can reduce viability and proliferation of cancer cells. Contrary to that, some studies emphasize the importance of SphK2 expression in tumor cells for immune cell polarization [25] and its suitability as a prognostic marker in cancer [182].

However, the reports of a paracrine S1P-S1PR1-STAT3 feed forward signaling loop, between tumor cells and immune cells, fueled the efforts on SphK and S1P research in the context of cancer. Besides, S1PR1 signaling itself has been shown to activate and modulate several pathways that promote cancer progression, cell proliferation, angiogenesis, cell migration and invasion [48, 49, 132, 194, 196, 210-213].

To explain if and how tumor-infiltrating immune cells contribute to tumor development, my work focused on the role of sphingosine kinases and S1PR1 signaling in two different cancer models.

1] To distinguish between the role of SphKs in tumor cells and bone marrow derived infiltrates, I performed bidirectional bone marrow transfer with wildtype and SphK1KO or SphK2KO mice. All knockout and chimera mice were injected with 3-MCA for tumor initiation

2] For analysis of the outcome in a different, human-relevant model, I utilized PyMT breast cancer mice, whose disease resembles the phenotype of human breast cancer

3] After finding significant alterations in tumor growth and metastasis formation in the macrophage-S1PR1 deficient PyMT mice, I purified primary TAM from both cancer model for mRNA micro-array

4] Finally, after the validation of the identified changes in TAM transcription, I started with an *in vitro* system to characterize the effect of S1PR1 deficiency on inflammatory signaling.

6.1 Human macrophage-S1PR1 regulation by alternative activation

The importance of S1PR1 signaling during alternative activation was first identified by the finding of apoptotic cells increasing macrophage survival *via* induction of Bcl-2 and Bcl-XL [64]. Although the exact mechanism remained unclear, further studies could show the requirement of heme-oxygenase 1 (HO-1) for pro-survival and anti-inflammatory signaling and its dependency on S1PR1 signaling [63]. An increase of S1PR1 expression after stimulation with apoptotic cells (AC) or AC supernatants (ACM) was observed, although the mechanism of S1PR1 induction was not further clarified. Within this setting, S1PR1 triggered activation of p38 MAPK, which caused an HO-1-dependent increase of macrophage survival. More interestingly, S1PR1 signaling induced the production of VEGF-A in a STAT-dependent manner, which in turn resulted in an autocrine, STAT1 and STAT3-dependent increase of cell survival. This finding is interesting, as STAT3 is known to be an essential regulator in anti-inflammatory signaling, for the termination of acute inflammation [214, 215] and the promotion of wound healing [216, 217].

Other studies revealed that dendritic cells – close relatives to macrophages – regulate their S1P receptor profile during their maturation process dependent on the stimulation of their surface receptors [56]. Indeed, stimulation of human macrophages with AC or ACM strongly induced their expression of S1PR1 and 3 whereas S1PR2 expression remained unaltered (Figure 6). However, the low S1PR3 mRNA expression was negligible compared to the pronounced expression of S1PR1.

Other than ACM-stimulation, LPS and IFNγ, both stimuli for classical (M1) inflammatory activation, were unable to induce S1PR1 expression (Figure 8).

Considering the role of S1PR1 on the induction of an alternative phenotype in macrophages and its role on migration of T-, B- and dendritic cells suggest a physiological role for termination of inflammation and re-establishing of tissue homeostasis. An induction of S1PR1, by phagocytosis of apoptotic cells for example, would render macrophages more receptive to autocrine, paracrine or endocrine S1P signaling. Consequently, the induction of alternative activation patterns through S1PR1 can reduce inflammatory signal transduction and initiate the phase of tissue regeneration [85, 164]. However, several stimuli for

alternative macrophage activation have been described, whereas the expression of S1PR1 was not determined so far. Peroxisome proliferator-activated receptor gamma (PPARγ) and liver X receptor (LXR) have both been described as important transcription factors for alternative macrophage activation [218-220], but surprisingly, only LXR activation was able to induce S1PR1 expression (Figure 11). IL-4, another commonly used inducer of alternative macrophage phenotypes [221], was able to induce S1PR1 expression significantly, just as LXR or ACM (Figure 8). Comparable to stimulation of mature macrophages, the incubation of specific stimuli on differentiating cells is known to influence the resulting phenotypes [222]. M-CSF-induced macrophage differentiation did not only mediate an alternative phenotype in mature macrophages, but resulted as well in a pronounced S1PR1 expression on macrophages when added to bone marrow cells or (immature) monocytes. Contrary to that, GM-CSF, which is known to generate rather classically activated macrophages, resulted in a much lower expression of S1PR1 (Figure 10). The increased expression of S1PR1 thus seems to be a frequent but not mandatory event during non-classical macrophage activation. This finding is in line with the postulate from Mosser and Edwards that not only one “alternative” macrophage phenotype exists, but rather a multiplicity of non-inflammatory phenotypes that can be induced by various anti-inflammative stimuli [223]. Thus, S1PR1-induction shapes up as another marker for alternative activation that might be used for routine analysis together with already established markers, such as CD206 and YM-1 [224]. Nevertheless, further experimental work will have to clarify which alternative stimuli in detail are able to regulate S1PR1 expression (Figure 45).

6.2 Alternative activation and macrophage migration

Since the discovery of highly specific S1P receptors about 15 years ago, several functional effects of S1P signaling have been identified (see 3.1.6). Best studied on immune cells are the induction of cell migration and trafficking mediated by S1PR1. T cell and B cell migration, as well as shuttling within lymphoid organs were diminished or completely abolished after treatment with the functional S1PR1 antagonist FTY720 (Fingolimod¦Gilenya®) [225]. Less well studied are the effects of S1P on innate phagocytes. For dendritic cells reports could show that S1PR signaling is able to modulate emigration to lymph nodes

[226], bacterial endocytosis [71] and affecting the effector functions, such as cytokine secretion and T cell polarization [227]. The localization of S1PR1 in the pseudopodia-like structures of macrophages after ACM-stimulation suggested similarly a functional involvement in stimulated macrophages [165]. Indeed, random migration (chemokinesis) (Figure 12), as well as directed migration (chemotaxis) (Figure 13) were induced *in vitro*, indicating a functional role of S1PR1 in macrophage migration. This effect was completely dependent on S1PR signaling, as the inhibition of S1PR1 with the compound VPC23019 completely abolished chemotaxis and strongly reduced chemokinesis *in vitro* (Figure 12). These findings are in line with earlier results of DC [73] and lymphocyte (T & B cells) migration [225] and emphasize a general role of S1PR1 in immune cell migration. However, IL-4, which equally potent induced S1PR1 mRNA and protein (Figure 8), did not result in S1P-mediated chemotaxis. This was quite surprising, as chemokinesis of macrophages was increased comparably to ACM. Why S1PR1 expression was increased following IL-4 secretion, but not shuttled to the cell membrane remains questionable (Figure 14). However, S1PR1 localization is not restricted to cell membrane or storage vesicles. Two independent research groups could show the localization of S1PR1 in the nuclear membrane or even within the nucleus [228, 229]. This alternative localization was even able to mediate opposing effects than membrane bound S1PR1. However, where exactly IL-4-induced S1PR1 was localized, and whether or how it affected cell migration, was not determined in my analyses.

Besides this alternative localization of S1PR1, transactivation is one possible pathway how IL-4 might affect chemokinesis. This indirect activation was been identified earlier for PGE_2-induced and EGFR-mediated migration [1, 230]. Indeed, the RTK inhibitor genistein was able to entirely prevent IL-4-mediated chemokinesis, suggesting RTK-mediated (trans-)activation as the cause for IL-4 stimulated and S1P-induced random migration (Figure 15) [1].

However, these *in vitro* experiments can hardly be used for final clarification of physiologic relevant processes. Therefore, I chose a model of acute peritonitis to explore the impact of S1PR1 on inflammation and macrophage migration. As peritoneal macrophages are not exposed to ACM during inflammation but to apoptotic neutrophils (AN), I wondered whether apoptosis of neutrophil

granulocytes could induce the same polarization effects I observed before. Indeed, termination of inflammation is in part mediated by the phagocytotic uptake of apoptotic neutrophils by macrophages, thereby clearing dead cells and limiting excessive tissue injury [231]. This efferocytotic process was first identified to switch the inflammatory activation of “M1” macrophages and to end inflammatory cytokine secretion *in vitro.* Likewise, efferocytosis was shown to be sufficient to prevent *in vivo* exacerbation of pulmonary or peritoneal inflammation through autocrine and paracrine signaling loops, involving mediators such as PGE_2, TGF-β, PAF or S1P [123, 232, 233]. In line with these findings, I could demonstrate that apoptotic human peripheral blood neutrophils are able to induce macrophage-S1PR1 to the same extent and functional outcome as ACM *in vitro* (Figure 16).

6.3 *In vivo* relevance of post-inflammatory S1PR1 regulation

The yeast cell membrane homopolysaccharide “zymosan A”, as inducer of peritoneal inflammation, has often been used and found suitable for *in vivo* studies on the resolution of inflammation [176, 234]. A low dose of zymosan A triggers a rapid infiltration of neutrophils into the peritoneal cavity peaking at about 12 hours [122] and subsequent phagocytosis of zymosan A particles. During the process of inflammation, infiltrated neutrophils, secreted MCP-1 and other inflammatory cytokines, as well as apoptotic neutrophils themselves, attract blood circulating inflammatory $Ly6C^+$ monocytes into the peritoneum, which then differentiate into macrophages [234, 235]. The subsequent efferocytosis of apoptotic cells provokes alternative-like activation of inflammatory macrophages and results in the secretion of anti-inflammatory mediators, such as IL-10 and TGF-β. The hereby generated macrophages are thus called “resolution phase macrophage” [176].

6.3.1 Conditional *in vivo* S1PR1 ablation

To determine the functional role of macrophage-S1PR1, I utilized a CRE-loxP recombination system with the F4/80 promoter inducing the CRE-recombinase [159] and loxP sequences flanking the S1PR1 gene [158]. The expression of S1PR1 6 days after induction of peritonitis was reduced as expected, although about 30 % of macrophages retained their S1PR1 expression (Figure 19). Except for a contamination with other immune cell types after macrophage

purification, this can be caused by immature macrophages that recently differentiated from monocytes and not yet reached their maximum of F4/80 promoter activity [236]. Another reason might be the heterogeneous F4/80 expression among the multiplicity of macrophage subsets. Whereas peritoneal resident macrophages (yolk sac originated macrophages) are long-lived and strongly express F4/80 [237], bone marrow derived macrophages (BMDM) are short-lived and achieve lower expression rates of F4/80. This reduced F4/80 promoter activity is accompanied by a lower CRE expression and accordingly, a lower probability of CRE-induced S1PR1 deletion. To validate the functionality of the knockout system, I used so called “mdT/meG, double-fluorescent CRE reporter mice” to visualize those cells that have undergone CRE-mediated recombination (Figure 17). As expected before, the highest CRE efficiency was observable in the peritoneal macrophages (Figure 18). In contrast, all other cell types showed markedly lower expression of the activated meGFP fluorochrome, indicating that CRE-mediated loxP recombination occurs almost exclusively in macrophages. Altogether, the F4/80 CRE model proved to be macrophage specific and the S1PR1 knockout was consistently sufficient to analyze changes in the macrophage populations between knockout and wildtype (Figure 19).

It was reported that surface F4/80 expression is important for the regulation of immune homeostasis in mice, especially for the induction of regulatory $CD8^+$ T cells to provide immune tolerance [238]. However, I did not observe alterations in the immune cell composition of untreated mice (Figure 23) indicating that neither F4/80 nor S1PR1 are critically involved in regulation of peritoneal homeostasis under steady-state conditions.

6.3.2 Acute inflammation in macrophage-S1PR1 deficient mice

The injection of zymosan A and elicitation of sterile inflammation caused in both genotypes the same early $CD11b^{high}F4/80^{high}$ macrophage disappearance reaction with a comparable reappearance at day 3 [239]. The infiltration of polymorphonuclear neutrophil granulocytes and the uptake of zymosan A particles occurred in both genotypes to the same extent (Figure 21). The subsequent attraction and infiltration of $Ly6C^+$ monocytes at day 3 was likewise identical in both genotypes (Figure 24) indicating the same initiation of inflammation in wildtype and S1PR1 KO.

Following their infiltration, monocytes immediately differentiate into macrophages and take up free zymosan A particles, resulting in a TLR2-mediated inflammatory activation [240]. After resolution of the acute inflammation, the polarized resolution phase macrophages successively emigrate into the lymphatic system [126]. In general, the immune cell composition, 6 days after the induction of inflammation, was not significantly altered (Figure 23). Unlike the general immune cell population, and in line with the initial hypothesis, macrophage numbers in the peritoneum were significantly elevated 6 days post-inflammation. Not only the total amount of macrophages was increased, but especially the percentage of macrophages that remained in the peritoneal cavity throughout the inflammatory event, identified by containing fluorescent zymosan A particles. Thus, I conclude that deficient S1PR1 upregulation prevents successful emigration from the post-inflammatory peritoneal cavity.

6.3.3 Macrophage-S1PR1 deficiency in resolving inflammation and macrophage survival

Several reports show that S1P can affect inflammatory cytokine secretion and propose a need for S1PR1 in macrophage polarization [25, 85]. Thus, it was unexpected to find the same cytokine signature in both genotypes (Figure 27). All mice revealed only minor amounts of secreted TNFα, IL-6 and MCP-1 indicating the termination of the inflammatory phase. Although IL-6 can be upregulated *via* STAT3 [241], the secretion profile and the polarization profile indicate the return to homeostatic conditions at day 6 (Figure 28). This might be due to low amounts of apoptotic cells in the peritoneum, or because of a completed resolution of inflammation and restored tissue homeostasis [176].

Not only migration, but also survival of macrophages or proliferation, [177, 242] are well known candidates to influence macrophage numbers in the peritoneum. However, macrophage-S1PR1 was shown to exert pro-survival and pro-proliferative functions on macrophages and should therefore result in an opposite phenotype as the one observed for S1PR1 KO mice [34, 64, 177]. Nevertheless, it was surprising that S1PR1 deficiency on macrophages did not alter the survival and proliferation rate of bone marrow derived macrophages after treatment with the appropriate stimulus (Figure 25). Hence I conclude that

the post-inflammatory upregulation of S1PR1 is dispensable for macrophage proliferation and survival.

As it was shown for dendritic cells and for resolution phase macrophages that alternative activation reduces their ability to efficiently engulf particles [71, 176], I analyzed whether the uptake of zymosan A particles might have altered the activation profile and the course of inflammation. However, I did not observe a change in zymosan A uptake in knockout *versus* wildtype macrophages following alternative activation, ruling out an effect of S1PR1 on zymosan A uptake (Figure 26).

Altogether, my data provide for the first time a link between regulation of S1PR1 and apoptotic cell clearance after inflammation. Comparable to dendritic cells, T, B and NK cells, macrophages regulate their S1P receptors according to their activation and emigrate after they fulfilled their task in inflammation. It is tempting to speculate that macrophages, similar to dendritic cells, enrich in the draining lymph nodes and modulate T cell priming [56]. However, this was not possible to determine with my chosen system and remains to be explored in following studies.

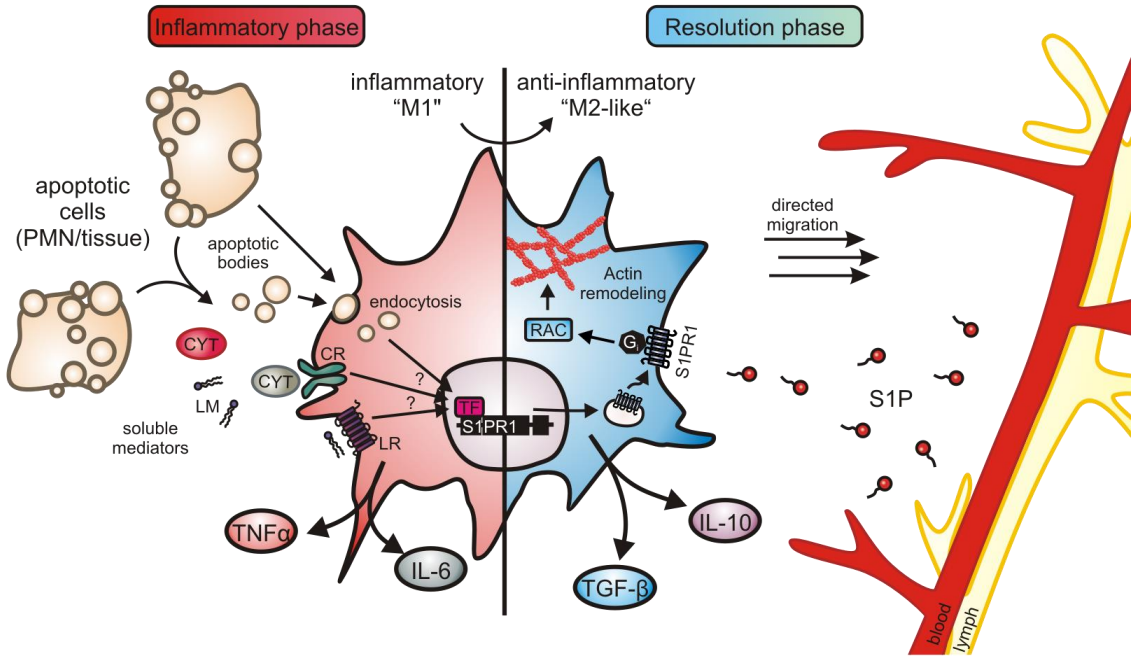

Figure 45. Macrophage regulation in acute inflammation

Apoptotic epithelial cells, apoptotic polymorphonuclear neutrophil granulocytes (PMN), apoptotic bodies and soluble mediators (*CYT* cytokine*, LM* lipid mediator) induce the phenotype-switch from "M1" inflammatory to "M2-like" anti-inflammatory through so far not identified mediators and signaling pathways (*CR* cytokine receptor, *LR* lipid receptor, *TF* transcription factor). Due to this phenotype switch, inflammatory mediators (e.g. TNFα, IL-6) are down- and anti-inflammatory mediators (e.g. TGF-β, IL-10) are upregulated. Simultaneously, S1PR1 is induced and increases G_i-dependent signaling. During the resolution phase, S1PR1 increases RAC-dependent actin remodeling and directs the polarized macrophages along the S1P-gradient out of the tissue into draining lymph-vessels.

6.4 S1P signaling in cancer

In the last decades several research groups focused on the role of ceramide and sphingolipids in cancer. After the discovery of its potent inhibitory effects on protein kinase C, sphingosine was suggested as a protector from tumor promotion [243]. Later findings in the 1990's could show that phosphorylation of the pro-apoptotic sphingosine converts the protector into a stimulator of proliferation, differentiation, adhesion and survival [8]. In the late 90's, the potential role of S1P in tumor development, vascularization and growth was introduced [33]. However, since these initial findings, our knowledge about signaling effects and pathways increased rapidly [244], establishing sphingolipid research as one of the major topics in cancer research.

6.4.1 The role of tissue and immune cell sphingosine kinases in inflammatory elicited cancer

Based on our observations in a xenograft mouse model, where knockdown of SphK2 in MCF-7 breast cancer cells diminished tumor growth by reduced alternative polarization of tumor-infiltrating macrophages [25], I wondered whether this is also true in endogenous tumorigenesis. Whereas SphK1 has already been found to be overexpressed in several cancer types and actively promotes tumor growth [209], the role of SphK2 in tumor development is rather doubtful. Cell culture data indicate a reduction of cell growth by S1P-mediated inhibition of HDAC1 and 2 [21, 189] or Bcl-XL inhibition through binding to the BH3 domain of SphK2 [245]. Hence, SphK2 overexpression was supposed to be a tumor suppressor rather than tumor promoter. Furthermore, it could be shown that loss of SphK2 in glioblastoma results in a faster growth than in SphK1 deficient cancer cells [246]. However, the finding that SphK2 knockout results in an increased tumor formation in an AOM/DSS colitis associated cancer mouse model was surprising, as SphK2 was not related to inflammatory cancer induction before. The researchers could show that this effect is caused by a hyper-inflammatory response, elicited by hematopoietic cells [132]. The loss of SphK2 resulted in a compensatory upregulation of SphK1 and increased serum S1P, leading to an intensified S1P-S1PR1-STAT3-IL-6 signaling, further enhancing cancer cell proliferation. Taking compensatory effects and the importance of immune cell *versus* tissue cell localization of sphingosine kinases into consideration, only a bidirectional bone marrow transfer from wildtype,

SphK1KO and SphK2KO mice allows the analysis of all constellations of sphingosine kinase expression and reduces compensatory effects.

I could show that a sub-lethal irradiation of the recipient mice and following transplantation of healthy bone marrow results in a stable engraftment and the generation of chimeras that remain stable for several months (Figure 29) [50].

The induction of carcinogenesis by injection of the carcinogen 3-methylcholanthrene has been extensively studied and found suitable for the analysis of inflammation elicited cancer [191]. Swann and colleagues could show with this model that inflammatory immune responses can cause opposing effects during tumorigenesis. Whereas excessive inflammation can induce cancer, diminished inflammation within an established tumor can increase tumor growth by failing immune surveillance. As SphK1 was determined to be an important effector, involved in TNFα inflammatory signaling [247, 248], its loss should reduce carcinogenesis comparable to MyD88 deficiency [191]. Unexpectedly, SphK1 deficiency did not alter the tumor incidence in my studies (Figure 30). Although, SphK1KO mice exhibited the lowest rate of cancer development, it coincided with the highest tumor burden at the end of the experiment. Hence I conclude that SphK1 knockout reduces the pro-inflammatory reaction towards the carcinogen MCA and thus tumor formation. Indeed, SphK1 inhibition was found to reduce carcinogenesis in persistent colon inflammation [249]. However, if a tumor is formed under SphK1KO conditions, the reduced inflammatory response itself should result in a reduced tumor immunosurveillance and thus, an increased tumor growth [250]. Indeed, this effect was detectable in the SphK1KO mice, although it was not reproducible in UbiC$^{GFP/+}$-BM-SphK1KO or SphK1KO-BM-UbiC$^{GFP/+}$ chimeric mice (Figure 32), raising the question if germline knockouts in general are suitable for this experimental setting. Many compensatory effects have been reported for germ line knockout mice [251, 252], but its outcome in such complex models as carcinogenesis remains yet undefined. Additionally, the persistence of long-living tissue-resident cells, such as resident macrophages or Langerhans cells, makes it hard to clearly assign the effects to certain cellular sources within the tissue of bone marrow chimeric mice [253].

Even more difficult to interpret are the results from the SphK2KO strain and its chimeras. Although most researchers conclude that SphK2 is dispensable for

inflammatory signaling or carcinogenesis, a few reports show that SphK2 deficiency in total or in the bone marrow is able to increase tumor formation [132]. However, SphK2 deficiency in the cancer originating tissue seems to be able to reduce tumor incidence and outgrowth [25]. In line with the report from the AOM/DSS colon cancer model, I observed an increase in tumor formation in mice that received SphK2KO bone marrow (Figure 31). Although more mice of this genotype developed tumors, the outgrowth was not altered during the experiment or at the day of sacrifice, indicating an effect on tumor initiation, but not on tumor promotion. In contrast, deficiency of SphK2 in the tumor tissue, significantly delayed the outgrowth of the tumor. Both parameters, tumor induction as well as time until sacrifice, were shifted to the benefit of SphK2KO-BM-UbiC$^{GFP/+}$ mice. This finding closely resembles the finding of the aforementioned xenograft mouse model where SphK2KO in tumor cells significantly reduced their outgrowth [25]. However, the process of tumor (out)growth requires growth promotion, which is commonly provided by stroma cells or infiltrated immune cells [254]. The mouse data therefore suggest that SphK2 deficient tumor cells have to struggle harder to overcome tumoricidal immune responses and polarize infiltrating cells towards growth promotion. But once they break the immune resistance, tumor outgrowth occurs comparable with the other genotypes, however, with the delay until tumor onset (Figure 32).

6.4.2 The role of S1P receptor 1 on macrophages in inflammation-induced cancer

SphK1 and SphK2 derived S1P, secreted or directly produced outside of the cell, affects all surrounding cells [20, 255]. Since multiple effects were found to be S1PR1-dependent, I used the aforementioned conditional macrophage-S1PR1 mice for the 3-methylcholanthrene cancer model as well. To my surprise, the tumor incidence was by trend increased in the S1PR1 KO mice and reached even 100 %, whereas the corresponding wildtype was equal to the UbiC$^{GFP/+}$ mice. Considering tissue inflammation as pro-carcinogenic, and macrophage-S1PR1 as anti-inflammatory by stimulating IL-10 production *via* STAT3 activation, the knockout might result in an exaggerated inflammation, thereby causing a higher cancer incidence [216, 256, 257]. Likewise, tumor promoting effects, due to reduced anti-inflammatory signaling, might as well account for the increased tumor burden in S1PR1 KO mice (Figure 32).

Interestingly, besides anti-inflammatory signaling, S1PR1 was identified to support chronic inflammation by STAT3-induced IL-6 and other inflammatory cytokines [258-260]. As MCA cancer induction is a matter of acute but not of smoldering inflammation, the deficiency of S1PR1 might predominantly result in missing anti-inflammation. If so, S1PR1 knockout should consequently result in the opposite effect and limit tumor growth in non-acute, smoldering inflammation-dependent cancer types (6.4.4) [261].

6.4.3 The role of sphingosine kinases in PyMT-induced breast cancer

The PyMT model is a well characterized endogenous breast cancer model and commonly used due to its analogy to human breast cancer [184]. Because the tumor development starts very early in life (first tumor foci are detectable 6 weeks after birth) a bone marrow transfer could only be performed after the stage of tumor initiation. Furthermore, the required irradiation of the recipient mice would affect and bias tumor development. Hence, I performed all breast cancer experiments with germline (SphK1&2KO) and conditional knockout mice (macrophage-S1PR1 KO).

Especially in breast cancer, SphK1 is often overexpressed and represents a suitable marker for patient prognosis [179, 262, 263]. Therefore, I expected SphK1 deficiency to result in a profound reduction of breast tumor growth. Surprisingly, SphK1 as well as SphK2 knockout mice exhibited the same amount of tumor bearing breast glands as the wildtype (Figure 33). Likewise, the time until sacrifice, the tumor burden, as well as the grown tumor mass were equal at the day of sacrifice. Although counterintuitive, this outcome might be explained by compensatory effects due to the germline deficiency of SphKs (see 6.4.1) [264].

In contrast to the 3-MCA model, the PyMT tumor model is a commonly used system for the analysis of lung metastasis formation. Although SphK1 inhibition was identified as one means to prevent metastasis, SphK1KO PyMT mice developed the highest number of pulmonary metastases of all genotypes (Figure 36). As exemplified under 6.4.1, inhibition of SphK1-dependent inflammatory signaling can cause a reduced tumor immune control and possibly enhances tumor growth and increases lung metastasis [191, 265]. Alternatively, compensatory effects by SphK2 cannot be excluded, although the effects of

compensatory SphK2 upregulation are yet largely unknown. Given the impact of SphK2 expression on gene transcription, it would be interesting to explore the outcome of SphK1 depletion on genes that are involved in metastatic processes such as epithelial-mesenchymal-transition (EMT) or tumor cell migration.

In contrast to SphK1KO mice, the SphK2KO PyMT mice did not reveal a particular phenotype. This might on the one hand reflect a dispensability of SphK2 within the process of cancer initiation and outgrowth in PyMT tumors. On the other hand, PyMT tumor initiation and (out)growth are not dependent on pronounced inflammation or extensive immune cell polarization, as in the 3-MCA model (6.4.1). The absence of effects in the PyMT model might thus reflect its individual relevance depending on the cancer type, such as glioblastoma or 3-MCA-induced cancer.

6.4.4 The role of S1P receptor 1 on macrophages in oncogene-driven breast cancer

Other than SphK1 and SphK2 PyMT mice, macrophage-S1PR1 KO PyMT mice revealed a substantial alteration in their tumor development (Figure 33). Although the number of tumor bearing breast glands was neither enhanced nor diminished in macrophage-S1PR1 knockout mice, the involvement in tumor progression and outgrowth was obvious. Compared to the wildtypes, it took significantly longer in the macrophage-S1PR1 KO mice to reach the defined tumor stages. As a result of this delay in tumor growth, it took as well significantly longer until the S1PR1 KO mice had to be sacrificed (Figure 34). To avoid any falsification in the following experiments, because of unequal developed tumor mass per mouse [184], I sacrificed all mice with the same estimated tumor burden instead of the same age. Nevertheless, the corresponding wildtype mice exhibited significantly more lung metastases than the S1PR1 KO mice (Figure 36). Given the role of myeloid derived cells in metastasis formation, especially macrophage and neutrophils precursors for preparing a metastatic niche [201], I compared the immune cell composition in the lung of all tumor bearing mice from both cancer models. Whereas the tumor bearers revealed a significant increase of lung immune cells, especially of myeloid derived suppressor cells (MDSC), there was no detectable difference between wildtype and macrophage-S1PR1 KO mice (Figure 38). All lungs from all tumor bearing mice revealed the same typical infiltration of $Ly6C^+$

mononuclear and Ly6G$^+$ polymorphonuclear MDSCs. Consequently, the reason for the discrepancy in metastasis formation is likely found in the primary tumor where the metastatic cells originate from.

The most common routes in tumor dissemination and metastasis formation are blood and lymph vessels [266], which commonly infiltrate into the tumor during its outgrowth [267]. The pronounced incorporation of lymph vessels into the primary tumor of wildtype mice was opposed by the almost complete deficiency of lymph vessels in the S1PR1 KO mice tumors (Figure 37), whereas the blood vessel density remained unaltered. How exactly the process of intratumoral neo-angiogenesis takes place is not yet clear. It is widely accepted that tumor cells themselves are able to secrete angiogenic factors, such as VEGF-C and VEGF-D that directly stimulate endothelial cell proliferation and migration [268, 269]. However, the more relevant induction of vessel development results presumably from the direct interaction of tumor cells and tumor-infiltrating immune cells [270, 271]. Secreted factors from viable, as well as apoptotic tumor cells, are able to alter the activation of tumor-resident immune cells and can induce the secretion of growth factors [85]. Especially the secretion of IL-6 during persistent inflammation is able to activate transcription factors, such as STAT3, that in turn induces the secretion of pro-survival mediators, angiogenic mediators and IL-6 [272, 273]. This self-amplifying loop can result in the promotion of tumor growth, vessel incorporation and metastasis development [206].

To identify the signaling pathways that mediate the observed phenotype, I first analyzed the tumor immune cell composition in detail by FACS analysis. As tumor development in general mediates a pronounced immune suppression in the whole organism, I expected an explicit increase of MDSCs in the primary tumor that actively suppresses T cell responses and survival through ARG1 and iNOS2 expression/activity [274]. However, the immune cell composition in the primary tumor was almost identical between both genotypes (Figure 39), highlighting that not only quantity, but especially the quality (activation profile) of macrophages determines the outcome. To address the question of macrophage activaton, I purified primary TAM and analyzed the gene expression profile by RNA microarray. Although, increasing evidence were found in the last 5 years that long-lasting S1PR1-STAT3-IL-6 signaling is critically involved in tumor

development [48, 49, 132], I could not determine alterations in this specific gene signature between S1PR1 KO and wildtype TAMs. Not even the expression of typical mediators for angiogenesis, such as the VEGF family, was altered. However, macrophages are not the only source of vascular growth factors in the tumor environment. Many publications document that other immune cells, fibroblasts, as well as tumor cells are able to produce sufficient amounts of growth factors for neo-angiogenesis [275-277]. Instead, I could identify the inflammasome component NLRP3 significantly reduced in the S1PR1 KO TAM. Even though Baluk et al. could demonstrate that IL-1β overexpression results in macrophage-mediated, persistent lymphangiogenesis in mouse airways [206], there has not yet been a link to the macrophage inflammasome.

Providing that IL-1β is able to selectively induce lymphangiogenesis through so far unexplored pathways, the connection of S1PR1 deficiency and NLRP3 regulation would provide a novel explanation how persistent inflammation is able to influence cancer progression (Figure 46).

6.4.5 The role of S1P receptor 1 in NLRP3-mediated IL-1β secretion

Only a few reports show a functional cooperation of S1PR1 and toll-like-receptor (TLR) signaling so far. Whereas stimulation with S1P alone did not relevantly induce inflammatory cytokine production, the simultaneous stimulation with LPS and S1P significantly induced the expression of inflammatory cytokines, such as IL-8 and IL-6 [204, 205]. This induction could be prevented either by inhibition of S1PR1 signaling *via* the G_i inhibitor pertussis toxin, or by inhibiting the activation of the transcription factors p38 or ERK1/2. Especially p38 and ERK1/2 have been shown to be of particular importance for the inflammatory response *via* NF-κB after stimulation with LPS and S1P in various cell lines and RAW264.7 macrophages [278, 279]. NLRP3 induction itself was shown to be regulated through the activation of NF-κB [280], which additionally increases the production of pro-IL-1β. But not only NF-κB is directly able to induce the transcription of NLRP3 [207]. A separate binding motif for AP-1 was found in the promoter region of NLRP3 [281], suggesting that both transcription factors together can further enhance the expression of NLRP3. Indeed, I could demonstrate in the system of LPS-stimulated human and mouse macrophages, that inhibition of S1PR1 signaling significantly reduces the secretion of IL-1β (Figure 43). Preliminary results could show that

the concentration of IL-1β within the primary tumor of PyMT mice is likewise significantly reduced (data not shown) (Figure 46).

My data thus suggest that S1PR1 on macrophages is involved in the activation of the inflammasome by enhancing the expression of NLRP3. This increased inflammatory machinery provides inflammatory cytokines, such as IL-1β and may cause a persistent, smoldering inflammation. Among others, I could demonstrate increased lymph vessel development in this context, which might explain the observation of altered metastasis development in the macrophage-S1PR1 deficient PyMT mice.

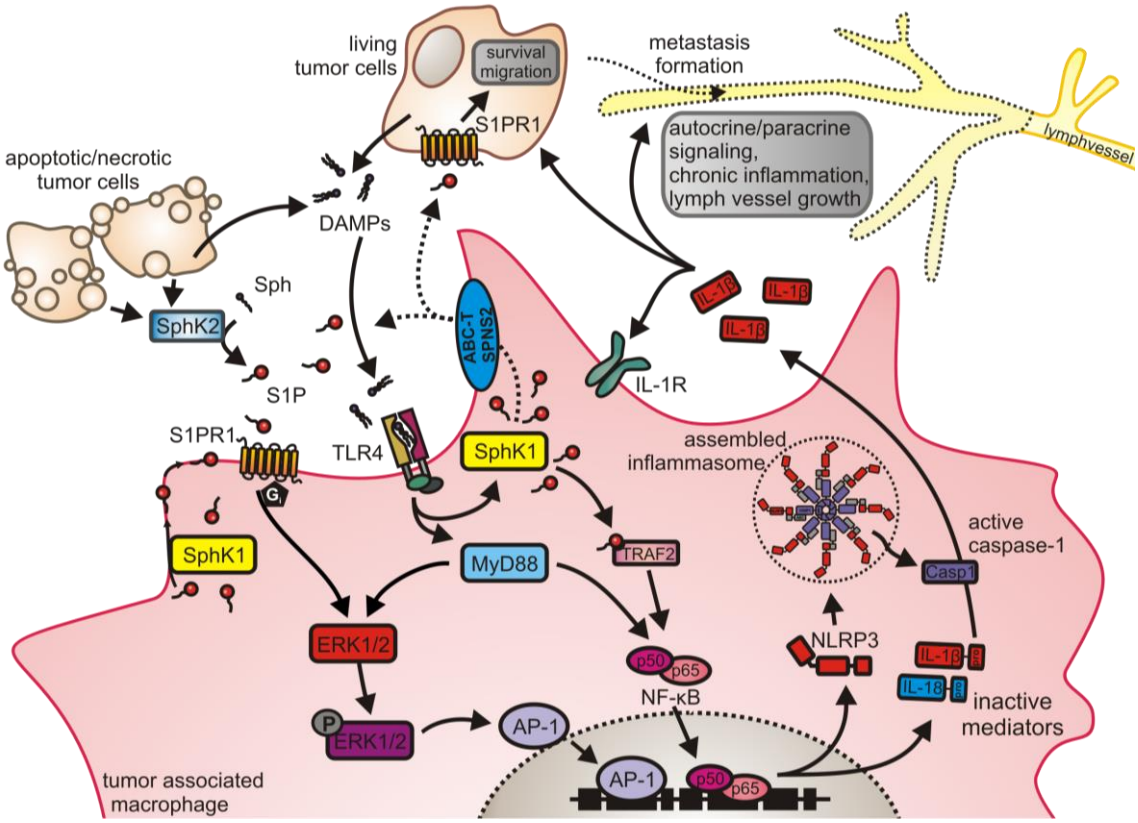

Figure 46. S1PR1-TLR co-signaling in cancer and lymphangiogenesis

Living tumor cells, apoptotic and necrotic tumor cells are able to secrete danger associated molecular patterns (DAMPs) and stimulate macrophage toll-like receptor 4 (TLR4). TLR4 is able to raise S1P production by activating sphingosine kinase 1 (SphK1). Intracellular S1P can bind to TNF receptor-associated factor 2 (TRAF2) and activate nuclear factor κB (NF-κB). By recruiting myeloid differentiation primary response gene (88) (MyD88), TLR4 can directly activate NF-κB and extracellular-signal-regulated kinases 1/2 (ERK1/2). Apoptotic cell-secreted sphingosine kinase 2 (SphK2) and activated SphK1 increase extracellular S1P levels after export of S1P through ABC transporters (ABC-T) and spinster homologue 2 (SPNS2). S1P binding to S1PR1 activates G_i proteins and can further enhance ERK1/2 activation. NF-κB and activator protein 1 (AP-1) together can induce NLRP3, pro-IL-1β and pro-IL-18 production. After activation of the cell by DAMPs, the inflammasome (see Figure 4)

assembles and activates caspase-1 (Casp1), which in turn activates IL-1β and IL-18 by proteolysis. The secretion of active IL-1β probably facilitates lymphangiogenesis through autocrine and paracrine signaling and can finally cause lymph-vessel dependent metastasis.

6.5 Et sequens

Although I could provide first evidence for the connection of S1P signaling, inflammation, lymphangiogenesis and metastasis, my experiments do not provide a final proof.

To prove the lymph vessel density as the exclusive cause for the development of metastasis, *in vivo* experiments are currently ongoing. The establishing of a cell settling assay was described in detail before [201, 282] and will demonstrate whether the metastasis development is equal in both genotypes after the induction of a metastatic niche by injection of hypoxic tumor cell supernatants.

Furthermore, lymphangiogenesis assays, such as embryoid body sprouting assays and matrigel plug assays, will identify the role of IL-1β in the macrophage supernatants after stimulation with tumor cells. Especially the addition and deprivation of IL-1β will provide substantial evidence for the role of this cytokine in lymphangiogenesis.

Finally, the use of primary human and mouse macrophages, in my already established *in vitro* system, will be the base for the elucidation of TLR and S1PR1 cooperation in NLRP3 expression.

7 References

1. Spiegel, S. and S. Milstien, *Sphingosine-1-phosphate: an enigmatic signalling lipid.* Nat Rev Mol Cell Biol, 2003. **4**(5): p. 397-407.
2. Merrill, A.H., Jr., Y.A. Hannun, and R.M. Bell, *Introduction: sphingolipids and their metabolites in cell regulation.* Adv Lipid Res, 1993. **25**: p. 1-24.
3. Hakomori, S. and Y. Zhang, *Glycosphingolipid antigens and cancer therapy.* Chem Biol, 1997. **4**(2): p. 97-104.
4. Hannun, Y.A. and L.M. Obeid, *The Ceramide-centric universe of lipid-mediated cell regulation: stress encounters of the lipid kind.* J Biol Chem, 2002. **277**(29): p. 25847-50.
5. Pettus, B.J., C.E. Chalfant, and Y.A. Hannun, *Ceramide in apoptosis: an overview and current perspectives.* Biochim Biophys Acta, 2002. **1585**(2-3): p. 114-25.
6. Heinrich, M., et al., *Ceramide as an activator lipid of cathepsin D.* Adv Exp Med Biol, 2000. **477**: p. 305-15.
7. Hung, W.C., H.C. Chang, and L.Y. Chuang, *Activation of caspase-3-like proteases in apoptosis induced by sphingosine and other long-chain bases in Hep3B hepatoma cells.* Biochem J, 1999. **338 (Pt 1)**: p. 161-6.
8. Goetzl, E.J., et al., *Dual mechanisms for lysophospholipid induction of proliferation of human breast carcinoma cells.* Cancer Res, 1999. **59**(18): p. 4732-7.
9. Pyne, N.J. and S. Pyne, *Sphingosine 1-phosphate and cancer.* Nat Rev Cancer, 2010. **10**(7): p. 489-503.
10. Clair, T., et al., *Autotaxin hydrolyzes sphingosylphosphorylcholine to produce the regulator of migration, sphingosine-1-phosphate.* Cancer Res, 2003. **63**(17): p. 5446-53.
11. Mastrandrea, L.D., S.M. Sessanna, and S.G. Laychock, *Sphingosine kinase activity and sphingosine-1 phosphate production in rat pancreatic islets and INS-1 cells: response to cytokines.* Diabetes, 2005. **54**(5): p. 1429-36.
12. Xia, P., et al., *Sphingosine kinase interacts with TRAF2 and dissects tumor necrosis factor-alpha signaling.* J Biol Chem, 2002. **277**(10): p. 7996-8003.
13. Hait, N.C., et al., *Role of sphingosine kinase 2 in cell migration toward epidermal growth factor.* J Biol Chem, 2005. **280**(33): p. 29462-9.
14. Shu, X., et al., *Sphingosine kinase mediates vascular endothelial growth factor-induced activation of ras and mitogen-activated protein kinases.* Mol Cell Biol, 2002. **22**(22): p. 7758-68.
15. Pebay, A., et al., *Essential roles of sphingosine-1-phosphate and platelet-derived growth factor in the maintenance of human embryonic stem cells.* Stem Cells, 2005. **23**(10): p. 1541-8.
16. Meyer zu Heringdorf, D., et al., *Stimulation of intracellular sphingosine-1-phosphate production by G-protein-coupled sphingosine-1-phosphate receptors.* Eur J Pharmacol, 2001. **414**(2-3): p. 145-54.
17. Hengst, J.A., et al., *Sphingosine kinase 1 localized to the plasma membrane lipid raft microdomain overcomes serum deprivation induced growth inhibition.* Arch Biochem Biophys, 2009. **492**(1-2): p. 62-73.
18. Barr, R.K., et al., *Deactivation of sphingosine kinase 1 by protein phosphatase 2A.* J Biol Chem, 2008. **283**(50): p. 34994-5002.

19. Hait, N.C., et al., *Sphingosine kinase type 2 activation by ERK-mediated phosphorylation.* J Biol Chem, 2007. **282**(16): p. 12058-65.
20. Weigert, A., et al., *Cleavage of sphingosine kinase 2 by caspase-1 provokes its release from apoptotic cells.* Blood, 2010. **115**(17): p. 3531-40.
21. Riccio, A., *New endogenous regulators of class I histone deacetylases.* Sci Signal, 2010. **3**(103): p. pe1.
22. Hait, N.C., et al., *Regulation of histone acetylation in the nucleus by sphingosine-1-phosphate.* Science, 2009. **325**(5945): p. 1254-7.
23. Gomez, L., et al., *A novel role for mitochondrial sphingosine-1-phosphate produced by sphingosine kinase-2 in PTP-mediated cell survival during cardioprotection.* Basic Res Cardiol, 2011. **106**(6): p. 1341-53.
24. Don, A.S. and H. Rosen, *A lipid binding domain in sphingosine kinase 2.* Biochem Biophys Res Commun, 2009. **380**(1): p. 87-92.
25. Weigert, A., et al., *Sphingosine kinase 2 deficient tumor xenografts show impaired growth and fail to polarize macrophages towards an anti-inflammatory phenotype.* Int J Cancer, 2009. **125**(9): p. 2114-21.
26. Maceyka, M., et al., *SphK1 and SphK2, sphingosine kinase isoenzymes with opposing functions in sphingolipid metabolism.* J Biol Chem, 2005. **280**(44): p. 37118-29.
27. Mizugishi, K., et al., *Maternal disturbance in activated sphingolipid metabolism causes pregnancy loss in mice.* J Clin Invest, 2007. **117**(10): p. 2993-3006.
28. Michaud, J., et al., *Normal acute and chronic inflammatory responses in sphingosine kinase 1 knockout mice.* FEBS Lett, 2006. **580**(19): p. 4607-12.
29. Mizugishi, K., et al., *Essential role for sphingosine kinases in neural and vascular development.* Mol Cell Biol, 2005. **25**(24): p. 11113-21.
30. Okada, T., et al., *Involvement of N-terminal-extended form of sphingosine kinase 2 in serum-dependent regulation of cell proliferation and apoptosis.* J Biol Chem, 2005. **280**(43): p. 36318-25.
31. Zhang, H., et al., *Sphingosine-1-phosphate, a novel lipid, involved in cellular proliferation.* J Cell Biol, 1991. **114**(1): p. 155-67.
32. Hisano, Y., T. Nishi, and A. Kawahara, *The functional roles of S1P in immunity.* J Biochem, 2012. **152**(4): p. 305-11.
33. Pyne, S. and N. Pyne, *Sphingosine 1-phosphate signalling via the endothelial differentiation gene family of G-protein-coupled receptors.* Pharmacol Ther, 2000. **88**(2): p. 115-31.
34. Spiegel, S. and S. Milstien, *The outs and the ins of sphingosine-1-phosphate in immunity.* Nat Rev Immunol, 2011. **11**(6): p. 403-15.
35. Oram, J.F. and A.M. Vaughan, *ABCA1-mediated transport of cellular cholesterol and phospholipids to HDL apolipoproteins.* Curr Opin Lipidol, 2000. **11**(3): p. 253-60.
36. Mitra, P., et al., *Role of ABCC1 in export of sphingosine-1-phosphate from mast cells.* Proc Natl Acad Sci U S A, 2006. **103**(44): p. 16394-9.
37. Takabe, K., et al., *Estradiol induces export of sphingosine 1-phosphate from breast cancer cells via ABCC1 and ABCG2.* J Biol Chem, 2010. **285**(14): p. 10477-86.
38. Lee, Y.M., et al., *A novel method to quantify sphingosine 1-phosphate by immobilized metal affinity chromatography (IMAC).* Prostaglandins Other Lipid Mediat, 2007. **84**(3-4): p. 154-62.

39. Takabe, K. and S. Spiegel, *Export of Sphingosine-1-Phosphate and Cancer Progression.* J Lipid Res, 2014.
40. Nagahashi, M., et al., *Spns2, a transporter of phosphorylated sphingoid bases, regulates their blood and lymph levels, and the lymphatic network.* FASEB J, 2013. **27**(3): p. 1001-11.
41. Venkataraman, K., et al., *Extracellular export of sphingosine kinase-1a contributes to the vascular S1P gradient.* Biochem J, 2006. **397**(3): p. 461-71.
42. Yatomi, Y., et al., *Sphingosine 1-phosphate induces platelet activation through an extracellular action and shares a platelet surface receptor with lysophosphatidic acid.* J Biol Chem, 1997. **272**(8): p. 5291-7.
43. Johnson, K.R., et al., *Role of human sphingosine-1-phosphate phosphatase 1 in the regulation of intra- and extracellular sphingosine-1-phosphate levels and cell viability.* J Biol Chem, 2003. **278**(36): p. 34541-7.
44. Bektas, M., et al., *Sphingosine 1-phosphate lyase deficiency disrupts lipid homeostasis in liver.* J Biol Chem, 2010. **285**(14): p. 10880-9.
45. Bernardini, M., et al., *High-resolution mapping of genomic imbalance and identification of gene expression profiles associated with differential chemotherapy response in serous epithelial ovarian cancer.* Neoplasia, 2005. **7**(6): p. 603-13.
46. Oskouian, B., et al., *Sphingosine-1-phosphate lyase potentiates apoptosis via p53- and p38-dependent pathways and is down-regulated in colon cancer.* Proc Natl Acad Sci U S A, 2006. **103**(46): p. 17384-9.
47. Sanchez, T. and T. Hla, *Structural and functional characteristics of S1P receptors.* J Cell Biochem, 2004. **92**(5): p. 913-22.
48. Lee, H., et al., *STAT3-induced S1PR1 expression is crucial for persistent STAT3 activation in tumors.* Nat Med, 2010. **16**(12): p. 1421-8.
49. Liu, Y., et al., *S1PR1 is an effective target to block STAT3 signaling in activated B cell-like diffuse large B-cell lymphoma.* Blood, 2012. **120**(7): p. 1458-65.
50. Du, W., et al., *S1P(2), the G protein-coupled receptor for sphingosine-1-phosphate, negatively regulates tumor angiogenesis and tumor growth in vivo in mice.* Cancer Res, 2010. **70**(2): p. 772-81.
51. Watters, R.J., et al., *Targeting sphingosine-1-phosphate receptors in cancer.* Anticancer Agents Med Chem, 2011. **11**(9): p. 810-7.
52. Wang, W., M.H. Graeler, and E.J. Goetzl, *Type 4 sphingosine 1-phosphate G protein-coupled receptor (S1P4) transduces S1P effects on T cell proliferation and cytokine secretion without signaling migration.* FASEB J, 2005. **19**(12): p. 1731-3.
53. Long, J.S., et al., *Sphingosine 1-phosphate receptor 4 uses HER2 (ERBB2) to regulate extracellular signal regulated kinase-1/2 in MDA-MB-453 breast cancer cells.* J Biol Chem, 2010. **285**(46): p. 35957-66.
54. Kohno, T., et al., *Sphingosine 1-phosphate promotes cell migration through the activation of Cdc42 in Edg-6/S1P4-expressing cells.* Genes Cells, 2003. **8**(8): p. 685-97.
55. Zheng, Y., Y. Kong, and E.J. Goetzl, *Lysophosphatidic acid receptor-selective effects on Jurkat T cell migration through a Matrigel model basement membrane.* J Immunol, 2001. **166**(4): p. 2317-22.

56. Idzko, M., et al., *Sphingosine 1-phosphate induces chemotaxis of immature and modulates cytokine-release in mature human dendritic cells for emergence of Th2 immune responses.* FASEB J, 2002. **16**(6): p. 625-7.
57. Xie, J.H., et al., *Sphingosine-1-phosphate receptor agonism impairs the efficiency of the local immune response by altering trafficking of naive and antigen-activated CD4+ T cells.* J Immunol, 2003. **170**(7): p. 3662-70.
58. Massberg, S., et al., *Immunosurveillance by hematopoietic progenitor cells trafficking through blood, lymph, and peripheral tissues.* Cell, 2007. **131**(5): p. 994-1008.
59. Duong, C.Q., et al., *Expression of the lysophospholipid receptor family and investigation of lysophospholipid-mediated responses in human macrophages.* Biochim Biophys Acta, 2004. **1682**(1-3): p. 112-9.
60. Fueller, M., et al., *Activation of human monocytic cells by lysophosphatidic acid and sphingosine-1-phosphate.* Cell Signal, 2003. **15**(4): p. 367-75.
61. Lewis, N.D., et al., *Circulating monocytes are reduced by sphingosine-1-phosphate receptor modulators independently of S1P3.* J Immunol, 2013. **190**(7): p. 3533-40.
62. Debien, E., et al., *S1PR5 is pivotal for the homeostasis of patrolling monocytes.* Eur J Immunol, 2013. **43**(6): p. 1667-75.
63. Weis, N., et al., *Heme oxygenase-1 contributes to an alternative macrophage activation profile induced by apoptotic cell supernatants.* Mol Biol Cell, 2009. **20**(5): p. 1280-8.
64. Weigert, A., et al., *Apoptotic cells promote macrophage survival by releasing the antiapoptotic mediator sphingosine-1-phosphate.* Blood, 2006. **108**(5): p. 1635-42.
65. Hughes, J.E., et al., *Sphingosine-1-phosphate induces an antiinflammatory phenotype in macrophages.* Circ Res, 2008. **102**(8): p. 950-8.
66. Wang, F., et al., *Sphingosine-1-phosphate receptor-2 deficiency leads to inhibition of macrophage proinflammatory activities and atherosclerosis in apoE-deficient mice.* J Clin Invest, 2010. **120**(11): p. 3979-95.
67. Skoura, A., et al., *Sphingosine-1-phosphate receptor-2 function in myeloid cells regulates vascular inflammation and atherosclerosis.* Arterioscler Thromb Vasc Biol, 2011. **31**(1): p. 81-5.
68. Weichand, B., et al., *Apoptotic cells enhance sphingosine-1-phosphate receptor 1 dependent macrophage migration.* Eur J Immunol, 2013. **43**(12): p. 3306-13.
69. Ocana-Morgner, C., et al., *Sphingosine 1-phosphate-induced motility and endocytosis of dendritic cells is regulated by SWAP-70 through RhoA.* J Immunol, 2011. **186**(9): p. 5345-55.
70. Ley, S., et al., *The role of TRKA signaling in IL-10 production by apoptotic tumor cell-activated macrophages.* Oncogene, 2013. **32**(5): p. 631-40.
71. Maeda, Y., et al., *Migration of CD4 T cells and dendritic cells toward sphingosine 1-phosphate (S1P) is mediated by different receptor subtypes: S1P regulates the functions of murine mature dendritic cells via S1P receptor type 3.* J Immunol, 2007. **178**(6): p. 3437-46.
72. Schulze, T., et al., *Sphingosine-1-phospate receptor 4 (S1P(4)) deficiency profoundly affects dendritic cell function and TH17-cell differentiation in a murine model.* FASEB J, 2011. **25**(11): p. 4024-36.

73. Czeloth, N., et al., *Sphingosine-1-phosphate mediates migration of mature dendritic cells.* J Immunol, 2005. **175**(5): p. 2960-7.
74. Rivera, J., R.L. Proia, and A. Olivera, *The alliance of sphingosine-1-phosphate and its receptors in immunity.* Nat Rev Immunol, 2008. **8**(10): p. 753-63.
75. Jenne, C.N., et al., *T-bet-dependent S1P5 expression in NK cells promotes egress from lymph nodes and bone marrow.* J Exp Med, 2009. **206**(11): p. 2469-81.
76. Finley, A., et al., *Sphingosine 1-phosphate mediates hyperalgesia via a neutrophil-dependent mechanism.* PLoS One, 2013. **8**(1): p. e55255.
77. Yokoo, E., et al., *Sphingosine 1-phosphate inhibits migration of RBL-2H3 cells via S1P2: cross-talk between platelets and mast cells.* J Biochem, 2004. **135**(6): p. 673-81.
78. Jolly, P.S., et al., *Transactivation of sphingosine-1-phosphate receptors by FcepsilonRI triggering is required for normal mast cell degranulation and chemotaxis.* J Exp Med, 2004. **199**(7): p. 959-70.
79. Kappos, L., et al., *Oral fingolimod (FTY720) for relapsing multiple sclerosis.* N Engl J Med, 2006. **355**(11): p. 1124-40.
80. Liu, G., et al., *The S1P(1)-mTOR axis directs the reciprocal differentiation of T(H)1 and T(reg) cells.* Nat Immunol, 2010. **11**(11): p. 1047-56.
81. Allende, M.L., et al., *S1P1 receptor directs the release of immature B cells from bone marrow into blood.* J Exp Med, 2010. **207**(5): p. 1113-24.
82. Schaphorst, K.L., et al., *Role of sphingosine-1 phosphate in the enhancement of endothelial barrier integrity by platelet-released products.* Am J Physiol Lung Cell Mol Physiol, 2003. **285**(1): p. L258-67.
83. Ogawa, R., et al., *A novel sphingosine-1-phosphate receptor agonist KRP-203 attenuates rat autoimmune myocarditis.* Biochem Biophys Res Commun, 2007. **361**(3): p. 621-8.
84. Dorsam, G., et al., *Transduction of multiple effects of sphingosine 1-phosphate (S1P) on T cell functions by the S1P1 G protein-coupled receptor.* J Immunol, 2003. **171**(7): p. 3500-7.
85. Weigert, A., et al., *Tumor cell apoptosis polarizes macrophages role of sphingosine-1-phosphate.* Mol Biol Cell, 2007. **18**(10): p. 3810-9.
86. Duenas, A.I., et al., *Selective attenuation of Toll-like receptor 2 signalling may explain the atheroprotective effect of sphingosine 1-phosphate.* Cardiovasc Res, 2008. **79**(3): p. 537-44.
87. Galluzzi, L. and G. Kroemer, *Necroptosis: a specialized pathway of programmed necrosis.* Cell, 2008. **135**(7): p. 1161-3.
88. Bergsbaken, T., S.L. Fink, and B.T. Cookson, *Pyroptosis: host cell death and inflammation.* Nat Rev Microbiol, 2009. **7**(2): p. 99-109.
89. Muzio, M., et al., *FLICE, a novel FADD-homologous ICE/CED-3-like protease, is recruited to the CD95 (Fas/APO-1) death--inducing signaling complex.* Cell, 1996. **85**(6): p. 817-27.
90. Varfolomeev, E.E., et al., *Targeted disruption of the mouse Caspase 8 gene ablates cell death induction by the TNF receptors, Fas/Apo1, and DR3 and is lethal prenatally.* Immunity, 1998. **9**(2): p. 267-76.
91. Kroemer, G. and J.C. Reed, *Mitochondrial control of cell death.* Nat Med, 2000. **6**(5): p. 513-9.
92. Hunter, A.M., E.C. LaCasse, and R.G. Korneluk, *The inhibitors of apoptosis (IAPs) as cancer targets.* Apoptosis, 2007. **12**(9): p. 1543-68.

93. Green, D.R., *Apoptotic pathways: ten minutes to dead.* Cell, 2005. **121**(5): p. 671-4.
94. Savill, J. and V. Fadok, *Corpse clearance defines the meaning of cell death.* Nature, 2000. **407**(6805): p. 784-8.
95. Majno, G. and I. Joris, *Apoptosis, oncosis, and necrosis. An overview of cell death.* Am J Pathol, 1995. **146**(1): p. 3-15.
96. Ogasawara, J., et al., *Lethal effect of the anti-Fas antibody in mice.* Nature, 1993. **364**(6440): p. 806-9.
97. Gatzka, M. and C.M. Walsh, *Apoptotic signal transduction and T cell tolerance.* Autoimmunity, 2007. **40**(6): p. 442-52.
98. Rossi, D. and G. Gaidano, *Messengers of cell death: apoptotic signaling in health and disease.* Haematologica, 2003. **88**(2): p. 212-8.
99. MacFarlane, M. and A.C. Williams, *Apoptosis and disease: a life or death decision.* EMBO Rep, 2004. **5**(7): p. 674-8.
100. Hanahan, D. and R.A. Weinberg, *Hallmarks of cancer: the next generation.* Cell, 2011. **144**(5): p. 646-74.
101. Gregory, C.D. and J.D. Pound, *Cell death in the neighbourhood: direct microenvironmental effects of apoptosis in normal and neoplastic tissues.* J Pathol, 2011. **223**(2): p. 177-94.
102. Huang, Q., et al., *Caspase 3-mediated stimulation of tumor cell repopulation during cancer radiotherapy.* Nat Med, 2011. **17**(7): p. 860-6.
103. Savill, J., et al., *A blast from the past: clearance of apoptotic cells regulates immune responses.* Nat Rev Immunol, 2002. **2**(12): p. 965-75.
104. Medzhitov, R., P. Preston-Hurlburt, and C.A. Janeway, Jr., *A human homologue of the Drosophila Toll protein signals activation of adaptive immunity.* Nature, 1997. **388**(6640): p. 394-7.
105. Matzinger, P., *Tolerance, danger, and the extended family.* Annu Rev Immunol, 1994. **12**: p. 991-1045.
106. Takeuchi, O. and S. Akira, *Pattern recognition receptors and inflammation.* Cell, 2010. **140**(6): p. 805-20.
107. Botos, I., D.M. Segal, and D.R. Davies, *The structural biology of Toll-like receptors.* Structure, 2011. **19**(4): p. 447-59.
108. Kawai, T. and S. Akira, *Toll-like receptors and their crosstalk with other innate receptors in infection and immunity.* Immunity, 2011. **34**(5): p. 637-50.
109. Alexopoulou, L., et al., *Recognition of double-stranded RNA and activation of NF-kappaB by Toll-like receptor 3.* Nature, 2001. **413**(6857): p. 732-8.
110. Andrade, W.A., et al., *Combined action of nucleic acid-sensing Toll-like receptors and TLR11/TLR12 heterodimers imparts resistance to Toxoplasma gondii in mice.* Cell Host Microbe, 2013. **13**(1): p. 42-53.
111. Oldenburg, M., et al., *TLR13 recognizes bacterial 23S rRNA devoid of erythromycin resistance-forming modification.* Science, 2012. **337**(6098): p. 1111-5.
112. Kenny, E.F. and L.A. O'Neill, *Signalling adaptors used by Toll-like receptors: an update.* Cytokine, 2008. **43**(3): p. 342-9.
113. Geijtenbeek, T.B. and S.I. Gringhuis, *Signalling through C-type lectin receptors: shaping immune responses.* Nat Rev Immunol, 2009. **9**(7): p. 465-79.
114. Apostolopoulos, V. and I.F. McKenzie, *Role of the mannose receptor in the immune response.* Curr Mol Med, 2001. **1**(4): p. 469-74.

115. Yoneyama, M. and T. Fujita, *Structural mechanism of RNA recognition by the RIG-I-like receptors.* Immunity, 2008. **29**(2): p. 178-81.
116. Wilmanski, J.M., T. Petnicki-Ocwieja, and K.S. Kobayashi, *NLR proteins: integral members of innate immunity and mediators of inflammatory diseases.* J Leukoc Biol, 2008. **83**(1): p. 13-30.
117. Mariathasan, S., et al., *Differential activation of the inflammasome by caspase-1 adaptors ASC and Ipaf.* Nature, 2004. **430**(6996): p. 213-8.
118. Tedder, T.F., et al., *The selectins: vascular adhesion molecules.* FASEB J, 1995. **9**(10): p. 866-73.
119. Akira, S., *Pathogen recognition by innate immunity and its signaling.* Proc Jpn Acad Ser B Phys Biol Sci, 2009. **85**(4): p. 143-56.
120. Sadik, C.D., N.D. Kim, and A.D. Luster, *Neutrophils cascading their way to inflammation.* Trends Immunol, 2011. **32**(10): p. 452-60.
121. Ortega-Gomez, A., M. Perretti, and O. Soehnlein, *Resolution of inflammation: an integrated view.* EMBO Mol Med, 2013. **5**(5): p. 661-74.
122. Serhan, C.N. and J. Savill, *Resolution of inflammation: the beginning programs the end.* Nat Immunol, 2005. **6**(12): p. 1191-7.
123. Fadok, V.A., et al., *Macrophages that have ingested apoptotic cells in vitro inhibit proinflammatory cytokine production through autocrine/paracrine mechanisms involving TGF-beta, PGE2, and PAF.* J Clin Invest, 1998. **101**(4): p. 890-8.
124. Byrne, A. and D.J. Reen, *Lipopolysaccharide induces rapid production of IL-10 by monocytes in the presence of apoptotic neutrophils.* J Immunol, 2002. **168**(4): p. 1968-77.
125. Golpon, H.A., et al., *Life after corpse engulfment: phagocytosis of apoptotic cells leads to VEGF secretion and cell growth.* FASEB J, 2004. **18**(14): p. 1716-8.
126. Bellingan, G.J., et al., *In vivo fate of the inflammatory macrophage during the resolution of inflammation: inflammatory macrophages do not die locally, but emigrate to the draining lymph nodes.* J Immunol, 1996. **157**(6): p. 2577-85.
127. Green, D.R. and G.I. Evan, *A matter of life and death.* Cancer Cell, 2002. **1**(1): p. 19-30.
128. Burstein, N.A. and L.W. Law, *Neonatal thymectomy and non-viral mammary tumours in mice.* Nature, 1971. **231**(5303): p. 450-2.
129. Grant, G.A. and J.F. Miller, *Effect of neonatal thymectomy on the induction of sarcomata in C57 BL mice.* Nature, 1965. **205**(976): p. 1124-5.
130. Swann, J.B. and M.J. Smyth, *Immune surveillance of tumors.* J Clin Invest, 2007. **117**(5): p. 1137-46.
131. Aguirre-Ghiso, J.A., *Models, mechanisms and clinical evidence for cancer dormancy.* Nat Rev Cancer, 2007. **7**(11): p. 834-46.
132. Liang, J., et al., *Sphingosine-1-phosphate links persistent STAT3 activation, chronic intestinal inflammation, and development of colitis-associated cancer.* Cancer Cell, 2013. **23**(1): p. 107-20.
133. Nishimura, H., et al., *Expression of sphingosine-1-phosphate receptor 1 in mantle cell lymphoma.* Mod Pathol, 2010. **23**(3): p. 439-49.
134. Yoshida, Y., et al., *The expression level of sphingosine-1-phosphate receptor type 1 is related to MIB-1 labeling index and predicts survival of glioblastoma patients.* J Neurooncol, 2010. **98**(1): p. 41-7.

135. Yoshida, Y., et al., *Sphingosine-1-phosphate receptor type 1 regulates glioma cell proliferation and correlates with patient survival.* Int J Cancer, 2010. **126**(10): p. 2341-52.
136. Watson, C., et al., *High expression of sphingosine 1-phosphate receptors, S1P1 and S1P3, sphingosine kinase 1, and extracellular signal-regulated kinase-1/2 is associated with development of tamoxifen resistance in estrogen receptor-positive breast cancer patients.* Am J Pathol, 2010. **177**(5): p. 2205-15.
137. Cattoretti, G., et al., *Targeted disruption of the S1P2 sphingosine 1-phosphate receptor gene leads to diffuse large B-cell lymphoma formation.* Cancer Res, 2009. **69**(22): p. 8686-92.
138. Lepley, D., et al., *The G protein-coupled receptor S1P2 regulates Rho/Rho kinase pathway to inhibit tumor cell migration.* Cancer Res, 2005. **65**(9): p. 3788-95.
139. Li, M.H., et al., *S1P/S1P2 signaling induces cyclooxygenase-2 expression in Wilms tumor.* J Urol, 2009. **181**(3): p. 1347-52.
140. Yamashita, H., et al., *Sphingosine 1-phosphate receptor expression profile in human gastric cancer cells: differential regulation on the migration and proliferation.* J Surg Res, 2006. **130**(1): p. 80-7.
141. Kim, E.S., et al., *Sphingosine 1-phosphate regulates matrix metalloproteinase-9 expression and breast cell invasion through S1P3-Galphaq coupling.* J Cell Sci, 2011. **124**(Pt 13): p. 2220-30.
142. Sukocheva, O., C. Wadham, and P. Xia, *Estrogen defines the dynamics and destination of transactivated EGF receptor in breast cancer cells: role of S1P(3) receptor and Cdc42.* Exp Cell Res, 2013. **319**(4): p. 455-65.
143. Harris, G.L., et al., *In vitro and in vivo antagonism of a G protein-coupled receptor (S1P3) with a novel blocking monoclonal antibody.* PLoS One, 2012. **7**(4): p. e35129.
144. Li, C., et al., *Involvement of sphingosine 1-phosphate (SIP)/S1P3 signaling in cholestasis-induced liver fibrosis.* Am J Pathol, 2009. **175**(4): p. 1464-72.
145. Ohotski, J., et al., *Sphingosine kinase 2 prevents the nuclear translocation of sphingosine 1-phosphate receptor-2 and tyrosine 416 phosphorylated c-Src and increases estrogen receptor negative MDA-MB-231 breast cancer cell growth: The role of sphingosine 1-phosphate receptor-4.* Cell Signal, 2014. **26**(5): p. 1040-7.
146. Chang, C.L., et al., *S1P(5) is required for sphingosine 1-phosphate-induced autophagy in human prostate cancer PC-3 cells.* Am J Physiol Cell Physiol, 2009. **297**(2): p. C451-8.
147. Hu, W.M., et al., *Effect of S1P5 on proliferation and migration of human esophageal cancer cells.* World J Gastroenterol, 2010. **16**(15): p. 1859-66.
148. Pyne, S. and N.J. Pyne, *New perspectives on the role of sphingosine 1-phosphate in cancer.* Handb Exp Pharmacol, 2013(216): p. 55-71.
149. Selvam, S.P. and B. Ogretmen, *Sphingosine kinase/sphingosine 1-phosphate signaling in cancer therapeutics and drug resistance.* Handb Exp Pharmacol, 2013(216): p. 3-27.
150. Shida, D., et al., *Targeting SphK1 as a new strategy against cancer.* Curr Drug Targets, 2008. **9**(8): p. 662-73.
151. Jonker, D.J., et al., *Cetuximab for the treatment of colorectal cancer.* N Engl J Med, 2007. **357**(20): p. 2040-8.

152. Soule, H.D., et al., *A human cell line from a pleural effusion derived from a breast carcinoma.* J Natl Cancer Inst, 1973. **51**(5): p. 1409-16.
153. Bertram, J.S. and P. Janik, *Establishment of a cloned line of Lewis Lung Carcinoma cells adapted to cell culture.* Cancer Lett, 1980. **11**(1): p. 63-73.
154. Sugiura, K. and C.C. Stock, *Studies in a tumor spectrum. I. Comparison of the action of methylbis (2-chloroethyl)amine and 3-bis(2-chloroethyl)aminomethyl-4-methoxymethyl -5-hydroxy-6-methylpyridine on the growth of a variety of mouse and rat tumors.* Cancer, 1952. **5**(2): p. 382-402.
155. Sirotnak, F.M., et al., *New folate analogs of the 10-deaza-aminopterin series. Further evidence for markedly increased antitumor efficacy compared with methotrexate in ascitic and solid murine tumor models.* Cancer Chemother Pharmacol, 1984. **12**(1): p. 26-30.
156. Muzumdar, M.D., et al., *A global double-fluorescent Cre reporter mouse.* Genesis, 2007. **45**(9): p. 593-605.
157. Guy, C.T., R.D. Cardiff, and W.J. Muller, *Induction of mammary tumors by expression of polyomavirus middle T oncogene: a transgenic mouse model for metastatic disease.* Mol Cell Biol, 1992. **12**(3): p. 954-61.
158. Allende, M.L., T. Yamashita, and R.L. Proia, *G-protein-coupled receptor S1P1 acts within endothelial cells to regulate vascular maturation.* Blood, 2003. **102**(10): p. 3665-7.
159. Schaller, E., et al., *Inactivation of the F4/80 glycoprotein in the mouse germ line.* Mol Cell Biol, 2002. **22**(22): p. 8035-43.
160. Allende, M.L., et al., *Mice deficient in sphingosine kinase 1 are rendered lymphopenic by FTY720.* J Biol Chem, 2004. **279**(50): p. 52487-92.
161. Schaefer, B.C., et al., *Observation of antigen-dependent CD8+ T-cell/ dendritic cell interactions in vivo.* Cell Immunol, 2001. **214**(2): p. 110-22.
162. Gantner, F., et al., *In vitro differentiation of human monocytes to macrophages: change of PDE profile and its relationship to suppression of tumour necrosis factor-alpha release by PDE inhibitors.* Br J Pharmacol, 1997. **121**(2): p. 221-31.
163. Wester, K., et al., *Zinc-based fixative improves preservation of genomic DNA and proteins in histoprocessing of human tissues.* Lab Invest, 2003. **83**(6): p. 889-99.
164. Weigert, A., B. Weichand, and B. Brune, *S1P regulation of macrophage functions in the context of cancer.* Anticancer Agents Med Chem, 2011. **11**(9): p. 818-29.
165. Weichand, B., et al., *Apoptotic cells enhance sphingosine-1-phosphate receptor 1 dependent macrophage migration.* Eur J Immunol, 2013.
166. Weis, N., *Role of Sphingosine-1-Phosphate Receptor 1 and Downstream Heme Oxygenase-1 Induction in Alternative Macrophage Activation Induced by Apoptotic Cells.* Univ.-Bibliothek Frankfurt am Main, 2009.
167. Ley, S., et al., *RNAi screen in apoptotic cancer cell-stimulated human macrophages reveals co-regulation of IL-6/IL-10 expression.* Immunobiology, 2013. **218**(1): p. 40-51.
168. Gordon, S., *Alternative activation of macrophages.* Nat Rev Immunol, 2003. **3**(1): p. 23-35.
169. Verreck, F.A., et al., *Human IL-23-producing type 1 macrophages promote but IL-10-producing type 2 macrophages subvert immunity to (myco)bacteria.* Proc Natl Acad Sci U S A, 2004. **101**(13): p. 4560-5.
170. Jiang, C., A.T. Ting, and B. Seed, *PPAR-gamma agonists inhibit production of monocyte inflammatory cytokines.* Nature, 1998. **391**(6662): p. 82-6.

171. Marathe, C., et al., *The arginase II gene is an anti-inflammatory target of liver X receptor in macrophages.* J Biol Chem, 2006. **281**(43): p. 32197-206.
172. Straus, D.S. and C.K. Glass, *Anti-inflammatory actions of PPAR ligands: new insights on cellular and molecular mechanisms.* Trends Immunol, 2007. **28**(12): p. 551-8.
173. Matloubian, M., et al., *Lymphocyte egress from thymus and peripheral lymphoid organs is dependent on S1P receptor 1.* Nature, 2004. **427**(6972): p. 355-60.
174. Mullershausen, F., et al., *Persistent signaling induced by FTY720-phosphate is mediated by internalized S1P1 receptors.* Nat Chem Biol, 2009. **5**(6): p. 428-34.
175. Bergelin, N., et al., *S1P1 and VEGFR-2 form a signaling complex with extracellularly regulated kinase 1/2 and protein kinase C-alpha regulating ML-1 thyroid carcinoma cell migration.* Endocrinology, 2010. **151**(7): p. 2994-3005.
176. Bystrom, J., et al., *Resolution-phase macrophages possess a unique inflammatory phenotype that is controlled by cAMP.* Blood, 2008. **112**(10): p. 4117-27.
177. Jenkins, S.J., et al., *Local macrophage proliferation, rather than recruitment from the blood, is a signature of TH2 inflammation.* Science, 2011. **332**(6035): p. 1284-8.
178. Xia, P., et al., *An oncogenic role of sphingosine kinase.* Curr Biol, 2000. **10**(23): p. 1527-30.
179. Ruckhaberle, E., et al., *Microarray analysis of altered sphingolipid metabolism reveals prognostic significance of sphingosine kinase 1 in breast cancer.* Breast Cancer Res Treat, 2008. **112**(1): p. 41-52.
180. Kohno, M., et al., *Intracellular role for sphingosine kinase 1 in intestinal adenoma cell proliferation.* Mol Cell Biol, 2006. **26**(19): p. 7211-23.
181. Johnson, K.R., et al., *Immunohistochemical distribution of sphingosine kinase 1 in normal and tumor lung tissue.* J Histochem Cytochem, 2005. **53**(9): p. 1159-66.
182. Wang, Q., et al., *Prognostic significance of sphingosine kinase 2 expression in non-small cell lung cancer.* Tumour Biol, 2013.
183. Schnitzer, S.E., et al., *Hypoxia enhances sphingosine kinase 2 activity and provokes sphingosine-1-phosphate-mediated chemoresistance in A549 lung cancer cells.* Mol Cancer Res, 2009. **7**(3): p. 393-401.
184. Lin, E.Y., et al., *Progression to malignancy in the polyoma middle T oncoprotein mouse breast cancer model provides a reliable model for human diseases.* Am J Pathol, 2003. **163**(5): p. 2113-26.
185. Olivera, A. and S. Spiegel, *Sphingosine-1-phosphate as second messenger in cell proliferation induced by PDGF and FCS mitogens.* Nature, 1993. **365**(6446): p. 557-60.
186. Cuvillier, O., et al., *Suppression of ceramide-mediated programmed cell death by sphingosine-1-phosphate.* Nature, 1996. **381**(6585): p. 800-3.
187. Baker, D.A., L.M. Obeid, and G.S. Gilkeson, *Impact of sphingosine kinase on inflammatory pathways in fibroblast-like synoviocytes.* Inflamm Allergy Drug Targets, 2011. **10**(6): p. 464-71.
188. Lai, W.Q., F.L. Chia, and B.P. Leung, *Sphingosine kinase and sphingosine-1-phosphate receptors: novel therapeutic targets of rheumatoid arthritis?* Future Med Chem, 2012. **4**(6): p. 727-33.
189. Igarashi, N., et al., *Sphingosine kinase 2 is a nuclear protein and inhibits DNA synthesis.* J Biol Chem, 2003. **278**(47): p. 46832-9.

190. Strub, G.M., et al., *Sphingosine-1-phosphate produced by sphingosine kinase 2 in mitochondria interacts with prohibitin 2 to regulate complex IV assembly and respiration.* FASEB J, 2011. **25**(2): p. 600-12.
191. Swann, J.B., et al., *Demonstration of inflammation-induced cancer and cancer immunoediting during primary tumorigenesis.* Proc Natl Acad Sci U S A, 2008. **105**(2): p. 652-6.
192. Fischer, I., et al., *Sphingosine kinase 1 and sphingosine 1-phosphate receptor 3 are functionally upregulated on astrocytes under pro-inflammatory conditions.* PLoS One, 2011. **6**(8): p. e23905.
193. Pchejetski, D., et al., *The involvement of sphingosine kinase 1 in LPS-induced Toll-like receptor 4-mediated accumulation of HIF-1alpha protein, activation of ASK1 and production of the pro-inflammatory cytokine IL-6.* Immunol Cell Biol, 2011. **89**(2): p. 268-74.
194. Theiss, A.L., *Sphingosine-1-phosphate: Driver of NFkappaB and STAT3 persistent activation in chronic intestinal inflammation and colitis-associated cancer.* JAKSTAT, 2013. **2**(3): p. e24150.
195. Deng, J., et al., *S1PR1-STAT3 signaling is crucial for myeloid cell colonization at future metastatic sites.* Cancer Cell, 2012. **21**(5): p. 642-54.
196. Bao, M., et al., *Sphingosine kinase 1 promotes tumour cell migration and invasion via the S1P/EDG1 axis in hepatocellular carcinoma.* Liver Int, 2012. **32**(2): p. 331-8.
197. Wood, G.W. and G.Y. Gillespie, *Studies on the role of macrophages in regulation of growth and metastasis of murine chemically induced fibrosarcomas.* Int J Cancer, 1975. **16**(6): p. 1022-9.
198. Yang, Y., et al., *Shp2 suppresses PyMT-induced transformation in mouse fibroblasts by inhibiting Stat3 activity.* Virology, 2011. **409**(2): p. 204-10.
199. Weigelt, B., J.L. Peterse, and L.J. van 't Veer, *Breast cancer metastasis: markers and models.* Nat Rev Cancer, 2005. **5**(8): p. 591-602.
200. Bonnomet, A., et al., *A dynamic in vivo model of epithelial-to-mesenchymal transitions in circulating tumor cells and metastases of breast cancer.* Oncogene, 2012. **31**(33): p. 3741-53.
201. Sceneay, J., et al., *Primary tumor hypoxia recruits CD11b+/Ly6Cmed/Ly6G+ immune suppressor cells and compromises NK cell cytotoxicity in the premetastatic niche.* Cancer Res, 2012. **72**(16): p. 3906-11.
202. Candido, J. and T. Hagemann, *Cancer-related inflammation.* J Clin Immunol, 2013. **33 Suppl 1**: p. S79-84.
203. Balkwill, F. and A. Mantovani, *Cancer and inflammation: implications for pharmacology and therapeutics.* Clin Pharmacol Ther, 2010. **87**(4): p. 401-6.
204. Eskan, M.A., et al., *TLR4 and S1P receptors cooperate to enhance inflammatory cytokine production in human gingival epithelial cells.* Eur J Immunol, 2008. **38**(4): p. 1138-47.
205. Fernandez-Pisonero, I., et al., *Lipopolysaccharide and sphingosine-1-phosphate cooperate to induce inflammatory molecules and leukocyte adhesion in endothelial cells.* J Immunol, 2012. **189**(11): p. 5402-10.
206. Baluk, P., et al., *Transgenic overexpression of interleukin-1beta induces persistent lymphangiogenesis but not angiogenesis in mouse airways.* Am J Pathol, 2013. **182**(4): p. 1434-47.

207. Qiao, Y., et al., *TLR-induced NF-kappaB activation regulates NLRP3 expression in murine macrophages.* FEBS Lett, 2012. **586**(7): p. 1022-6.
208. Pettus, B.J., et al., *The sphingosine kinase 1/sphingosine-1-phosphate pathway mediates COX-2 induction and PGE2 production in response to TNF-alpha.* FASEB J, 2003. **17**(11): p. 1411-21.
209. Olivera, A., et al., *Sphingosine kinase expression increases intracellular sphingosine-1-phosphate and promotes cell growth and survival.* J Cell Biol, 1999. **147**(3): p. 545-58.
210. Yang, L., et al., *Sphingosine kinase/sphingosine 1-phosphate (S1P)/S1P receptor axis is involved in liver fibrosis-associated angiogenesis.* J Hepatol, 2013. **59**(1): p. 114-23.
211. Yang, F., et al., *Sorafenib inhibits endogenous and IL-6/S1P induced JAK2-STAT3 signaling in human neuroblastoma, associated with growth suppression and apoptosis.* Cancer Biol Ther, 2012. **13**(7): p. 534-41.
212. Sekine, Y., K. Suzuki, and A.T. Remaley, *HDL and sphingosine-1-phosphate activate stat3 in prostate cancer DU145 cells via ERK1/2 and S1P receptors, and promote cell migration and invasion.* Prostate, 2011. **71**(7): p. 690-9.
213. Loh, K.C., et al., *Sphingosine-1-phosphate enhances satellite cell activation in dystrophic muscles through a S1PR2/STAT3 signaling pathway.* PLoS One, 2012. **7**(5): p. e37218.
214. Benkhart, E.M., et al., *Role of Stat3 in lipopolysaccharide-induced IL-10 gene expression.* J Immunol, 2000. **165**(3): p. 1612-7.
215. Ouyang, W., et al., *Regulation and functions of the IL-10 family of cytokines in inflammation and disease.* Annu Rev Immunol, 2011. **29**: p. 71-109.
216. Yu, H., M. Kortylewski, and D. Pardoll, *Crosstalk between cancer and immune cells: role of STAT3 in the tumour microenvironment.* Nat Rev Immunol, 2007. **7**(1): p. 41-51.
217. Yu, H., D. Pardoll, and R. Jove, *STATs in cancer inflammation and immunity: a leading role for STAT3.* Nat Rev Cancer, 2009. **9**(11): p. 798-809.
218. Walcher, D., et al., *LXR activation reduces proinflammatory cytokine expression in human CD4-positive lymphocytes.* Arterioscler Thromb Vasc Biol, 2006. **26**(5): p. 1022-8.
219. Hasegawa-Moriyama, M., et al., *Peroxisome proliferator-activated receptor-gamma agonist rosiglitazone attenuates postincisional pain by regulating macrophage polarization.* Biochem Biophys Res Commun, 2012. **426**(1): p. 76-82.
220. Hasegawa-Moriyama, M., et al., *Peroxisome proliferator-activated receptor-gamma agonist rosiglitazone attenuates inflammatory pain through the induction of heme oxygenase-1 in macrophages.* Pain, 2013. **154**(8): p. 1402-12.
221. Stein, M., et al., *Interleukin 4 potently enhances murine macrophage mannose receptor activity: a marker of alternative immunologic macrophage activation.* J Exp Med, 1992. **176**(1): p. 287-92.
222. Geissmann, F., et al., *Development of monocytes, macrophages, and dendritic cells.* Science, 2010. **327**(5966): p. 656-61.
223. Mosser, D.M. and J.P. Edwards, *Exploring the full spectrum of macrophage activation.* Nat Rev Immunol, 2008. **8**(12): p. 958-69.
224. Mantovani, A., A. Sica, and M. Locati, *Macrophage polarization comes of age.* Immunity, 2005. **23**(4): p. 344-6.

225. Graler, M.H. and E.J. Goetzl, *The immunosuppressant FTY720 down-regulates sphingosine 1-phosphate G-protein-coupled receptors.* FASEB J, 2004. **18**(3): p. 551-3.
226. Lan, Y.Y., et al., *The sphingosine-1-phosphate receptor agonist FTY720 modulates dendritic cell trafficking in vivo.* Am J Transplant, 2005. **5**(11): p. 2649-59.
227. Muller, H., et al., *The immunomodulator FTY720 interferes with effector functions of human monocyte-derived dendritic cells.* Eur J Immunol, 2005. **35**(2): p. 533-45.
228. Estrada, R., et al., *Ligand-induced nuclear translocation of S1P(1) receptors mediates Cyr61 and CTGF transcription in endothelial cells.* Histochem Cell Biol, 2009. **131**(2): p. 239-49.
229. Liao, J.J., et al., *Distinctive T cell-suppressive signals from nuclearized type 1 sphingosine 1-phosphate G protein-coupled receptors.* J Biol Chem, 2007. **282**(3): p. 1964-72.
230. Buchanan, F.G., et al., *Prostaglandin E2 regulates cell migration via the intracellular activation of the epidermal growth factor receptor.* J Biol Chem, 2003. **278**(37): p. 35451-7.
231. Savill, J.S., et al., *Macrophage phagocytosis of aging neutrophils in inflammation. Programmed cell death in the neutrophil leads to its recognition by macrophages.* J Clin Invest, 1989. **83**(3): p. 865-75.
232. Cox, G., J. Crossley, and Z. Xing, *Macrophage engulfment of apoptotic neutrophils contributes to the resolution of acute pulmonary inflammation in vivo.* Am J Respir Cell Mol Biol, 1995. **12**(2): p. 232-7.
233. Mitchell, S., et al., *Lipoxins, aspirin-triggered epi-lipoxins, lipoxin stable analogues, and the resolution of inflammation: stimulation of macrophage phagocytosis of apoptotic neutrophils in vivo.* J Am Soc Nephrol, 2002. **13**(10): p. 2497-507.
234. Lawrence, T., D.A. Willoughby, and D.W. Gilroy, *Anti-inflammatory lipid mediators and insights into the resolution of inflammation.* Nat Rev Immunol, 2002. **2**(10): p. 787-95.
235. Ajuebor, M.N., et al., *Endogenous monocyte chemoattractant protein-1 recruits monocytes in the zymosan peritonitis model.* J Leukoc Biol, 1998. **63**(1): p. 108-16.
236. Hirsch, S., J.M. Austyn, and S. Gordon, *Expression of the macrophage-specific antigen F4/80 during differentiation of mouse bone marrow cells in culture.* J Exp Med, 1981. **154**(3): p. 713-25.
237. Cain, D.W., et al., *Identification of a tissue-specific, C/EBPbeta-dependent pathway of differentiation for murine peritoneal macrophages.* J Immunol, 2013. **191**(9): p. 4665-75.
238. Lin, H.H., et al., *The macrophage F4/80 receptor is required for the induction of antigen-specific efferent regulatory T cells in peripheral tolerance.* J Exp Med, 2005. **201**(10): p. 1615-25.
239. Barth, M.W., et al., *Review of the macrophage disappearance reaction.* J Leukoc Biol, 1995. **57**(3): p. 361-7.
240. Underhill, D.M., *Macrophage recognition of zymosan particles.* J Endotoxin Res, 2003. **9**(3): p. 176-80.
241. Hodge, D.R., E.M. Hurt, and W.L. Farrar, *The role of IL-6 and STAT3 in inflammation and cancer.* Eur J Cancer, 2005. **41**(16): p. 2502-12.

242. Conte, D., et al., *Inhibitor of apoptosis protein cIAP2 is essential for lipopolysaccharide-induced macrophage survival.* Mol Cell Biol, 2006. **26**(2): p. 699-708.
243. Merrill, A.H., Jr. and V.L. Stevens, *Modulation of protein kinase C and diverse cell functions by sphingosine--a pharmacologically interesting compound linking sphingolipids and signal transduction.* Biochim Biophys Acta, 1989. **1010**(2): p. 131-9.
244. Goetzl, E.J., et al., *Mechanisms of lysolipid phosphate effects on cellular survival and proliferation.* Ann N Y Acad Sci, 2000. **905**: p. 177-87.
245. Liu, H., et al., *Sphingosine kinase type 2 is a putative BH3-only protein that induces apoptosis.* J Biol Chem, 2003. **278**(41): p. 40330-6.
246. Van Brocklyn, J.R., et al., *Sphingosine kinase-1 expression correlates with poor survival of patients with glioblastoma multiforme: roles of sphingosine kinase isoforms in growth of glioblastoma cell lines.* J Neuropathol Exp Neurol, 2005. **64**(8): p. 695-705.
247. Baker, D.A., et al., *Genetic sphingosine kinase 1 deficiency significantly decreases synovial inflammation and joint erosions in murine TNF-alpha-induced arthritis.* J Immunol, 2010. **185**(4): p. 2570-9.
248. Chen, X.L., et al., *Sphingosine kinase-1 mediates TNF-alpha-induced MCP-1 gene expression in endothelial cells: upregulation by oscillatory flow.* Am J Physiol Heart Circ Physiol, 2004. **287**(4): p. H1452-8.
249. Maines, L.W., et al., *Suppression of ulcerative colitis in mice by orally available inhibitors of sphingosine kinase.* Dig Dis Sci, 2008. **53**(4): p. 997-1012.
250. Bui, J.D. and R.D. Schreiber, *Cancer immunosurveillance, immunoediting and inflammation: independent or interdependent processes?* Curr Opin Immunol, 2007. **19**(2): p. 203-8.
251. Meng, H., Y. Yuan, and V.M. Lee, *Loss of sphingosine kinase 1/S1P signaling impairs cell growth and survival of neurons and progenitor cells in the developing sensory ganglia.* PLoS One, 2011. **6**(11): p. e27150.
252. Kanno, T., et al., *Regulation of synaptic strength by sphingosine 1-phosphate in the hippocampus.* Neuroscience, 2010. **171**(4): p. 973-80.
253. Gordon, S. and P.R. Taylor, *Monocyte and macrophage heterogeneity.* Nat Rev Immunol, 2005. **5**(12): p. 953-64.
254. Ibe, S., et al., *Tumor rejection by disturbing tumor stroma cell interactions.* J Exp Med, 2001. **194**(11): p. 1549-59.
255. Hisano, Y., et al., *Mouse SPNS2 functions as a sphingosine-1-phosphate transporter in vascular endothelial cells.* PLoS One, 2012. **7**(6): p. e38941.
256. Kuhn, R., et al., *Interleukin-10-deficient mice develop chronic enterocolitis.* Cell, 1993. **75**(2): p. 263-74.
257. Mantovani, A., et al., *Cancer-related inflammation.* Nature, 2008. **454**(7203): p. 436-44.
258. Nguyen, A.V., et al., *STAT3 in epithelial cells regulates inflammation and tumor progression to malignant state in colon.* Neoplasia, 2013. **15**(9): p. 998-1008.
259. Pyne, N.J. and S. Pyne, *Sphingosine 1-phosphate is a missing link between chronic inflammation and colon cancer.* Cancer Cell, 2013. **23**(1): p. 5-7.
260. Taniguchi, K. and M. Karin, *IL-6 and related cytokines as the critical lynchpins between inflammation and cancer.* Semin Immunol, 2014. **26**(1): p. 54-74.

261. Chang, Q., et al., *The IL-6/JAK/Stat3 feed-forward loop drives tumorigenesis and metastasis.* Neoplasia, 2013. **15**(7): p. 848-62.
262. Ruckhaberle, E., et al., *Predictive value of sphingosine kinase 1 expression in neoadjuvant treatment of breast cancer.* J Cancer Res Clin Oncol, 2013. **139**(10): p. 1681-9.
263. Nagahashi, M., et al., *Sphingosine-1-phosphate produced by sphingosine kinase 1 promotes breast cancer progression by stimulating angiogenesis and lymphangiogenesis.* Cancer Res, 2012. **72**(3): p. 726-35.
264. Maceyka, M., S. Milstien, and S. Spiegel, *Sphingosine-1-phosphate: the Swiss army knife of sphingolipid signaling.* J Lipid Res, 2009. **50 Suppl**: p. S272-6.
265. Prakash, H., et al., *Sphingosine kinase-1 (SphK-1) regulates Mycobacterium smegmatis infection in macrophages.* PLoS One, 2010. **5**(5): p. e10657.
266. Bono, P., et al., *High LYVE-1-positive lymphatic vessel numbers are associated with poor outcome in breast cancer.* Clin Cancer Res, 2004. **10**(21): p. 7144-9.
267. Skobe, M., et al., *Induction of tumor lymphangiogenesis by VEGF-C promotes breast cancer metastasis.* Nat Med, 2001. **7**(2): p. 192-8.
268. Achen, M.G., et al., *Vascular endothelial growth factor D (VEGF-D) is a ligand for the tyrosine kinases VEGF receptor 2 (Flk1) and VEGF receptor 3 (Flt4).* Proc Natl Acad Sci U S A, 1998. **95**(2): p. 548-53.
269. Joukov, V., et al., *A novel vascular endothelial growth factor, VEGF-C, is a ligand for the Flt4 (VEGFR-3) and KDR (VEGFR-2) receptor tyrosine kinases.* EMBO J, 1996. **15**(2): p. 290-98.
270. Kerjaschki, D., *The crucial role of macrophages in lymphangiogenesis.* J Clin Invest, 2005. **115**(9): p. 2316-9.
271. Schoppmann, S.F., et al., *Tumor-associated macrophages express lymphatic endothelial growth factors and are related to peritumoral lymphangiogenesis.* Am J Pathol, 2002. **161**(3): p. 947-56.
272. Shinriki, S., et al., *Interleukin-6 signalling regulates vascular endothelial growth factor-C synthesis and lymphangiogenesis in human oral squamous cell carcinoma.* J Pathol, 2011. **225**(1): p. 142-50.
273. Leu, C.M., et al., *Interleukin-6 acts as an antiapoptotic factor in human esophageal carcinoma cells through the activation of both STAT3 and mitogen-activated protein kinase pathways.* Oncogene, 2003. **22**(49): p. 7809-18.
274. Srivastava, M.K., et al., *Myeloid suppressor cells and immune modulation in lung cancer.* Immunotherapy, 2012. **4**(3): p. 291-304.
275. Popa, E.R., et al., *Circulating CD34+ progenitor cells modulate host angiogenesis and inflammation in vivo.* J Mol Cell Cardiol, 2006. **41**(1): p. 86-96.
276. Kalluri, R. and M. Zeisberg, *Fibroblasts in cancer.* Nat Rev Cancer, 2006. **6**(5): p. 392-401.
277. Dankbar, B., et al., *Vascular endothelial growth factor and interleukin-6 in paracrine tumor-stromal cell interactions in multiple myeloma.* Blood, 2000. **95**(8): p. 2630-6.
278. Hammad, S.M., et al., *Dual and distinct roles for sphingosine kinase 1 and sphingosine 1 phosphate in the response to inflammatory stimuli in RAW macrophages.* Prostaglandins Other Lipid Mediat, 2008. **85**(3-4): p. 107-14.
279. Hsieh, H.L., et al., *Sphingosine-1-phosphate induces COX-2 expression via PI3K/Akt and p42/p44 MAPK pathways in rat vascular smooth muscle cells.* J Cell Physiol, 2006. **207**(3): p. 757-66.

280. Bauernfeind, F.G., et al., *Cutting edge: NF-kappaB activating pattern recognition and cytokine receptors license NLRP3 inflammasome activation by regulating NLRP3 expression.* J Immunol, 2009. **183**(2): p. 787-91.
281. Busillo, J.M., K.M. Azzam, and J.A. Cidlowski, *Glucocorticoids sensitize the innate immune system through regulation of the NLRP3 inflammasome.* J Biol Chem, 2011. **286**(44): p. 38703-13.
282. Sceneay, J., et al., *Hypoxia-driven immunosuppression contributes to the pre-metastatic niche.* Oncoimmunology, 2013. **2**(1): p. e22355.

8 Publications

Weigert, A., **Weichand, B.** and Brüne, B., S1P regulation of macrophage functions in the context of cancer. *Anticancer Agents Med Chem* 2011. 11: 818-829.

Weigert, A.*, **Weichand, B.***, Sekar, D., Sha, W., Hahn, C., Mora, J., Ley, S., Essler, S., Dehne, N. and Brüne, B., HIF-1alpha is a negative regulator of plasmacytoid DC development *in vitro* and *in vivo*. *Blood* 2012. 120: 3001-3006.

Ley, S., Weigert, A., **Weichand, B.**, Henke, N., Mille-Baker, B., Janssen, R. A. and Brune, B., The role of TRKA signaling in IL-10 production by apoptotic tumor cell-activated macrophages. *Oncogene* 2013. 32: 631-640.

Weichand, B.*, Weis, N.*, Weigert, A., Grossmann, N., Levkau, B. and Brüne, B., Apoptotic cells enhance sphingosine-1-phosphate receptor 1 dependent macrophage migration. *Eur J Immunol* 2013. 43: 3306-3313.

Schiffmann, S., Weigert, A., Mannich, J., Eberle, M., Birod, K., Haussler, A., Ferreiros, N., Schreiber, Y., Kunkel, H., Grez, M., **Weichand, B**., Brüne, B., Pfeilschifter, W., Nusing, R., Niederberger, E., Grosch, S., Scholich, K. and Geisslinger, G., PGE2/EP4 signaling in peripheral immune cells promotes development of experimental autoimmune encephalomyelitis. *Biochem Pharmacol* 2014. 87: 625-635.

Schuh, C. D., Pierre, S., Weigert, A., **Weichand, B**., Altenrath, K., Schreiber, Y., Ferreiros, N., Zhang, D. D., Suo, J., Treutlein, E. M., Henke, M., Kunkel, H., Grez, M., Nusing, R., Brüne, B., Geisslinger, G. and Scholich, K., Prostacyclin mediates neuropathic pain through interleukin 1beta-expressing resident macrophages. *Pain* 2014. 155: 545-555.

* contributed equally

9 Acknowledgements

10 Curriculum vitae

11 Erklärung

Ich erkläre hiermit an Eides Statt, dass ich die dem Fachbereich Biologie, Chemie und Pharmazie der Johann Wolfgang Goethe-Universität Frankfurt am Main zur Promotionsprüfung eingereichte Dissertation mit dem Titel

The role of sphingosine-1-phosphate and its receptor S1PR1 in inflammation and cancer

am Institut der Biochemie I / Pathobiochemie unter Betreuung und Anleitung von Professor Dr. Bernhard Brüne mit Unterstützung durch PD. Dr. Andreas Weigert ohne sonstige Hilfe selbst durchgeführt und bei der Abfassung der Arbeit keine anderen als die in der Dissertation angeführten Hilfsmittel benutzt habe. Darüber hinaus versichere ich, nicht die Hilfe einer kommerziellen Promotionsvermittlung in Anspruch genommen zu haben.

Ich versichere, die Grundsätze der guten wissenschaftlichen Praxis beachtet, und nicht die Hilfe einer kommerziellen Promotionsvermittlung in Anspruch genommen zu haben

Vorliegende Ergebnisse der Arbeit wurden in den folgenden Publikationsorganen veröffentlicht:

Weigert, A., Weichand, B. and Brüne, B., S1P regulation of macrophage functions in the context of cancer. Anticancer Agents Med Chem 2011. 11: 818-829.

Weichand, B., Weis, N., Weigert, A., Grossmann, N., Levkau, B. and Brüne, B., Apoptotic cells enhance sphingosine-1-phosphate receptor 1 dependent macrophage migration. Eur J Immunol 2013. 43: 3306-3313.

Frankfurt am Main, 28.07.2014